Use of k-dimensional space, "affigraphy", to predict phase diagram structure for n-component, (n+k)-phase multisystems

Bernard Guy

USE OF K-DIMENSIONAL SPACE, « AFFIGRAPHY », TO PREDICT PHASE DIAGRAM STRUCTURE FOR N-COMPONENT, (N + K)-PHASE MULTISYSTEMS

Bernard GUY

Part 2

Captions of tables and figures

Tables

Figures

CAPTIONS OF TABLES AND FIGURES

CAPTIONS OF TABLES

TABLE 1

Correspondence between bases and cobases for *affigraphy* region n° I (labelled by *) in Fig. 26B. The different stability levels are indicated. Different sets of bases may be obtained in *chemography* regions 1 to 7 (Fig. 26A); the bases are rewritten in the corresponding columns 1 to 7 of the table. By reading the columns vertically, the list of bases for each chemography region is obtained with their stability index; intensive parameters correspond to region I of affigraphy. The relative positions of the Gibbs free energy of the phases are represented in Fig. 26C.

TABLE 2

Characteristic numbers for phase diagrams, depending on the value of k; the numbers are related to points, lines and domains respectively; numbers of affinity vectors and stability levels are given for each geometric item.

TABLE 3

Stability « *successions* » (or sequences) of points along univariant lines in the case k = 5. The four points follow in successive order along each univariant line. To each point is attached three affinity vectors whose positive or negative part is concerned. All the possible sequences are obtained by geometric transformations from one single sequence; use is made of the symmetries with respect to the varieties defined by all possible groups of basic affinity vectors. Sequence number one corresponds to that on Δ_1, Fig. 39A, and has been chosen as starting one. The others are obtained by symmetries on affigraphy vectors as explained in the text. Sequence number 11 is the monotonic sequence that might also be chosen as the starting one; sequence 6 corresponds to it in reverse order (so are associated sequences 2 and 4 and so on).

TABLE 4

Number of affigraphy vectors whose sign changes when a linear variety of dimension p (horizontal axis) is crossed along a linear variety of dimension q (vertical axis). The varieties are themselves defined by groups of affigraphy vectors. The numbers express the generalized stability level changes of the multi-dimensional domains.

TABLE 5

Correspondence between the different types of diagrams: chemography, affigraphy, chemical potential saturation diagram, reaction space. Two operations are responsible for the correspondences: combinatorial duality (a set of phases is replaced by the supplementary set with respect to the whole set; vertical axis; the dimension is changed) and geometric duality (a variety of dimension p is replaced by a variety of dimension m - p where m is the dimension of the space; horizontal axis; the dimension is unchanged). The basic diagrams are labelled A, B, C and D. Additional operations result in composite diagrams: - horizontal substitution of one intensive / one extensive variable (dimension unchanged) leads to composite diagrams I (μ, $\mathbf{x}$; dim. n) or II ($\boldsymbol{A}$, ξ; dim. k); - vertical addition of diagrams lead to integrated n + k diagrams, III ($\underline{\mu}$, $\underline{\xi}$), IV ($\underline{\mathbf{x}}$, $\underline{\boldsymbol{A}}$), V ($\underline{\mathbf{x}}$, $\underline{\xi}$), VI ($\underline{\boldsymbol{A}}$, $\underline{\mu}$). The names of the pertinent variables are indicated in the table so are the constraints for the basic diagrams A to D. Corresponding algabraic problems are defined in Table 6.

TABLE 6

The different types of linear programming problems corresponding to the different choices of variables and constraints. Basic problems are labelled P_1 and P_2 and their dual counterparts are P_1^* and P_2^* respectively. In order to solve P_1 or P_1^* the knowledge of vector $\underline{\mathbf{c}}$ (dim. n) and of vector $\mathbf{g}$ (n + k) are requested; similarly, in order to solve P_2 or P_2^* the knowledge of $\mathbf{x}_0$ (n + k) and of $\underline{\boldsymbol{a}}$ (k) -k stands for the k independent reactions- is requested. When going from one problem to its dual form, the minimum condition is replaced by a maximum. Exclusion relations relating variables in duality are indicated. Problems 1 and 2 may also be expressed with no optimum criterion but with the help

of all the constraints and the exclusion relations (second column). Refer to Appendix A4.

TABLE 7

Nature of the different geometrical operations (projections / intersections) in the n + k dimensional composition and affinity spaces allowing the definition of chemography, affigraphy, chemical potential space, reaction space and four other « *residual* » diagrams.

TABLE 8

Nomenclature of different « *solutions* » of phase diagrams according to the nature of information available.

CAPTIONS OF FIGURES

FIGURE 1

Figure 1A (P, T) diagram for a simple 1 + 2 system of H_2O type (one component, three phases: liquid, solid, vapor). One invariant point, three univariant lines, three two-dimensional domains. No scale.

Figure 1B Three-dimensional affigraphy for a simple 1 + 3 system, the sulfur system (S_α, S_β, S_l, S_v). One invariant hyperpoint Ω, four affinity phase absent vectors. By intersecting the affinity vectors by a two-dimensional plane, a (P, T) diagram is obtained: three invariant points limiting one closed domain and three open ones. No scale.

FIGURE 2

Points and hyperplanes of the chemography; an example on a 3 + 3 system. Positions of points and equations of hyperplanes are given by composition matrix **C** as explained in the text. For example, the equation of hyperplane (here line) BF in basis ABC is A - .5C = 0.

FIGURE 3

Points and hyperplanes of the affigraphy corresponding to the example of Fig. 2 (3 + 3) system; positions of points and equations of hyperplanes are given by **R** matrix as explained in the text. For example the equation of hyperplane (here plane) (C)(D) in cobasis (D) (E) (F) is $A^{(E)} - 0.5A^{(F)} = 0$ also written (E) - 0.5(F) = 0. The intersection of plane (C)(D) with plane (E)(F) is line $A^{(E)} = 0.5A^{(F)}$. The origin of the affigraphy is named Ω.

FIGURE 4

Figure 4A Affine representation of the affigraphy for the 3 + 3 system of Fig. 2 and 3; the figure is obtained by cutting the affinity vectors of Fig. 3 by the hyperplane $\Sigma A^i = 1$. The positive part of an affinity vector gives a black point in the intersecting hyperplane and the negative part a white point.

Figure 4B Convex polyhedron corresponding to the affigraphy of Fig. 3; the polyhedron is formed with the extremities of the affinity vectors as apices. The important is the direction of the vectors, not their lengths and these may be changed so that the polyhedron is convex or drawn on a hypersphere. The construction of a convex hyperpolyhedron is founded on the affigraphy vectors in the general k-dimensional case. It is a complicated task not discussed here. The affine representation of Fig. 4A corresponds to the upper horizontal face of the polyhedron.

Figure 4C The polyhedron of Fig. 4B may be deformed so that it has a cylindrical shape.

Figure 4D Another affine representation of the affigraphy (cf. Fig. 4A). It corresponds to the cutting of the affigraphy by the hyperplane $\Sigma A^i = -1$. When compared to Fig. 4A, black and white points are permuted.

FIGURE 5

Figure 5A Total modal space for a three phase system (variables x_A, x_B, and x_C); n = 1, k = 2, composition matrix **C** is

	A	B	C
A	1	1	1

Variety V (**C**.**x** = $\underline{\mathbf{c}}$) is here a two-dimensional plane; perpendicular variety W_0, a line, is also represented. Initial composition x_0 belongs to V and may be pointed out on the diagram. Systems with one single phase among A, B and C correspond to the intersection of V with the co-ordinate axes.

Figure 5B Vectorial chemography corresponding to the system of Fig. 5A. It is obtained by projecting the basic phase vectors A, B and C of Fig. 5A onto the variety W_0. One independent chemical variable is needed, for instance x_A. The three phases A, B and C project in the same point. Total content $\underline{\mathbf{c}}$ and initial composition $\mathbf{x}_0$ project at the same point; here this point is also the same as projected A, B and C phases.

Figure 5C Total affinity diagram; variables $A^{(A)}$, $A^{(B)}$, and $A^{(C)}$. Basic co-ordinate planes represent absent phases (A) (B and C present), (B) (A and C present) and (C) (A and B present). Variety V', equation $\mathbf{R}\boldsymbol{A}^{T} = \underline{\boldsymbol{a}}^{T}$, is here a line; initial affinity $\underline{\boldsymbol{A}}_0$ also belongs to V'. Variety W'_0 is perpendicular to V' and contains Ω. Here **R** is

	(A)	(B)	(C)
(B)	-1	1	0
(C)	-1	0	1

Figure 5D Affigraphy of the system, obtained by projecting the basic vectors (A) (B) and (C) onto plane W'_0. The projection is independent of the initial affinity $\underline{\boldsymbol{A}}_0$ which projects at the same point as $\underline{\boldsymbol{a}}$. The three basic affinity vectors are the column vectors of **R** matrix.

FIGURE 6

Figure 6A Chemography of a 3 + 2 system. Corresponding **C** matrix is

	A	B	C	D	E
A	1	0	0	1	2.5
B	0	1	0	4	1
C	0	0	1	1.5	1.5

Figure 6B Affigraphy related to Fig. 6A. Chemical reaction matrix is:

	(A)	(B)	(C)	(D)	(E)
(D)	-1	-4	-1.5	1	0
(E)	-2.5	-1	-1.5	0	1

FIGURE 7

The corresponding regions of chemography and affigraphy are represented together (cf. Fig. 6A and B). In this simple example the list

of bases and associated cobases and the corresponding regions of chemography and affigraphy may be decided by mere inspection of the figure. The general method to find out the associated regions is by parametrization of the simplex tableau as explained in App. 2. The ten bases are: ABC, ABD, ABE, ACD, ACE, ADE, BCD, BCE, BDE and CDE; they are systematically explored. The corresponding cobases (D)(E), (C)(E), (C)(D), (B)(E), (B)(D), (B)(C), (A)(E), (A)(D), (A)(C) and (A)(B) are discovered and represented by corresponding regions of the affigraphy (Fig. 7A through J).

FIGURE 8

Summary of Fig. 7 in the form of two associate diagrams.

Figure 8A Chemography. Within each domain of the chemography, the composition of the global system may be generated by several bases. Each of these bases corresponds to a domain of the affigraphy; by summing these affigraphy domains, a restricted affigraphy for each chemography domain is obtained and represented in insert in the chemography domain; in the insert, the names of the chemography bases could be gained by the sole knowledge of the affigraphy vectors; they are written here for clarity.

Figure 8B Affigraphy. Conversely each affigraphy domain corresponds to several bases of the chemography that are represented as insert.

FIGURE 9

Figure 9 General representation of hyperplanes and vectors of the affigraphy. Each chemical reaction corresponds to one hyperplane defined by k - 1 vectors taken among the n + k vectors of the affigraphy. If $A^{(Pi1)}$ is the unitary dissociation affinity vector of phase P_{i1}, hyperplane containing vectors $A^{(Pi1)}...A^{(Pik-1)}$ corresponds to the chemical reaction that brings together all the phases but the k - 1 phases $P_{i1}...P_{ik-1}$.

FIGURES 10 to 19

Corresponding chemographies and affigraphies for different values of n and k. The relevant **C** and **R** matrices are specified. The affinity vectors

of the dissociation reactions of the phases are simply labelled by the names of the phases, between brackets. For each case of (n, k) values, chemography is illustrated in Fig. A, vectorial affigraphy in Fig. B, an arbitrarily chosen affine affigraphy in Fig. C (ruled by $\Sigma A^{(l)} = 1$), and a possible affinity polyhedron in Fig. D. It may happen (k = 4) that only an affine representation of the affigraphy is possible. Conventions on black and white points is the same as explained in Fig. 4. Arrows are used for affinity vectors. Unit value for affinity vectors are not indicated; the length of these vectors matter less than the directions.

Figure 10: n = 1, k = 2.
Matrix **C**:

	A	B	C
A	1	1	1

Matrix **R**:

	(A)	(B)	(C)
(B)	-1	1	0
(C)	-1	0	1

10A: chemography; 10B: affigraphy; 10C: affine affigraphy

Figure 11: n = 1, k = 3
C:

	A	B	C	D
A	1	1	1	1

R:

	(A)	(B)	(C)	(D)
(B)	-1	1	0	0
(C)	-1	0	1	0
(D)	-1	0	0	1

11A: chemography; 11B: affigraphy; 11C: affine affigraphy; 11D: polyhedron. Letters A, C and D refer to tetrahedron faces (B)(C)(D), (A)(B)(D) and (A)(B)(C) respectively.

Figure 12: n = 1, k = 4

C:

	A	B	C	D	E
A	1	1	1	1	1

R:

	(A)	(B)	(C)	(D)	(E)
(B)	-1	1	0	0	0
(C)	-1	0	1	0	0
(D)	-1	0	0	1	0
(E)	-1	0	0	0	1

12A: chemography; 12B: affine affigraphy.

Figure 13: n = 2, k = 2

C:

	A	B	C	D
A	1	0	8	2
B	0	1	2	8

R:

	(A)	(B)	(C)	(D)
(C)	-8	-2	1	0
(D)	-2	-8	0	1

13A: chemography; 13B: affigraphy; 13C: affine affigraphy

Figure 14: n = 2, k = 3

C:

	A	B	C	D	E
A	1	0	8	5	2
B	0	1	2	5	8

R:

	(A)	(B)	(C)	(D)	(E)
(C)	-8	-2	1	0	0
(D)	-5	-5	0	1	0
(E)	-2	-2	0	0	1

14A: chemography; 14B: affigraphy; 14C: affine affigraphy; 14D: polyhedron.

Figure 15: n = 2, k = 4

C:

	A	B	C	D	E	F
A	1	0	4	3	2	1
B	0	1	1	2	3	4

R:

	(A)	(B)	(C)	(D)	(E)	(F)
(C)	-4	-1	1	0	0	0
(D)	-3	-2	0	1	0	0
(E)	-2	- 3	0	0	1	0
(F)	-1	-4	0	0	0	1

15A: chemography; 15B: affine affigraphy.

Figure 16: n = 3, k = 4

C:

	A	B	C	D	E	F	G
A	1	0	0	6	3	3	2
B	0	1	0	1	3	6	3
C	0	0	1	3	4	1	5

R:

	(A)	(B)	(C)	(D)	(E)	(F)	(G)
(D)	-6	-1	-3	1	0	0	0
(E)	-3	-3	-4	0	1	0	0
(F)	-3	-6	-1	0	0	1	0
(G)	-2	-3	-5	0	0	0	1

16A: chemography; 16B: affine affigraphy

Figure 17: n = 4, k = 2

C

	A	B	C	D	E	F
A	1	0	0	0	6	3
B	0	1	0	0	2	2
C	0	0	1	0	1	2
D	0	0	0	1	1	3

R:

	(A)	(B)	(C)	(D)	(E)	(F)
(E)	-6	-2	-1	-1	1	0
(F)	-3	-2	-2	-3	0	1

17A: chemography; 17B: affigraphy; 17C: affine affigraphy.

Figure 18: n = 4, k = 3

C:

	A	B	C	D	E	F	G
A	1	0	0	0	6	3	1
B	0	1	0	0	2	2	1
C	0	0	1	0	1	2	2
D	0	0	0	1	1	3	6

R:

	(A)	(B)	(C)	(D)	(E)	(F)	(G)
(E)	-6	-2	-1	-1	1	0	0
(F)	-3	-2	-2	-3	0	1	0
(G)	-1	-1	-2	-6	0	0	1

18A: chemography; 18B: affigraphy; 18C: affine affigraphy; 18D: polyhedron.

Figure 19: n = 4, k = 4

C:

	A	B	C	D	E	F	G	H
A	1	0	0	0	6	3	1	2
B	0	1	0	0	2	2	1	2
C	0	0	1	0	1	2	2	3
D	0	0	0	1	1	3	6	3

R:

	(A)	(B)	(C)	(D)	(E)	(F)	(G)	(H)
(E)	-6	-2	-1	-1	1	0	0	0
(F)	-3	-2	-2	-3	0	1	0	0
(G)	-1	-1	-2	-6	0	0	1	0
(H)	-2	-2	-3	-3	0	0	0	1

19A: chemography; 19B: affine affigraphy

FIGURE 20

In Fig. 20 to 22, examples are given of associated chemographies and affigraphies, for three different arrangements of the chemography of a 3 + 3 system. For each example, the chemography, affigraphy, affine representation of affigraphy and representative polyhedron are given in successive order. A first example of a 3 + 3 system has already been studied in Fig. 4. In Fig. 20, the hexagonal arrangement is chosen. It has proved convenient in a first step to use chemical elements a, b and c as references in the composition matrix, and then to take sets of three phases as new bases; a new **C** matrix is obtained by pivoting, from which a **R** reaction matrix is then constructed.

Figure 20A: chemography

	A	B	C	D	E	F
a	3	1	0	0	1	3
b	1	3	3	1	0	0
c	0	0	1	3	3	1

Let us choose basis ACE; matrix becomes

	A	B	C	D	E	F
A	1	.43	0	-.29	0	.86
C	0	.86	1	.43	0	-.29
E	0	-.29	0	.86	1	.43

Figure 20B: affigraphy; from the preceding matrix it is easy to derive a matrix of chemical reactions

	(A)	(B)	(C)	(D)	(E)	(F)
(B)	-.43	1	-.86	0	.29	0
(D)	.29	0	-.43	1	-.86	0
(F)	-.86	0	.29	0	-.43	1

Figure 20C: affine affigraphy

Figure 20D: polyhedron. Indifferent crossing points on line (D)(F) are represented (see Sect. 6.4). They correspond to intersections of plane (D)(F) with the planes defined by pairs of vectors among (A), (B), (C) and (E). The six indifferent crossing points on line (D)(F) (or plane (D)(F)) are thus $(-DF, -A\text{-}B)_{ic}$, $(-DF, -AC)_{ic}$, $(DF, -A\text{-}E)_{ic}$, $(D\text{-}F, -B\text{-}C)_{ic}$, $(DF, B\text{-}E)_{ic}$, $(DF, -C\text{-}E)_{ic}$. Each of the vectors in the four vector set of one indifferent crossing point has a positive or negative sign depending on the corresponding affinity vector sector. In order to construct the points, horizontal plane BDF has been used so as its intersections with the negative vectors (-A), (-C) and (-E). An example is given for point $(DF, B\text{-}E)_{ic}$ by use of vectors (B) and (-E). Line Δ $(AF, DC)_{ic}$ has also been represented.

FIGURE 21

Pentagonal arrangement for a 3 + 3 system

Figure 21A: chemography

	A	B	C	D	E	F
a	3	1	0	0	1	1
b	1	3	1	0	0	1
D	0	0	1	1	1	1

Basis ABD is chosen and matrix becomes

	A	B	C	D	E	F
A	1	0	-.12	0	.37	.25
B	0	1	.37	0	-.12	.25
D	0	0	1	1	1	1

Figure 21B: affigraphy; the matrix of chemical reactions in co-basis (C) (E) (F) is easily derived from the preceding matrix

Figure 21C: affine representation of the affigraphy

Figure 21D: representation polyhedron; (A), (B), (C), (D) have all a negative co-ordinate on (F); line (A) (B) lies between point (D) and line (C)(E) contrary to the chemography where EC is between D and AB; the polyhedron is a pyramid with pentagonal basis.

FIGURE 22

Quadrilateral arrangement for a 3 + 3 system

Figure 22A: chemography

	A	B	C	D	E	F
a	3	1	0	1	.8	1.6
b	1	3	1	0	1.2	.8
c	0	0	1	1	.8	.8

Similarly to what is done in the preceding figures a new composition matrix is computed for basis ABC, from which the chemical reaction matrix for co-basis (D) (E) (F) is derived but not reported here.

Figure 22B: affigraphy

Figure 22C: affine representation of the affigraphy

Figure 22D: representation polyhedron

FIGURE 23

Affigraphy of simple 1 + 2 system; in the region in-between (C) and negative part of (A) noted (-A), phase A is the most stable; B is less stable, then C; this is noted $A^{\circ} < B^{1} < C^{2}$. In the other region identified by a star the sequence is $B^{\circ} < C^{1} < A^{2}$; corresponding co-bases are listed: (AC), (A-B), (-B-C).

FIGURE 24

Affigraphy of a 1 + 3 system; in the region identified by the arrow the following phases may appear in increasing metastability order: $A^{\circ} < D^{1} < B^{2} < C^{3}$. Affigraphy planes intersect along other vectors than the basic affinity vectors. These define « *indifferent crossing (i.c.) points* » as discussed in Sect. 6.4 below. Such points, for instance $(\text{-A-B, CD})_{ic}$ are represented in plane (B) (C) (D).

FIGURE 25

Stability sequences for a 2 + 2 system.

Figure 25A: chemography. *25B*: affigraphy. The value of overall system affinity is chosen in the region comprised between (A) and (D). For this region, the list of the generalized co-bases, i.e. with possible negative part vectors, is indicated. The correspondence between bases and cobases for each chemography region, and for the chosen affigraphy region, is given in the following table. The stability of the bases is determined by the number of negative vectors of the corresponding co-basis:

cobases	bases		
	region AB	region BC	region CD
(AB)			CD^0
(A-C))		BD^1	BD^1
(AD)		BC^0	
(-B-C)	AD^2	AD^2	AD^2
(-BD)	AC^1	AC^1	
(CD)	AB^0		

With the use of this table, sets of bases are written below the chemographic bar with their stability index. In the composition domain between B and C two subdomains may be defined, the precise location of the limit is unknown. Location of point « ? » depends on the thermodynamic values of the phases. On the left side (B side) basis BD^1 is more stable than AC^1; on the right side (C side) AC^1 is more stable than BD^1. In Fig. 25A, an example of possible relations between the g's of the phase associations is represented along the vertical axis. This allows to locate point « ? » in the BC domain.

Figure 25C Graphical representation of basis stability sequences in each affigraphy region. Three bars are added to the ordinary stable chemographic bar. They represent possible phase associations with

higher free energy. For instance, in the affigraphy region between (-C) and (D) and for composition between A and B, association of A and C has metastability level equal to one (dashed lower intermediate bar), and association of A and D has metastability level equal to two (dotted higher bar).

FIGURE 26

Stability sequences for a 3 + 2 system (cf. Fig. 6 to 8). The procedure is the same as for Fig. 25: 1) choice of affigraphy region marked by a star * (region I) and list of generalized cobases and associated bases with their stability index (Table 1). 2) writing of the list of possible bases with their stability indices for each of the 7 chemography regions (the stability sequences all fit to the chosen affigraphy region).

Figure 26A: chemography

Figure 26B: affigraphy corresponding to Fig. 26A.

Figure 26C: possible position of the G planes for affigraphy region number I. This allows to rank the bases with the same intermediate stability level of 1.

FIGURE 27

Graphical representation of basis stability sequences in each affigraphy region. For a given composition and a given affigraphy region (from I to X) the possible bases with their stability level may be determined from the figure. They are represented in four triangles, one for stable bases (stab. level 0), one for doubly metastable bases (stab. level 2), and, because of the relatively large number of singly metastable bases, two triangles are given in order overlapping stab. level 1 bases are clearly distinguished. Domains corresponding to stable bases are filled by a solid line, to singly metastable bases by a dashed line and to doubly metastable basis by a dotted line. In some cases, two bases with same stability level one are accessible to the same composition domain. The hierarchy between them is given by phase thermodynamic data. Bases with stab. level 0 exchange with bases with stab. level 2 in the regions that are symmetric to the origin; in that case bases with stab. level 1 are unchanged.

FIGURE 28

Construction of (P, T) plane by affigraphy intersection and notation of points and lines. The illustration is artificial because one is limited by dimension 3; the purpose is for general understanding. The extremity of the k-dimensional affinity vector of the system, $\underline{a}$, (projection of n + k dimensional total affinity $\boldsymbol{A}_{tot}$ onto affigraphy space), describes a two-dimensional surface in the affigraphy described by the two parameters P and T. This surface can be approximated by a linear variety of two dimensions: a plane. Some basic affinity vectors are represented; their intersection with (P, T) plane will give the structure of the (P, T) diagrams. The (P, T) plane may cut the positive or negative part of each of the basic affinity vectors. The chemical reactions correspond to hyperplanes defined by collections of k - 1 affinity vectors of the affigraphy; the univariant lines of the (P, T) diagram are the intersections of these hyperplanes with the (P, T) plane. In the collection of k - 1 vectors, the number of negative parts may be zero, one, two, ..., k - 1; invariant points result from the intersection of k - 2 vectors (among the k - 1 of the reaction) with the (P, T) plane. Similarly zero to k - 2 vectors may be negative in the collection. A typographic type of line and point must be chosen for each of these combinations. In the figure, the two neighbouring points have stability level p and p - 1 respectively, and univariant portions have stability level p, p - 1 and p - 2 respectively.

FIGURE 29

Examples of relations of affigraphy with (P, T) plane

Figure 29A In the case k = 2, the (P, T) plane coincides with the affigraphy, reduced to two dimensions. The example is taken from Fig. 10 (one component, three phase system): the axes of affigraphy are $A^{(B)}$ and $A^{(C)}$. The affinities $A^{(B)}$ and $A^{(C)}$ are function of P and T and conversely, P and T can be derived from $A^{(B)}$ and $A^{(C)}$: arbitrary P and T axes are drawn in the figure (the location of the axes depend on the thermodynamic values g^j). P and T axes are straight lines in the

affigraphy because of the linear dependence hypothesis of the g's on P and T.

Figure 29B Case k = 5. Like in Fig. 28, the representation is artificial and merely intends to illustrate the notations. Each univariant line is defined by a set of four affinity vectors; the line contains four points defined each by three vectors taken in the four vector set. Stability levels are defined by the number of negative parts of affinity vectors; this number is indicated and a special type of symbol is chosen for each type of point and each type of univariant line portion.

FIGURE 30 A through G

Examples of (P, T) diagrams obtained by the intersection of the affigraphy by a two-dimensional plane in the case k = 3, n = 1 (cf. Fig. 11). Four cases are portrayed according to the position of the plane: arbitrary of first type (three positive vectors, one negative, Fig. 30A), parallel to one affinity vector (30B), parallel to two vectors (30C), arbitrary of second type (three negative negative vectors, one positive, 30D). Points and line portions are labelled according to corresponding affinity vectors. The portions between the different types of points taken two by two are stable, singly metastable and doubly metastable respectively and three types of lines have been chosen.

Thermodynamic degeneracy occurs when the intersecting two-dimensional plane contains the hyperpoint Ω (Fig. 30 E, F, G). The plane may contain zero vector (30E), but in addition to Ω, it may contain one (30F) or two (30G) affinity vectors.

Figure 30E (P, T) plane contains Ω; all univariant lines are present, but they have but one invariant point, Ω itself. Only the semi-infinite parts of Fig. 30A are present, the parts between the invariant points are reduced to zero. The stability level of the line portions shifts from the level at one extremity to the level at the other extremity of the lines of Fig. 30A.

Figure 30F (P, T) plane contains Ω and vector (B). Line (B) is at the same time (AB), (BC) and (BD) that coincide. Other lines are as in Fig. 30E.

Figure 30G (P, T) plane contains Ω and vectors (B) and (D). Line (B) coincides with all the lines that contain (B): (AB), (BC) and (BD); similarly line (D) coincides with (AD), (BD) and (CD).

FIGURE 31

Another example of a (P,T) diagram obtained by the intersection of the affigraphy by a two-dimensional plane; n = 3, k = 3, cf. Fig. 20. (P, T) plane is parallel to the quadrilateral face of Fig. 20D polyhedron.

FIGURE 32

Projection of an hyperpolyhedron (n = 1, k = 5; six phases). The hyperpolyhedron gathers the affigraphy information and thus that on all possible phase diagrams. In the example, each apex is connected to the five others. Invariant points correspond to groups of three phases and univariant lines groups of four phases. The hyperpolyhedron indicates how points and lines may be related.

FIGURE 33

Figure 33A An univariant line in a n + 4 system belongs to a three dimensional hyperplane defined by a set of three affinity vectors, (A) (B) and (C). The line is obtained by intersecting this three-dimensional volume by the two-dimensional (P, T) plane. This cannot be represented in the figure because in general the plane does not belong to the three-dimensional volume. Examples of lines are given. Notations of intersecting points and stability levels depend on the plane sector defined by pairs of vectors (same rules as in previous figures). Two univariant lines Δ_1 and Δ_2 are represented; Δ_1 yields stability succession 1 of Fig. 34, Δ_2 succession 3. Δ_1 and Δ_2 define plane (P).

An affine representation of the three-dimensional hyperplane may be obtained by cutting it by a two-dimensional plane; affigraphy itself may be represented in a three-dimensional affine section. By inspection of the two-dimensional planes, one determines the rules for noting the intersections of an affine representation of the four-dimensional affigraphy. Synthesis of the rules is given in Fig. 36 and the construction

of a (P, T) diagram with the k = 4 affine affigraphy method is given in Fig. 37.

Figure 33B Other intersections of univariant lines with one chemical reaction three-plane set in the n + 4 system, yielding other stability successions. Δ_1 yields succession 2, Δ_2 succession 5 and Δ_3 succession 6 (synthesis in Fig. 34).

FIGURE 34

All univariant line stability successions for n + 4 systems. The successions may be found by the geometrical method illustrated in previous figures, or by the operation of all types of symmetries of the problem on one single succession.

FIGURE 35

Two examples of univariant loops for n + 4 system. The structure of Fig. 33A is cut by a two-dimensional plane containing the origin. Same notations as in previous figures.

FIGURE 36

Rules for noting the intersections of the affine four-dimensional affigraphy by two-dimensional planes. The invariant points of n + 4 systems may be obtained in two steps. First cut the affigraphy vectors by a three-dimensional hyperplane. The resulting points are black or white depending on the positive or negative part of affigraphy vector. Pairs of black / white points define lines. Second, cut the preceding lines with a two-dimensional plane. All types of lines and intersections are represented in the figure; three types of invariant points come out (stable, singly metastable, doubly metastable), also recognized by the number of signs + or - in the letters for the points.

FIGURE 37

Example of the geometric construction of a (P,T) diagram for a 1 + 4 system. An affine tetrahedron in three-dimensional space (four black points, an inner white point) is first obtained by intersecting the affigraphy vectors with a three-dimensional hyperplane. Then the edges

of this tetrahedron intersect a two-dimensional plane and this yields the diagram. The two-dimensional plane is the horizontal plane corresponding to the lower part of the figure below line Δ. The intersection is determined by two associated two-dimensional representations by use of descriptive geometry (Monge, 1800): vertical projection above ground line Δ, horizontal projection below line Δ. Types of invariant points and univariant line portions are determined according to the rules exposed in the preceding figures.

FIGURE 38

Equivalence classes for k = 4 systems (Usdansky, 1987). The classes are understood as resulting from the intersection of a polyhedron by a rotating plane in three-dimensional space. The three-dimensional polyhedron results from a (first) intersection of the affigraphy by a three-dimensional hyperplane. By intersecting the plane, pairs of polyhedron apices of different stability level will give rise to invariant points in the (P, T) diagram. The rotation of the (P, T) plane does not change the intermediate stability level whereas the most and least stable level points are interchanged in correspondence with Usdansky's classes. Point symbols as in Fig. 34.

FIGURE 39

Figure 39A and B

The affine four-dimensional restriction of the chemical reaction hyperplane of the n + 5 systems is a tetrahedron. Univariant lines are obtained by cutting the tetrahedron by one-dimensional lines. Two examples are given. In Fig. 39A the lines yield stability successions 1 (Δ_1) and 7 (Δ_2) of Fig. 40, in Fig. 39B successions 10 and 8. Similar rules as in previous figures; captions for points and lines in Fig. 40.

FIGURE 40

Univariant line stability successions in n + 5 systems. Succession 1 corresponds to Δ_1 (Fig. 39A). All successions are given in Table 3.

FIGURE 41

Thermodynamic degeneracies for k = 4, 5 systems.

Figure 41A k = 4 systems; the degeneracy corresponds to the intersection of a univariant line Δ with one affinity vector in Fig. 33A. Next step when Δ contains Ω. In this final situation, there are two types of univariant lines left.

Figure 41B k = 5 systems; degeneracy when univariant line Δ cuts an edge such as (B)(D) in Fig. 39; next step when Δ contains a point; next step when Δ contains Ω. All degeneracies may be obtained by skipping 1, 2, ..., k - 2 portions on the univariant lines represented in Fig. 34 and 40. No special symbols are chosen here to represent these particular invariant points resulting from the merging of two or more ordinary invariant points. For instance point (B) is here kept as a black point. In the final case where the univariant line contains Ω, there are three cases of line types left.

FIGURE 42

Rules for univariant line portion and adjoining invariant point symbols illustrated on a k = 4 system. a) Portion comprised between points AB and B-C is AB-C. b) After crossing point B-C, next portion is -AB-C; sign of vector A, not included in the definition of point B-C has been changed. c) Next point on the line may be either -A-C or -AB: vector -A must take the place either of B or of -C. Brackets omitted.

FIGURE 43

Two-dimensional stability patterns for k = 3. A two-dimensional domain results from the intersection of three affigraphy (hyper)planes with the (P, T) plane, giving rise to three lines and three invariant points. Depending on the stability levels of the points and lines, eight « *patterns* » are obtained. The stability levels of the two-dimensional domains are indicated on two examples. The corresponding bases (parageneses) are contoured by lines of special type depending on the stability level.

FIGURE 44

Two-dimensional stability patterns in the case k = 4.

Figure 44A The two-dimensional domains result from the intersection of four affigraphy hyperplanes with the (P, T) plane, giving rise to four lines.

Four lines define one closed quadrilateral, two triangles, four open three-sided sectors, three open two-sided sectors and one open four-sided sector (the domains are labelled by « o » or « c » for open or closed, and by a number for the number of lines).

Figure 44B Among the several possibilities to start with, the three apices of one triangle have been chosen to be stable points; each point corresponds to two affigraphy vectors. The stable paragenesis (ABCD) is obtained inside the triangle. The same paragenesis is obtained in the other domains, with other stability levels. The sixteen cases of stability patterns are indicated. They correspond to the different sets of stability levels for the six basic points of the four line, four-dimensional, polyhedric cone. The complete set of absent phase letters with their positive or negative sign in the two-dimensional domains is indicated only for cases 1 and 5; in order to distinguish the stability level for each domain, the letters are surrounded by a frame with a special type of line for each stability level (see caption at the end of figure). In other figures, the stability levels of the domains may be found by considering the stability of the boundering invariant points.

FIGURE 45

Morey-Schreinemakers rule. Assemblage (P_{i1}, P_{i2}), phases P_{i1} and P_{i2} lacking, is bounded by curves (P_{i1}) and (P_{i2}). In the k-dimensional case the n-present (k lacking) phase assemblage (P_{i1}, ..., P_{ik}) is the convex cone bounded by the k affinity vectors (P_{i1})... (P_{ik}).

FIGURE 46

Overlap rule: in the cone containing, or overlapping, (P_j)...(P_k) vectors, corresponding phases P_j ,..., P_k are not absent since they are not involved in the definition of the cone, whatever their sign. So they are present (they are stably present when the negative part of the vector is overlapped). This may be generalized in the k-dimensional frame.

FIGURE 47

180° rule. The vectorial sum of the affinity vectors is equal to zero. So in the case k = 2, no angle in the plane is greater than 180°; in the k-

dimensional case, all vectors are not on the same side of any hyperplane.

FIGURE 48

Univariant scheme. The rule is derived from the properties of **R** matrix. If reaction (A) is written B + C = D + E, (B) and (C) are on one side of (A), and (C) and (D) are on the other. In other words, one does not know exactly where are vectors (C) and (D) but they are on the (A) > 0 side, and the same for (D) and (E) on the (A) < 0 side. The univariant scheme may be generalized to the k-dimensional space. If one chemical reaction reads $A_1 + A_2 + ... = B_1 + B_2 + ...$, the absent phases from the reaction being C_1, C_2, ..., C_{k-1}, then vectors (A_1) (A_2)... lie on one side of hyperplane $\{(C_1)\ (C_2)\ ...\ (C_{k-1})\}$ and vectors (B_1) (B_2) ... lie on the other side. In the case k = 3 of Fig. 20D, reaction (D, F) is written A + C = E + B; (A) and (C) are on one side of (D, F) plane and (E) and (B) on the other.

FIGURE 49

When crossing hyperinvariant point Ω all the signs of the affinity vectors defining the k-dimensional sector (cone) are changed (Table 4).

FIGURE 50

The *fundamental axiom* is illustrated in the case k = 2. (A) and (B) are on both sides of (C). On one side of (C), stable sector is (AC) and singly metastable sector is (C, -B). On the other side, stable sector is (BC) and metastable sector is (-A, C). In terms of present phases, B is stable on one side of (C), sector (AC), where A is metastable (the sector also corresponds to (B, -C)); A is stable on the other side of (C), sector BC, where B is metastable (the sector also corresponds to (-AC)). See also Table 4.

FIGURE 51

Figure 51A: Mirror image rule. The (P,T) plane is obtained by intersecting affigraphy by a two-dimensional plane. The plane may be observed from one side or the other, so the orientation of the co-ordinate

axes in the plane is unknown. This leads to the two mirror image possibilities.

Figure 51B Another « *topological* » rule in the case k = 2 (Hillert, 1985). The number of phases in a domain is given by the number of negative part vectors in the domain. In domain α, zero negative part, n + 2 phases; in domain β_1 and β_2, one negative part, n + 1 phases; in domain γ, two negative parts, n phases.

FIGURE 52

Chemography and affigraphy in the case phase A' is counted as negative. A' = -A of Fig. 6. When compared to Fig. 6, A' is symmetric to A with respect to BC in the chemography (Fig. 52A), and (A') is symmetric to (A) with respect to Ω in the affigraphy (Fig. 52B).

FIGURE 53

Two-dimensional chemography (n = 3) seen as a thermodynamic diagram. The points representing the phases may be seen as invariant points (Fig. 53A) and the labelling of the hyperplanes (here lines, k = 2) emanating from these points is made according to the adjoining phases (Fig. 53B).

Figure 53B « *Reactions* » between absent phases (or « *co-reactions* ») may be read on the chemography. A is on one side of line CE, B and D on the other. So co-reaction CE is (A) = (B) + (D). The affigraphy vectors are reported on both sides of line CE (Fig. 6A). Their position also allows to write the co-reaction. Organization of ordinary reactions around an ordinary invariant point is also portrayed to show the duality between both representations.

FIGURE 54

Stability sequences (or « *co-sequences* ») for the cobases depending on the chemography domains for a 2 + 2 system. The origin of the composition space O is represented. By joining it to the phases A, B, C and D of the chemographic bar, eight composition domains are defined. In some of them (IV to VIII) one or two of the phases of the corresponding paragenesis is in negative amount. For example, in

region V, the following bases are defined: -A-B, -A-C, -A-D, -BC, -BD, -CD; corresponding co-bases are CD^2, BD^2, BC^2, AD^1, AC^1, AB^1 (brackets have been omitted for the co-bases). In each composition sector the possible co-bases are indicated with their stability (or « *co-stability* ») index; the figure in duality to Fig. 27 where the stability of the bases were indicated depending on the affigraphy sector in a 3 + 2 system. For example in sector V, co-bases (B)(C), (C)(D) and (D)(B) have co-stability index equal to 2 and co-bases (B)(A), (A)(D) and (A)(C) have co-stability index equal to 1. The co-stability indices are decided according to the signs of the phases in the different composition sectors.

FIGURE 55
Degenerate system, n = 2, k = 2; chemography (55A) and affigraphy (55B). B and D coincide on the same side of A and C, so (A) and (C) coincide stable to metastable.

FIGURE 56
Degenerate system, n = 2, k = 2; chemography (56A) and affigraphy (56B); C and D coincide and A and B are on opposite sides of CD, so (A) and (B) coincide stable to stable.

FIGURE 57
Degenerate system, n = 2, k = 3; chemography (57A), affigraphy (57B). A and B coincide. So (C), (D) and (E) are coplanar. In order to represent a possible phase diagram, an intersection of the affigraphy by a two-dimensional plane is given (Fig. 57C). C, D and E are on the same side of A and B, so the sequence of point stability levels (C), (D), (E) on degenerate univariant line (CDE) is of the alternate type: stable (C) - metastable (-D) - stable (E).

FIGURE 58
Doubly degenerate system, n = 3, k = 3; chemography (58A), affigraphy (58B). B, D and E coincide, so (A), (C) and (F) are doubly coplanar, i.e. colinear. Since indifferent phases A, C, F are on the same side of degenerate phases, all affinity vectors (A), (C) and (F) have not the same direction. On the two-dimensional intersection of the affigraphy

(Fig. 58C), coincident invariant points (A), (C) and (-F) have not the same stability level.

FIGURE 59

Doubly degenerate system, n = 3, k = 3; chemography (59A), affigraphy (59B). B and D coincide, so as E and F; (A) and (C) coincide stable to stable and they belong to the intersection of plane (EF) and plane (BD). The intersection of the affigraphy by a two-dimensional plane (Fig. 59C) gives another representation of this situation.

FIGURE 60

Doubly degenerate system, n = 3, k = 2; chemography (60A) and affigraphy (60B). Phases A, D and C are colinear so as phases C, B and E. (A) and (D) coincide stable to metastable, so as (B) and (E). In Fig. 60B only the stable portions of the reactions are represented.

FIGURE 61

Chemography and affigraphy in the case with solid solution for a 3 + 2 system; *Figure 61A*: chemography; D_a phase, counted for one, possess solution from D_0 to D_1 represented by a portion of solid line. *Figure 61B*: affigraphy; (A) and (B) vectors are variable according to solution parameter a; for a = ½ phases $D_{1/2}$, C and E are colinear (case of degeneracy) and so ($A_{1/2}$) and ($B_{1/2}$) coincide (« singular » situation). Because the indifferent phases A and B are on opposite sides of C, $D_{1/2}$, E, the coincidence of ($A_{1/2}$) and ($B_{1/2}$) is stable to stable.

FIGURE 62

Chemography and affigraphy in the case with solid solution for a 3 + 3 system. Chemography (62A); solution D is represented by its end members D_0 and D_1 and is counted for two phases. This is another representation of Fig. 61 system. Affigraphy (Fig. 62B) is now three-dimensional. The projection of affigraphy in the plane (D_0) (D_1) perpendicular to (E) (Fig. 62C) better shows the symmetry of the system with respect to (CE) reduced to (C). Vector ($D_{1/2}$) that can be constructed in intermediate position between (D_0) and (D_1) will be coplanar to (C) and (E). In Fig. 62D, relations between neighbouring Fig. 62C invariant

points are represented when the composition parameter has several values i-δi, i, i + δi, i + 2δi. Additional reactions (A), (B) and (C) are represented only at the invariant point $P_{i-\delta i,i}$. When δi goes to zero, these reaction vanish. The collection of stable invariant points P define the enveloppe for reaction R (Fig. 62E). Individual reactions for values of a equal to i and j are straight lines R_i and R_j tangent to R in P_i and P_j. Away from points P_i and P_j, lines R_i and R_j have an infinity of stability levels and an infinity of metastable invariant points that cannot be represented.

FIGURE 63

Chemography and affigraphy in the case with solid solution for a 2 + 2 system or equivalent (depending on the choice to represent the solution) 2 + 3 system. Chemography (63A). Solution C_a may alternatively be represented as solid line between C_0 and C_1 or by the two end members C_0 and C_1. Affigraphy (k = 2 representation, Fig. 63B). (A) and (B) vectors are variable according to solution parameter a. For a = 0 C_0 coincides with A; D and B are on the same side of degenerate phases so the indifferent phase affigraphy vectors (D) and (B_0) coincide stable to metastable. Figure 63C: affigraphy, k = 3 representation. (D), (B) and (C_1) are coplanar. Figure 63D: intersection of Fig. 63C affigraphy by a two-dimensional plane. Line (DC_1) is singular line common to all chemical reactions (BC) and (CD). It connects the two singular points (B) and (D).

FIGURE 64

Synthesis of the different mathematical - thermodynamic spaces of interest. Orthogonal n- and k- dimensional spaces are artificially represented by perpendicular two-dimensional planes in order the relations between the different spaces are clearly understood.

Figure 64A Composition and related spaces

The (n + k)-dimensional composition modal space is generated by the unit vectors P_1, ..., P_{n+k} representing each of the n + k phases. Closed system constraint imposes the total composition **x** of the system verifies $\mathbf{C.x} = \mathbf{C.x_0} = \underline{\mathbf{c}}$. This defines k-dimensional variety V; $\mathbf{x_0}$ is the initial

composition, chosen as the origin in V. Inside V, the initial composition is fixed and **x** variable becomes $\xi = \mathbf{x} - \mathbf{x}_0$. The unit composition vectors taken by groups of n + k - 1 define basic hyperplanes that give boundaries to the V variety; this defines admissible reaction space, intersection of positive orthant with V. Constraint $\mathbf{C}.\mathbf{x} = 0$ defines V_0 containing the origin O. Optimal (equilibrium) $\mathbf{x}^*$ will be a point at the border, generally an apex, of reaction space V where k of the co-ordinates will be zero and n non-zero.

Variety perpendicular to V and containting the origin is named W_0. It is n-dimensional; its equation is $\mathbf{R}.\mathbf{x} = 0$. The projection of total composition **x** onto W_0 is constant. It is $\underline{\mathbf{c}}$, which is also simply the intersection of W_0 and V. The projections of the unit n + k vectors onto W_0 give the structure of chemography. Space W is parallel to W_0 and contains initial composition x_0; its equation is $\mathbf{R}.\mathbf{x} = \mathbf{R}.\mathbf{x}_0$. In the figure, the points **x**, $\mathbf{x}_0$, $\mathbf{x}^*$ and $\underline{\mathbf{c}}$ are represented on the same line in order to show they have the same projection $\underline{\mathbf{c}}$ in W_0. Actually they simply belong to the same space, all points of which project in $\underline{\mathbf{c}}$ (including the optimal solution $\mathbf{x}^*$). When $\mathbf{x}_0$ is varied, the optimum composition $\mathbf{x}^*$ also varies and describes an n-dimensional space corresponding to the n non-zero coordinates of the corresponding basis of n-dimensional composition space.

Once a basis is chosen to represent the composition of the system, a specific writing for composition matrix **C** is derived, as well as a total composition $\underline{\mathbf{c}}$, corresponding to a specific $\mathbf{x}_0$. This choice fixes the definition of all spaces used. **R** is the reaction matrix corresponding to **C**.

Chemography may be cut by two-dimensional planes to simulate systems with two inert components, the others being mobile. This kind of diagram could be represented by a line inside W_0 like (P,T) in affigraphy, Fig. 64B.

Figure 64B. Total affinity and related spaces.

The n + k dimensional total affinity space is generated by the unit vectors (P_1), ..., (P_{n+k}) for each of the n + k phases. The constraint that the intensive conditions on the system are fixed (k conditions in $\underline{\boldsymbol{a}}$), imposes that the total affinity $\boldsymbol{A}$ of the system verifies $\mathbf{R}.\boldsymbol{A}^T = \mathbf{R}.\boldsymbol{A}^T_0 = \underline{\mathbf{a}}^T$; this defines an n-dimensional variety V'; $\boldsymbol{A}_0$ is the initial affinity vector chosen as the origin in V'. Admissible (stable) potential space is limited

to the positive orthant; the basic hyperplanes defined by sets of n + k - 1 unit vectors give boundaries on the V' variety; the limit may be called « *saturation surface* » (intersection of positive orthant with V'). Constraint $\mathbf{R}.\boldsymbol{A}^T = 0$ defines V'_0 containing the origin Ω. The optimum equilibrium affinity $\boldsymbol{A}^*$ will be a border, generally an apex, of the saturation potential surface. For this point k co-ordinates are non-zero and n are zero.

The variety perpendicular to V' and containting the origin Ω is named W'_0. It is k-dimensional; its equation is $\mathbf{C}.\boldsymbol{A}^T = 0$. The projection of total affinity $\boldsymbol{A}$ onto W'_0 is constant. It is $\underline{\boldsymbol{a}}$, which is also simply the intersection of W'_0 and V'. The points $\boldsymbol{A}$, $\boldsymbol{A}_0$ and $\underline{\boldsymbol{a}}$ are represented on the same line in order to show they have the same projection $\underline{\boldsymbol{a}}$ in W'_0. Actually they simply belong to the same space, all points of which project in $\underline{\boldsymbol{a}}$ (including the optimal solution $\boldsymbol{A}^*$).

The projections of the unit n + k vectors onto W'_0 give the structure of affigraphy. Space W' is parallel to W'_0 and contains initial affinity $\boldsymbol{A}_0$; the equation is $\mathbf{C}.\boldsymbol{A}^T = \mathbf{C}.\boldsymbol{A}^T_0$. Inside affigraphy, physical $\underline{\boldsymbol{a}}$ belongs to a two-dimensional plane (P, T) here represented as a line. Chemical potential surface belongs to space V' perpendicular to space W'_0 that contains (P,T); it thus corresponds to fixed values of P and T. So the affinity variables become potential in V' thanks to $\mu = g(P, T) - A$. When $\boldsymbol{A}_0$ is varied, the optimum composition $\boldsymbol{A}^*$ also varies and describes a k-dimensional space corresponding to the k non-zero coordinates of the corresponding co-basis of k-dimensional affinity space.

Chemical potential grid corresponds to the same situation as the (P, T) plane and results from the intersection of affigraphy by a plane.

FIGURE 65

Different associated n + k -, n -, and k - dimensional diagrams illustrated for a n = 1, k = 2 system (three phases A, B and C).

Figure 65A: modal space. The quantities of the three phases in the system define the three co-ordinate axes. Pure A, B and C phases are represented as unit vectors on the three axes. The positivity constraints $x_A, x_B, x_C \geq 0$ limit the permitted modal space to the positive orthant. Linear variety (plane) V represents the closed system constraint ($\mathbf{Cx} = 1$;

total quantity is one for simplicity). V_0 is plane parallel to V and containing the origin ($\mathbf{Cx} = 0$). x_0 is the initial content of the phases in the system ($\mathbf{Cx} = \mathbf{Cx_0} = \underline{\mathbf{c}} = 1$ = constant). W is the linear variety (here a line) perpendicular to V and containing x_0. W_0 is parallel to W in O. Line BC corresponding to the absence of A is labelled (A) and similarly for lines AC = (B) and AB = (C). W_0 cuts V in point M limiting a line portion OM whose length is $\sqrt{3}/3$; OM corresponds to vector $\underline{\mathbf{c}}$ closed system composition.

Figure 65B. Reaction space, obtained by the intersection of variety V with the positive orthant (variable x), or equivalently by the intersection of V_0 with the constraints $\xi \geq - x_0$ (variable ξ). The origin corresponds to x_0 in Fig. 65A and the co-ordinate axes to the extent of independent reactions $\xi_B = x_B - x_{0B}$ and $\xi_C = x_C - x_{0C}$. It is bounded by the lines (A), (B) and (C) representing complete resorption of phases A, B and C. Unit vectors of modal space perpendicular to basic hyperplanes (here lines) may also be represented in reaction space; they are perpendicular to the basic phase resorption lines.

Figure 65C. Chemography, obtained by projecting the basic vectors of modal space onto W_0. One independent chemical parameter is chosen: x_A. The three unit phases A, B and C project in the same point together with the initial composition x_0 and the total content of the independent chemical component expressed in A content, $\underline{\mathbf{c}}$. The region at the left of origin O ($x_A < 0$) is forbidden in the stable representation.

Figure 65D. Total affinity space. The basic dissociation affinities A^A, A^B, A^C of the three phases are represented along the three co-ordinate axes. Along each basic plane, phases A, B and C are present respectively since $A = 0$, i.e. $\mu = g$. Along each basic vector, two phases are present and the third, corresponding to the axis A of the same name, is lacking. Inside the positive orthant, the phases are absent, their dissociation affinities are strictly positive. The linear variety V' $\mathbf{R}.\boldsymbol{A}^T = \mathbf{R}\boldsymbol{A_0}^T = \underline{\boldsymbol{a}}^T$ containing vector $\boldsymbol{A_0}$ is represented; two independent reaction affinities are specified and V' is a line; W'_0 is perpendicular to it and contains the origin Ω. The total affinity of the system remains in V' and the projection

$\underline{a}$ on W'_0 is constant. W' is perpendicular to V' and contains $\boldsymbol{A}_0$ and V'_0 is perpendicular to W' and contains Ω.

Figure 65E: affigraphy. Projection of the three unit affinity vectors onto plane W'_0, parallel to V'. Total affinity $\boldsymbol{A}$ and initial affinity $\boldsymbol{A}_0$ project in the same point $\underline{a}$ in the affigraphy. When the total affinity is in Ω three phases coexist. When it is along the basic affinity vectors, two phases coexist, one is lacking; when it is in the sectors bounded by pairs of affinity vectors one phase is present, two lacking.

Figure 65F: chemical potential saturation space. This space is obtained by intersecting V' with the basic affinity (hyper)planes. At point O (face A of the cube) saturation in phase A is obtained. Points $<A^{(A)}>$, $<A^{(B)}>$ and $<A^{(C)}>$ (unit affinities) project at the same point together with A_0.

Figure 65G: reaction space combined with affigraphy. The admissible directions of affinity vectors are reported. For instance, along the A phase missing boundary, vector A_{tot} in the basis $A^{(B)}$ $A^{(C)}$ must be perpendicular to the boundary according to the direction indicated. This property corresponds to the fact that the basic affinity vectors are orthogonal to the hyperplanes representing the dissociation of the phases in reaction space.

FIGURE 66

Different associated (n + k) -, n -, and k - dimensional diagrams illustrated for a n = 2, k = 1 system (three phases A, B and C). The definitions of the varieties and of the geometrical operations are virtually the same as in Fig. 65 to which one may report for more detailed captions.

Figure 66A: modal space. Space V is here a line (closed system constraint), space W is a plane. It is limited by the positive orthant.

Figure 66B: reaction space. Intersection of V with the positive orthant. There is one independent chemical reaction. The dissociation of A has

been chosen. Space is limited on one side by the complete consumption of the phase and on the other by its precipitation in quantity x_0.

Figure 66C: chemography, vectorial and affine representation. The projections of the three unitary basic composition vectors onto W_0 are represented. The affine representation is obtained by intersecting the vectors by a line, yielding three points.

Figure 66D: total chemical potential space. Space W' is a plane, space V' is a line. $\boldsymbol{A}_0$ is the initial total affinity vector.

Figure 66E: affigraphy; projection of the three unit affigraphy vectors $A^{(A)}$, $A^{(B)}$, $A^{(C)}$ onto line V'_0 parallel to W'. $\boldsymbol{A}_0$ is also projected. In the affine representation the vectors coincide in one point corresponding to two positive and one negative part (or two negative one positive).

Figure 66F: chemical potential space in affinity and in chemical potential form. This space is obtained by the intersection of W' with the affinity orthant.

FIGURE 67

Combined (n + k)-dimensional space associating chemography and affigraphy. Example of a 2 + 2 system. Chemography is represented along the horizontal axis (four phases A, B, C, D); affine representation gains one dimension. Three composition domains are defined. Affigraphy is represented in the vertical plane (four vectors (A), (B), (C), (D)). Four affinity sectors are defined. By extending the composition domains and affinity sectors to the whole space,12 cells are defined. 10 are represented (for simplification, the metastable cells are not represented). The corresponding stable parageneses are indicated inside each of the ten stable cells.

FIGURE 68

Figure 68A Perspective representation of planes P_1 and P_2 in the chemography + affigraphy space of Fig. 67. Resulting intersecting diagrams are represented in subsequent figures.

Figure 68B Intersecting affinity - composition diagram corresponding to plane P_1 in Fig. 68A. Composition is represented along the horizontal axis (phases A, B, C, D), affinity or chemical potential along the vertical axis (affinity vectors (-A), (-B), (C), (D)). Three stable cells are defined. Stable parageneses are represented in the plane. Only phases A and B are stable in the whole composition range.

Figure 68C

Intersecting affinity - composition diagram corresponding to plane P_2 in Fig. 68A. Same caption as in Fig. 68B; stable parageneses are indicated. In the cell defined by composition range AC and potential range (-C) (B) the metastable associations are also indicated.

FIGURE 69

Composition - temperature diagram for a solid solution with one two-phase (liquid + solid) spindle-shaped domain bounded by liquidus and solidus curves. An understanding of the diagram by use of pseudocompounds and affigraphy approach may be given. Composition is fractionnated into several pseudocompounds i, j, k and so on. The system is degenerate in that each pseudocompound is two phase, solid and liquid. Temperature axis represents a combination of basic affinities and is also fractionnated in several domains because of the reactions between all pseudocompounds. All the cells in the diagram are two phase domains; corresponding written associations are more stable than all other possible pairs of phases (pseudocompounds) defining the same global composition. The horizontal lines represent (n + 2) four-phases invariant points at fixed temperature; because of the high degree of degeneracy each horizontal line actually represents a superposition of many such lines. The different degenerate reactions are of the type solid = liquid or $j^l = j^s$ and so on for the different pseudocompounds. The vertical lines are co-reactions defined by one present phase (n - 1 phase with n = 2); their writing in terms of absent phases would require a very large number of absent phase vectors. In terms of stable associations of phases, the co-reactions correspond to the change of an association of the type $i^s + m^l$ to one of the type $m^l + n^l$ simply written $i^s \rightarrow n^l$ when the

composition of the system crosses m pseudocompound composition; co-reaction equivalently corresponds to the change from a two solid association to an one solid + one liquid phase association when the composition of the system crosses the composition of a pseudocompounds. The same co-reaction may involve other pseudocompounds in higher metastability level associations.

TABLE 1

		List of bases with their stability indices for chemography regions whose numbers are:						
cobases for affigraphy region I	*corresponding bases*	1	2	3	4	5	6	7
A-B	CDE^{1}				CDE^{1}			
A-C	BDE^{1}						BDE^{1}	BDE^{1}
-AD	BCE^{1}		BCE^{1}		BCE^{1}		BCE^{1}	BCE^{1}
-A-E	BCD^{2}		BCD^{2}					
-BC	ADE^{1}					ADE^{1}		ADE^{1}
-BD	ACE^{1}	ACE^{1}						
-B-E	ACD^{2}	ACD^{2}			ACD^{2}	ACD^{2}		ACD^{2}
-CD	ABE^{1}			ABE^{1}		ABE^{1}		
-C-E	ABD^{2}			ABD^{2}			ABD^{2}	
DE	ABC^{0}	ABC^{0}	ABC^{0}	ABC^{0}	ABC^{0}	ABC^{0}	ABC^{0}	ABC^{0}

TABLE 2

	POINTS			LINES		DOMAINS	
value of k	*number of invariant points per univar. line*	*number of affinity vectors per inv. point*	*number of inv. point stability levels*	*number of affinity vectors per univ. line*	*number of univ. line stability levels*	*number of affinity vectors per domain*	*number of domain stability levels*
k	k - 1	k - 2	k - 1	k - 1	k	k	k + 1
2	1	0	1	1	2	2	3
3	2	1	2	2	3	3	4
4	3	2	3	3	4	4	5
5	4	3	4	4	5	5	6

TABLE 3

succession number (= number of univariant line)	*affinity vectors for point 1*	*affinity vectors for point 2*	*affinity vectors for point 3*	*affinity vectors for point 4*
1	AB-C	ABD	BCD	-ACD
2	-AB-C	-ABD	BCD	ACD
3	A-B-C	A-BD	-BCD	-ACD
4	ABC	ABD	B-CD	-A-CD
5	AB-C	AB-D	BC-D	-AC-D
6	-A-B-C	-A-BD	-BCD	ACD
7	-ABC	-ABD	B-CD	A-CD
8	-AB-C	-AB-D	BC-D	AC-D
9	A-BC	A-BD	-B-CD	-A-CD
10	A-B-C	A-B-D	-BC-D	-AC-D
11	ABC	AB-D	B-C-D	-A-C-D
12	-A-BC	-A-BD	-B-CD	A-CD
13	-A-B-C	-A-B-D	-BC-D	AC-D
14	A-BC	A-B-D	-B-C-D	-A-C-D
15	-ABC	-AB-D	B-C-D	A-C-D
16	-A-BC	-A-B-D	-B-C-D	A-C-D

TABLE 4

		Dimension of the intersected variety					
		0 (point)	*1 (vector)*	*2*	...	*k - 2*	*k - 1 (hyperplane)*
dimension of the intersec-ting variety	*1 (vector)*	1 vector changes..	2 vectors change...	3 vectors change	...	k - 1	k vector change...
	2	2	1	2	...	k - 2	k - 1
	...	...	...	...	...	...	...
	k - 2	k - 2	k - 3	k - 4	...	2	3
	k - 1 (hyperpl.)	k - 1	k - 2	k - 3	...	1	2
	k (domain)	k vectors change	k - 1 vect. change	k - 2 vect change	...	2	1 vector changes

TABLE 5

geometric duality

	A **Chemography** dim. n $\underline{c}$, **x** **C.x** = $\underline{c}$	**I** substitution of some $\underline{x}_j$ to some $\underline{\mu}^j$ composite ($\underline{x}$, $\underline{\mu}$) diagram dim.n	**B** **Chemical potential saturation space** dim. n $\underline{\mu}$, **g** $\underline{\mu}$.**C** ≤ **g**
combinatorial duality	**IV** dim. n + k or less (proj. / sections) integrated $\underline{x}$ + $\underline{A}$ (or $\underline{c}$ + $\underline{a}$)diagram	**V** dim. n + k $\underline{x}$ + $\underline{\xi}$ (or ξ / **x**: total adv./ total comp. (modal) space) **VI** $\underline{A}$ + $\underline{\mu}$ (or ***A*** / **μ**: total aff./ total chem. pot. space)	**III** dim. n + k or less (proj. / sections) integrated $\underline{\mu}$ + $\underline{\xi}$ diagram
	C **Affigraphy** dim. k $\underline{a}$, ***A*** **R.*A*** ^{T} = $\underline{a}^T$	**II** substitution of some $\underline{A}^j$ to some $\underline{\xi}_j$ composite ($\underline{A}$, $\underline{\xi}$) diagram dim. k	**D** **Reaction space** dim. k $\underline{\xi}$, $\mathbf{x_0}$ $\underline{\xi}^T$ **.R** ≥ - $\mathbf{x_0}^T$

TABLE 6

P1 Find x $(n + k)$: Min gx $Cx = \underline{c}$ $x \geq 0$ $\underline{c}$ (n) and g $(n+k)$ are known	Find x $(n + k)$ and $\underline{\mu}$ (k): $Cx = c$ $\underline{\mu}C \leq g$ $(g - \underline{\mu}C)x = 0$ $x \geq 0$ (μ)	**P1*** Find $\underline{\mu}$ (k) Max $\underline{\mu}\underline{c}$ $\underline{\mu}C \leq g$ (μ) c (n) and g $(n + k)$ are known	exclusion relations $(g - \underline{\mu}C)x = 0$
P2 Find A $(n+k)$ Min $A.x_0$ $R.A^T = \underline{a}^T$ $A \geq 0$ $\underline{a}$ (k) and x_0 $(n+k)$ are known	Find A $(n + k)$ and $\underline{\xi}$ (k) $RA^T = \underline{a}^T$ $A \geq 0$ $\underline{\xi}^T.R \geq - x_0^T$ $A.(x_0 + R^T.\underline{\xi}) = 0$ (ξ)	**P2*** Find $\underline{\xi}$ (k): Max $\underline{a}.\underline{\xi}$ $\underline{\xi}^T.R \geq - x_0^T$ (ξ) $\underline{a}$ (k) and x_0 $(n + k)$ are known	exclusion relations $A.(x_0 + R^T.\underline{\xi}) = 0$

TABLE 7

nature of varieties	***Nature of geometrical operation in (n + k)-dimensional space***	
	projection of basic vectors	*intersection of varieties with basic co-ordinate hyperplanes*
dimension k V	vectors $\perp$ to hyperplanes of reaction space	reaction space
W'_0	affigraphy	« *complementary* » chemical potential space
dimension n W_0	chemography	« *complementary* » reaction space
V'	vectors $\perp$ to hyperplanes of chemical potential saturation space	chemical potential saturation space

TABLE 8

Nomenclature of different « *solutions* » of phase diagrams

symbol	**name**	**nature of informations available dimension of space**
α_j	combinatorially possible affigraphy n° i	number of components and phases; dimension k
θ_{ij}	combinatorially possible solution n° i for affigraphy n° j	number of components and phases; dimension 2
Θ	total number of combinatorially possible solutions for all combinatorially possible affigraphies	number of components and phases; dimension 2
δ_j	mathematically possible affigraphy n°j	number of components and phases; thermo-mathematical structure; dimension k
π_{ij}	mathematically possible solution n° i for affigraphy n°j	number of components and phases; thermo-mathematical structure; dimension 2
Π	number of mathematically possible solutions for all chemographic arrangements	number of components and phases; thermo-mathematical structure; dimension 2
δ_0 δ_0^*	unique affigraphy for specified composition 0 affigraphy in case of generalized composition (with negative phases...)	number of components and phases; thermo-mathematical structure; composition; dimension k
π_{i0} π_{i0}^*	potential solution n° i for affigraphy δ_0 in case of generalized composition	number of components and phases; thermo-mathematical structure; composition; dimension 2
Π_0	number of potential solutions for composition 0	number of components and phases; thermo-mathematical structure; composition; dimension 2
ν_{li0}	isoclinal variant n° l for potential solution n° i corresponding to composition 0	number of components and phases, composition, molar volumes and entropies; dimension 2
γ_0	unique physical solution for composition 0	all informations: number of components and phases, composition, free energies; dimension 2

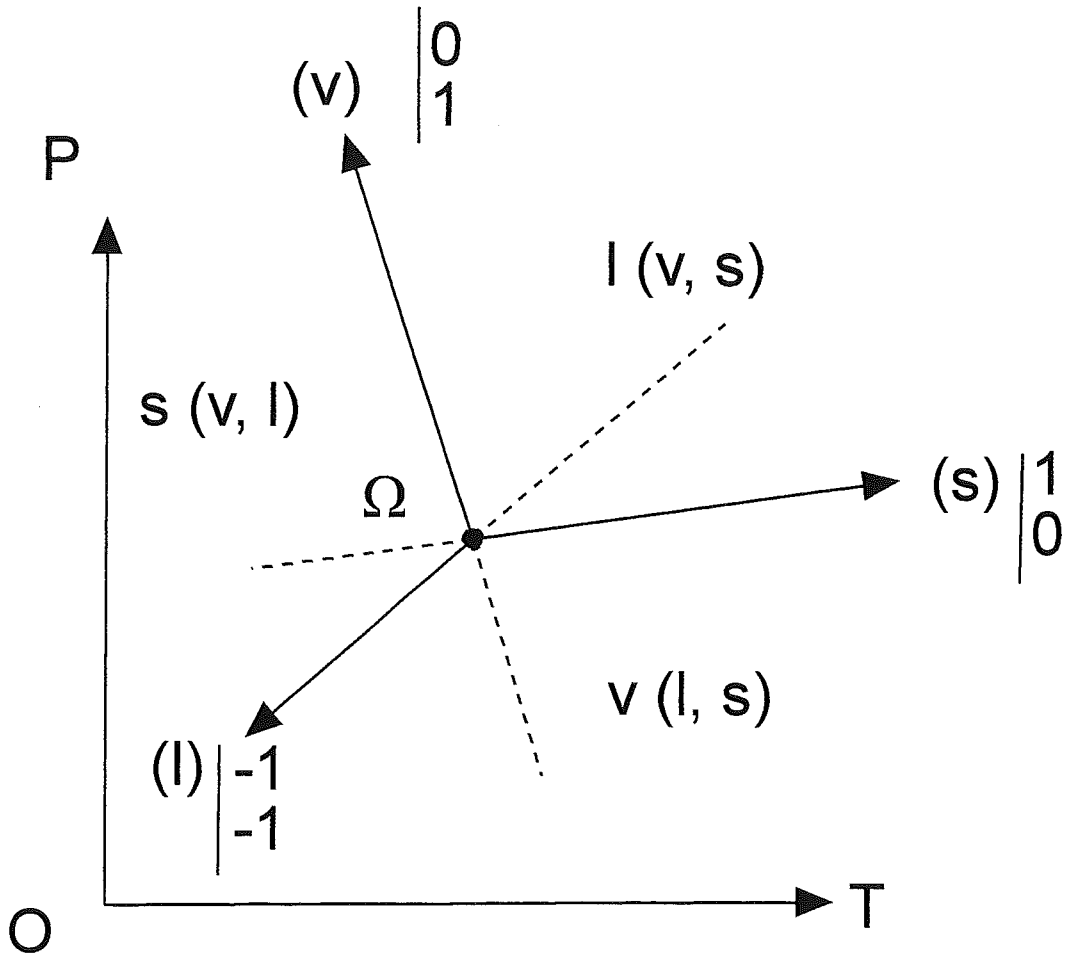

Fig. 1A

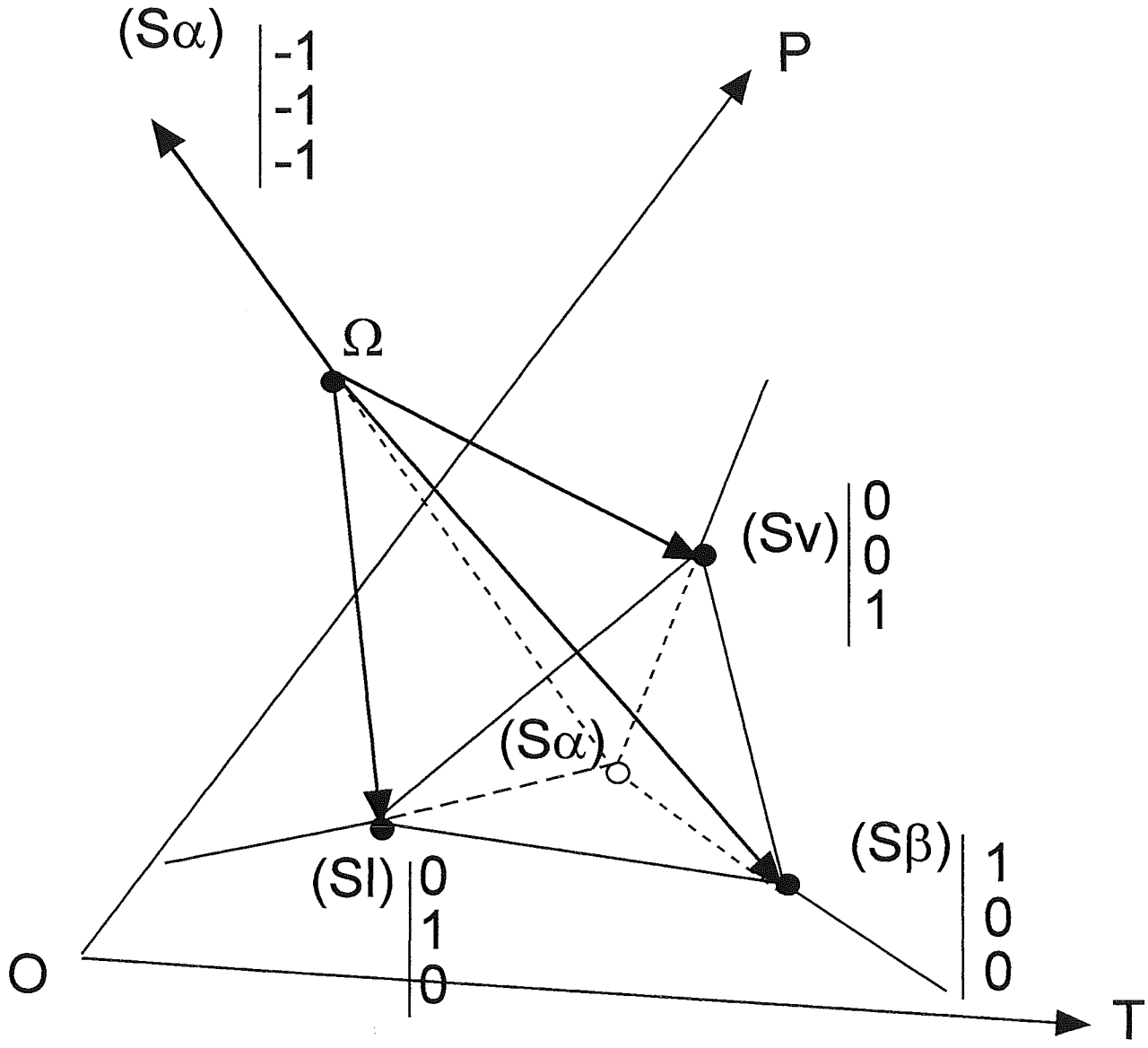

Fig. 1B

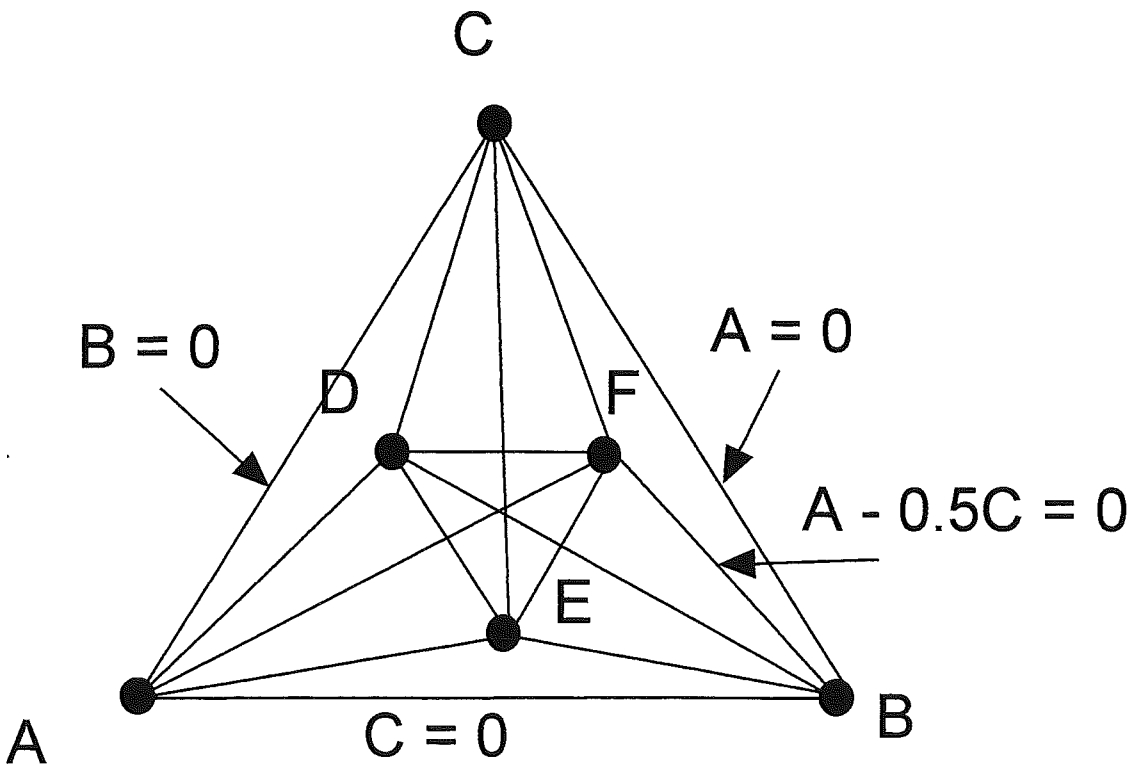

Fig. 2

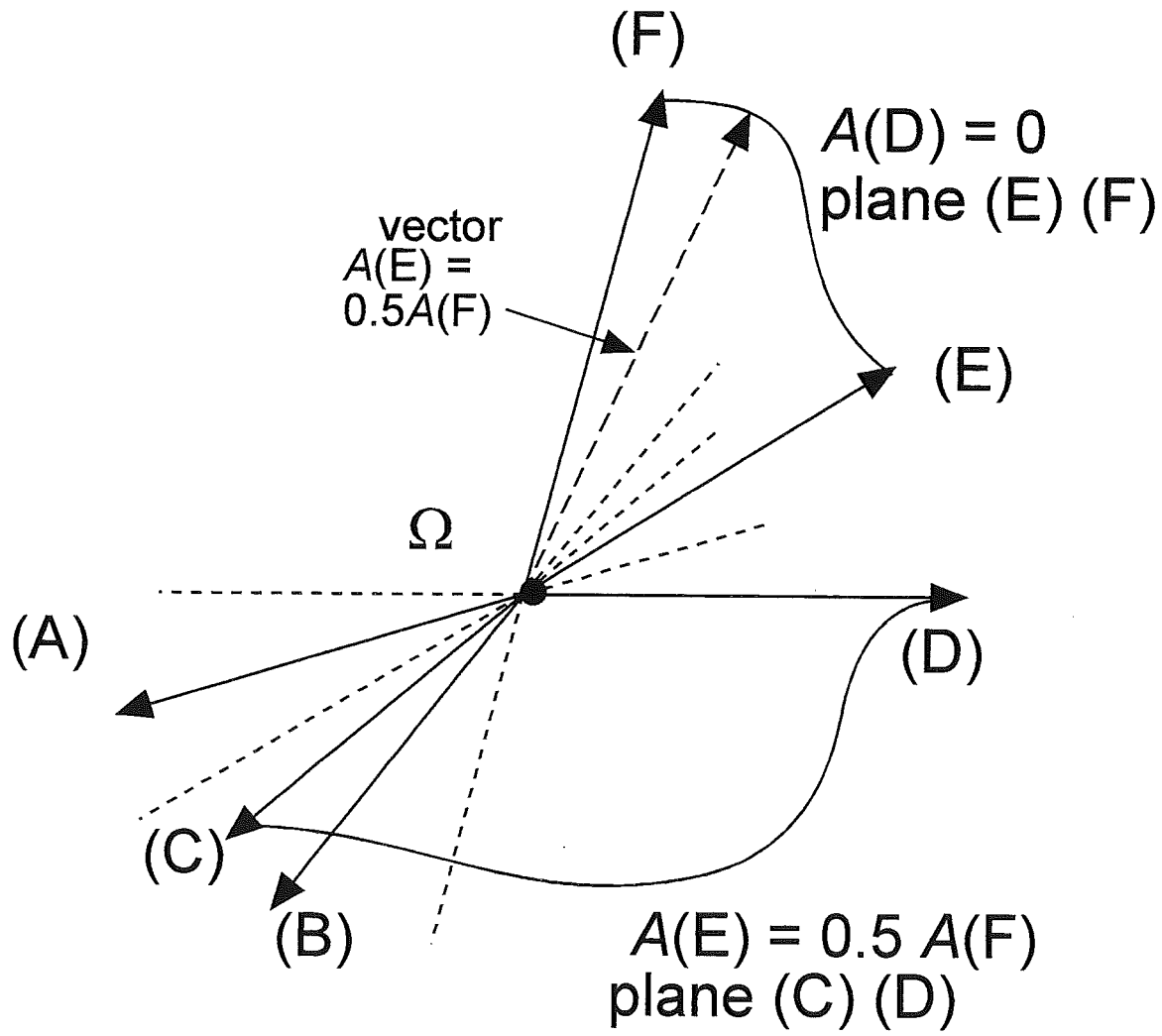

Fig. 3

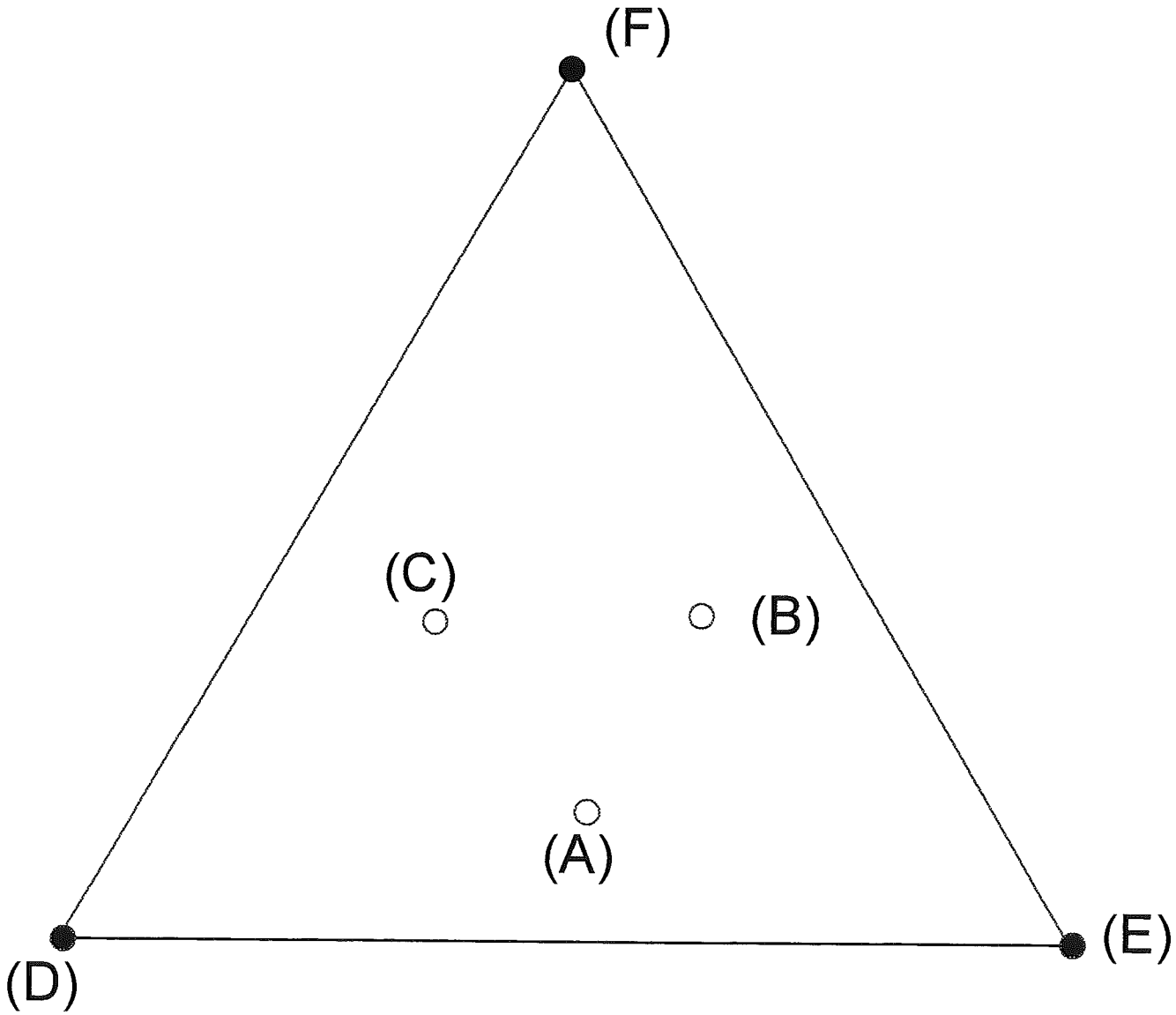

Fig. 4A

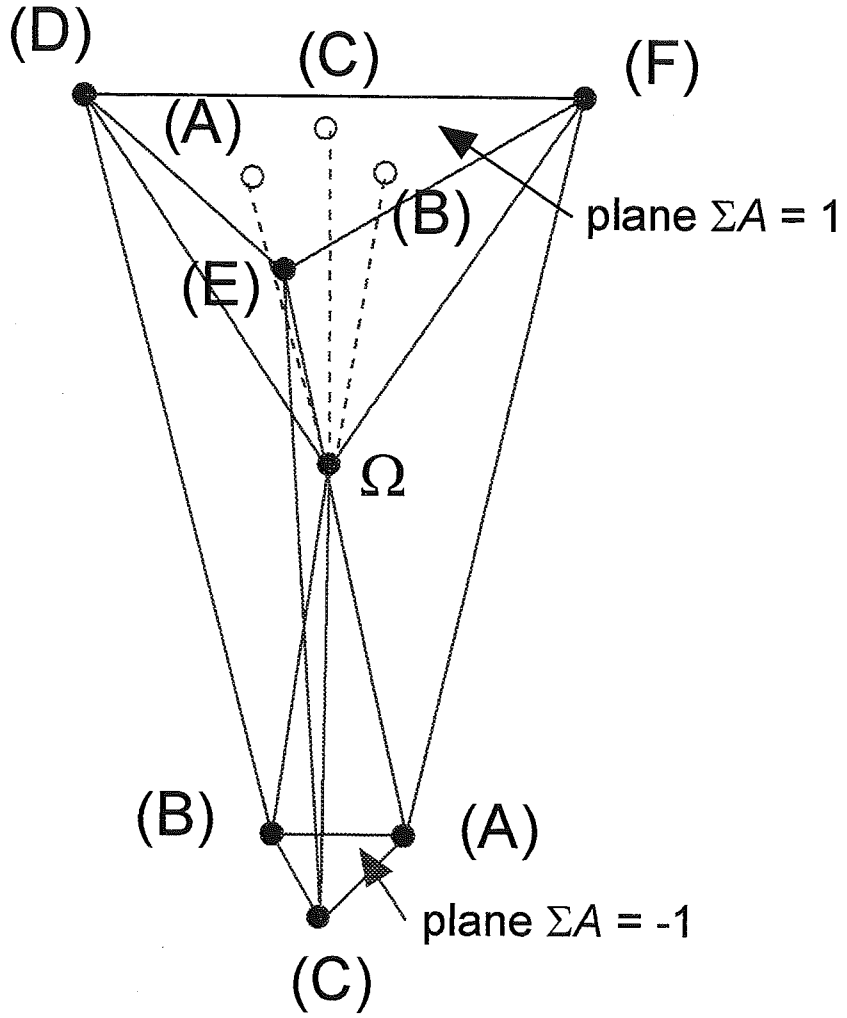

Fig. 4B

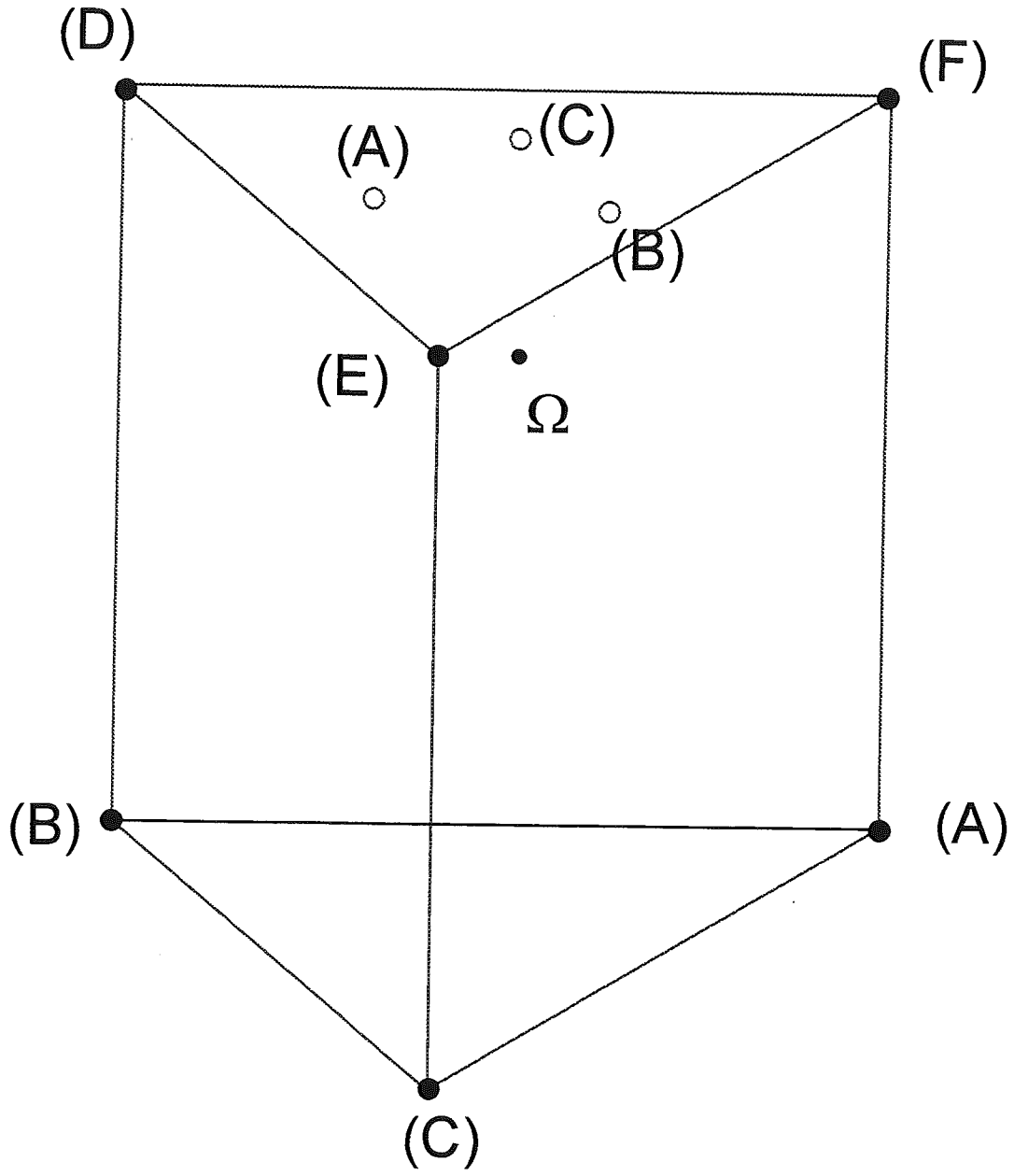

FIG 4C

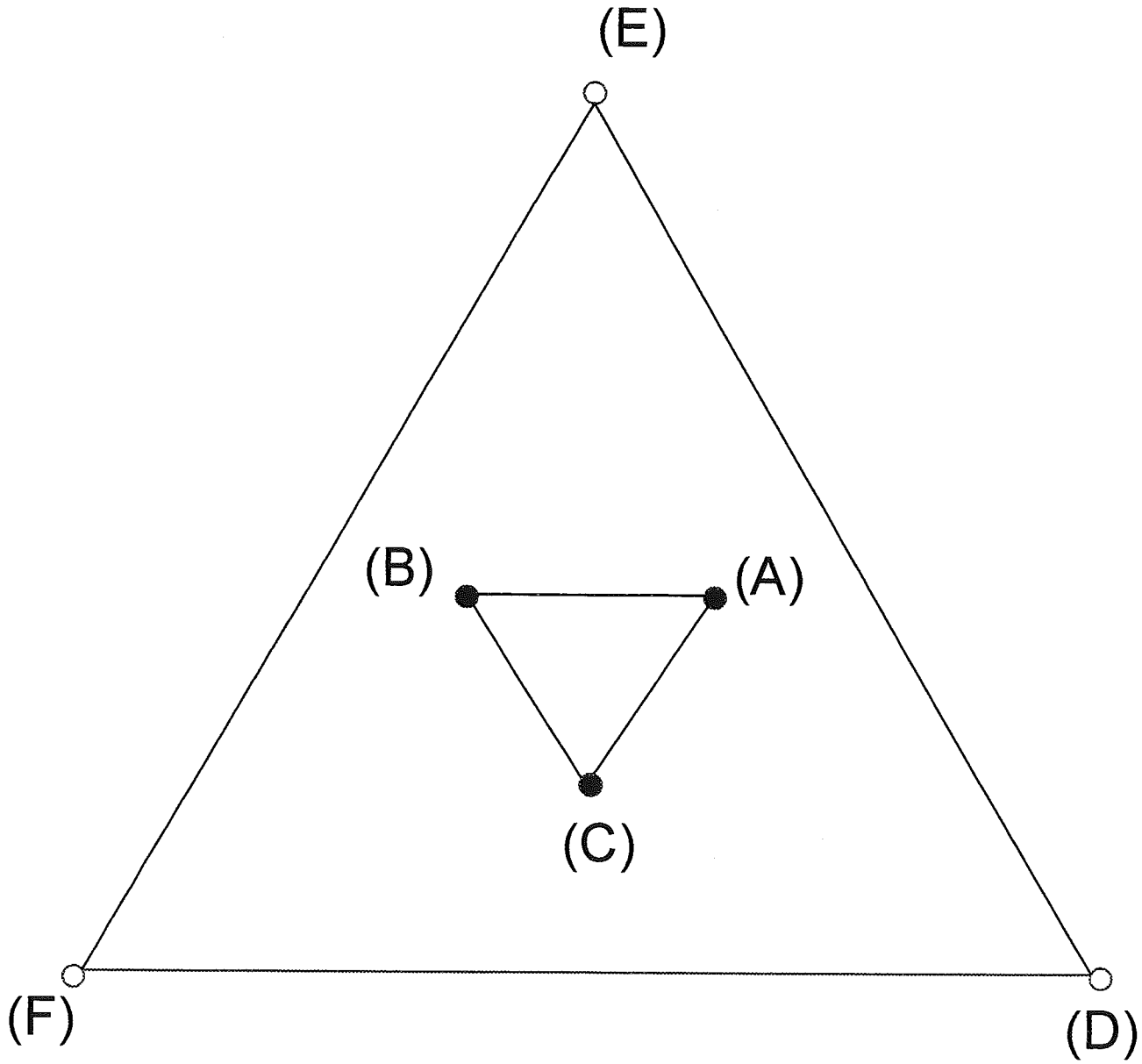

Fig. 4D

A

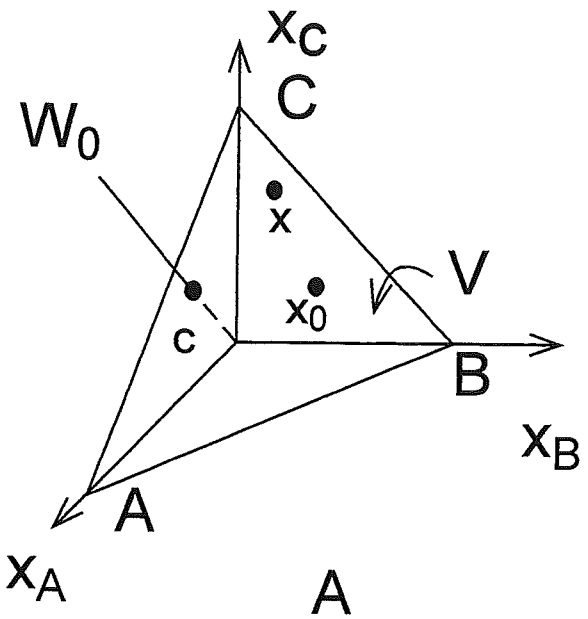

B

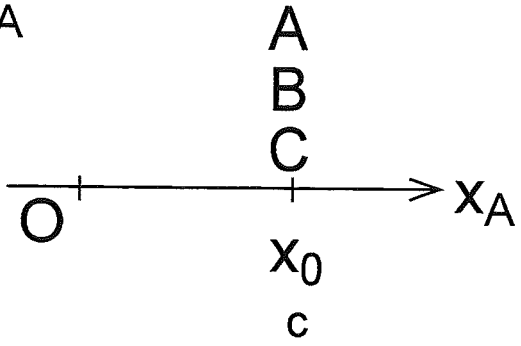

C

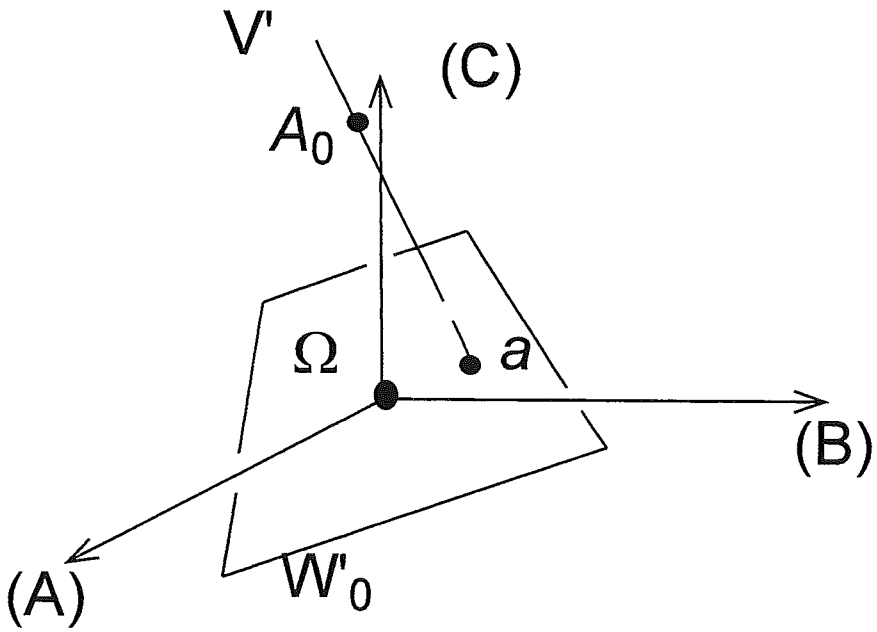

D

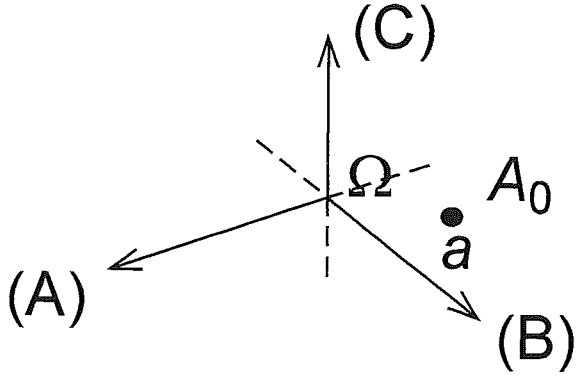

Fig. 5

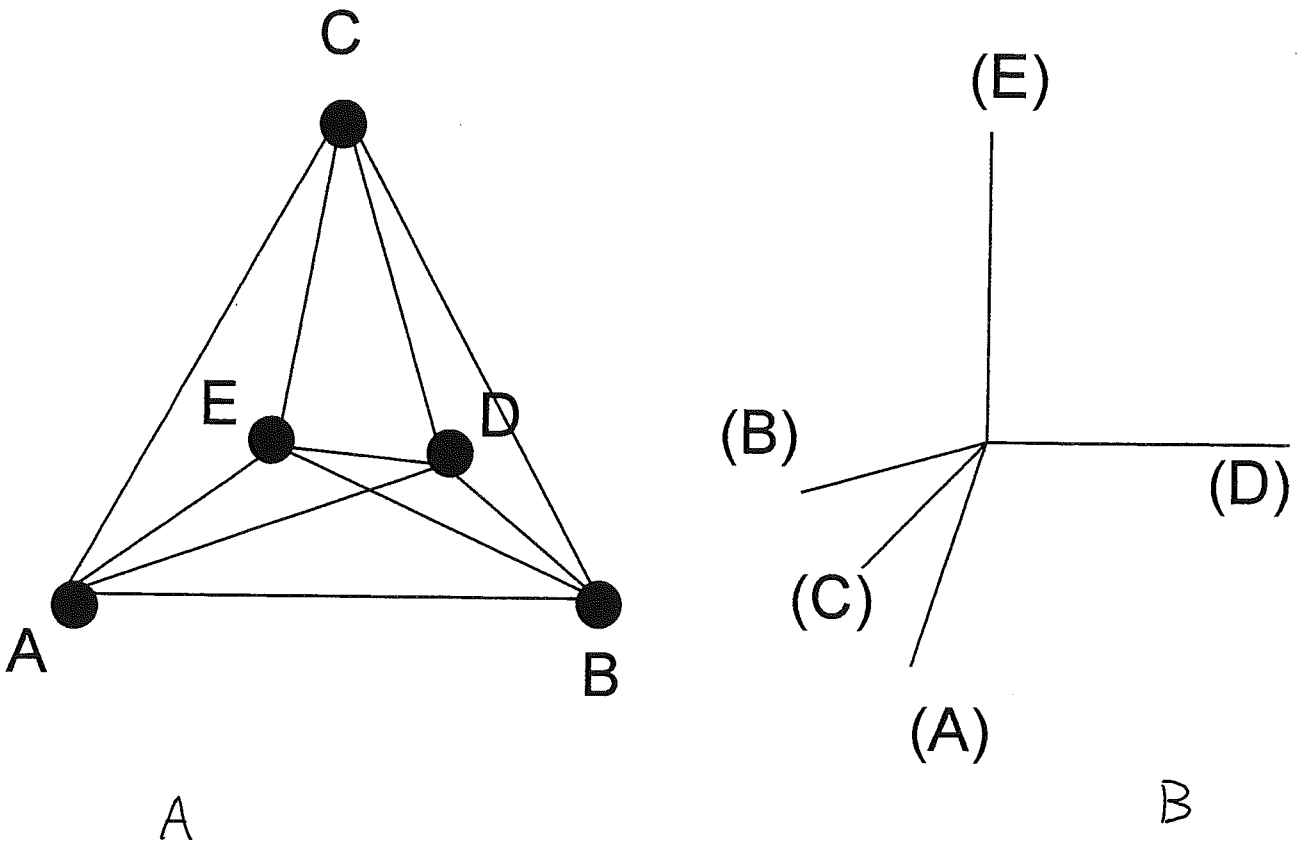

A B

Fig. 6

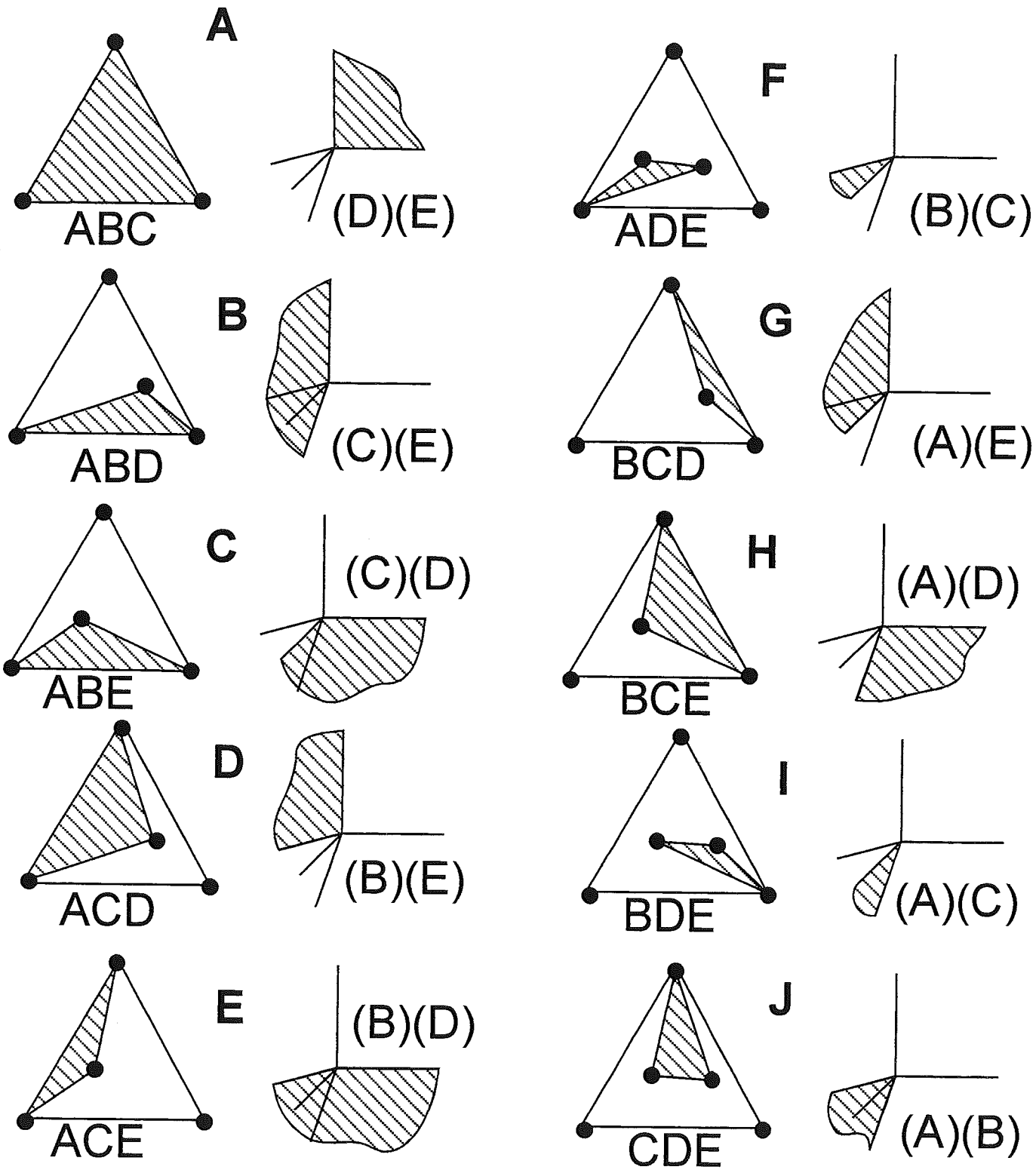
A
ABC
(D)(E)
B
ABD
(C)(E)
C
ABE
(C)(D)
D
ACD
(B)(E)
E
ACE
(B)(D)
F
ADE
(B)(C)
G
BCD
(A)(E)
H
BCE
(A)(D)
I
BDE
(A)(C)
J
CDE
(A)(B)

Fig. 7

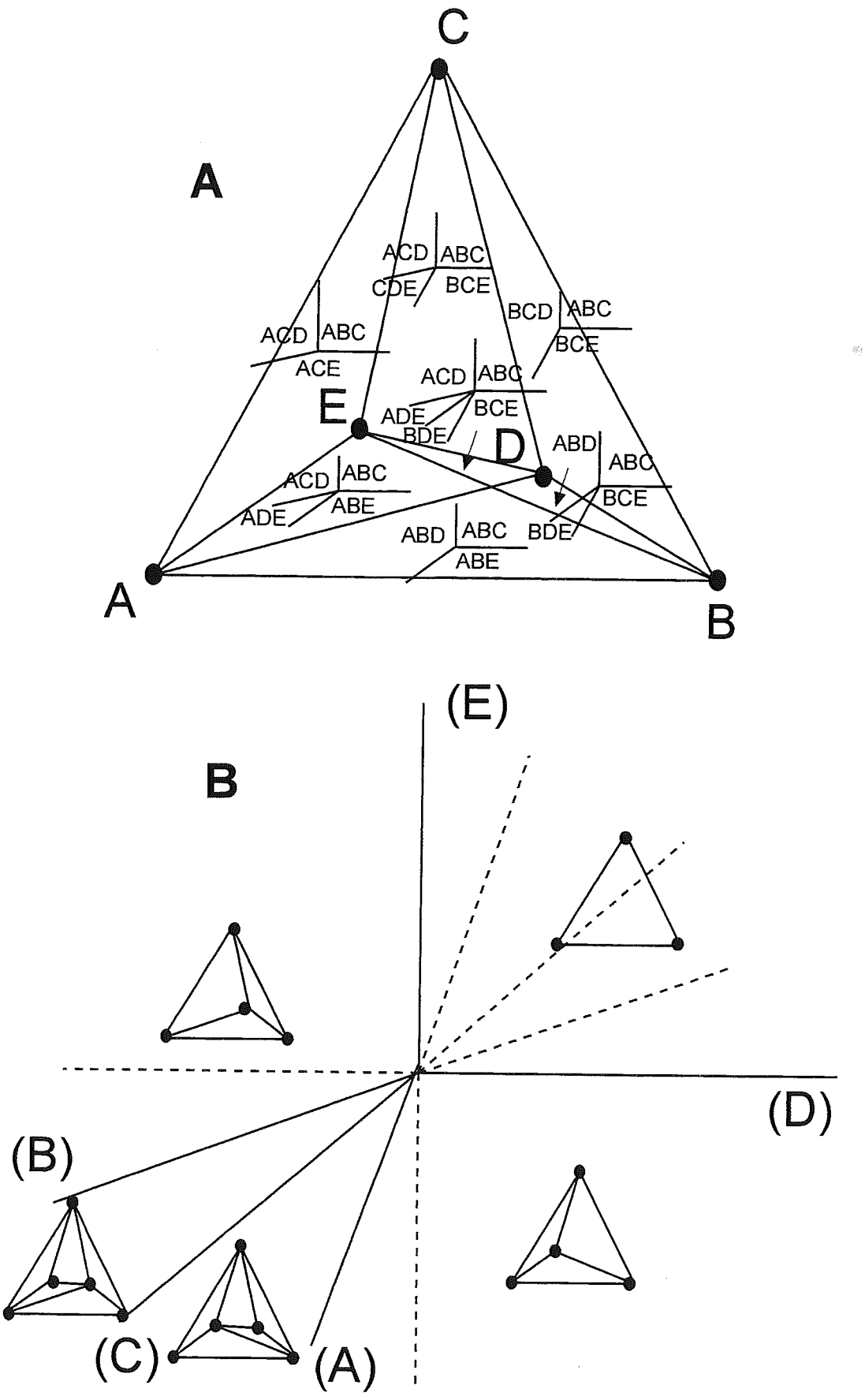
C
A
ACD
ABC
CDE
BCE
BCD
ABC
BCE
ACD
ABC
ACE
ACD
ABC
E
ADE
BCE
BDE
D
ABD
ABC
ACD
ABC
BCE
ADE
ABE
ABD
ABC
BDE
ABE
A
B
(E)
B
(D)
(B)
(C)
(A)

Fig. 8

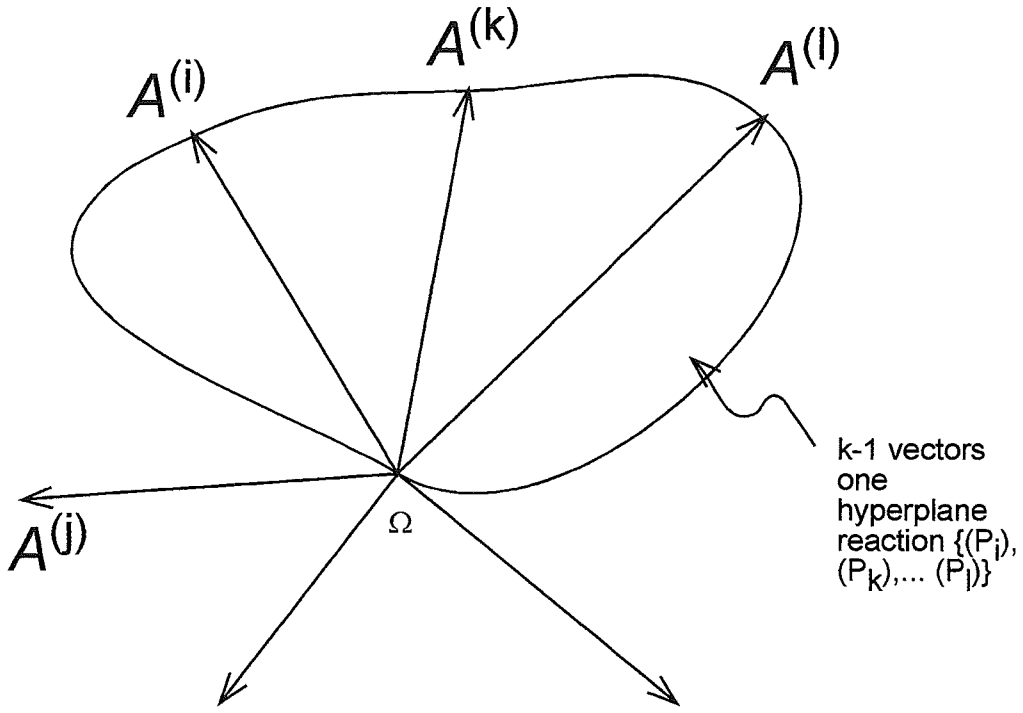

Fig. 9

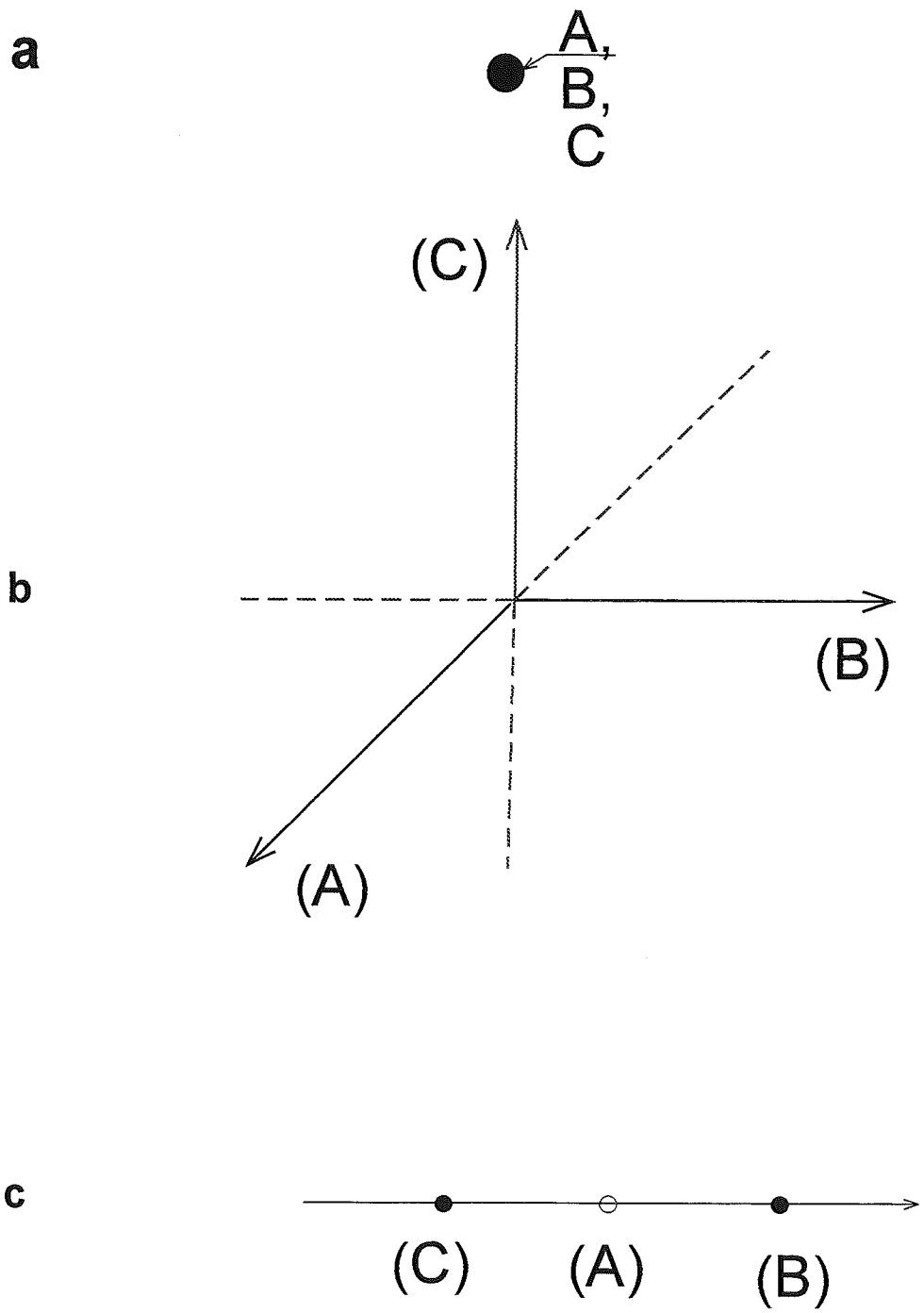

Fig. 10

A

B

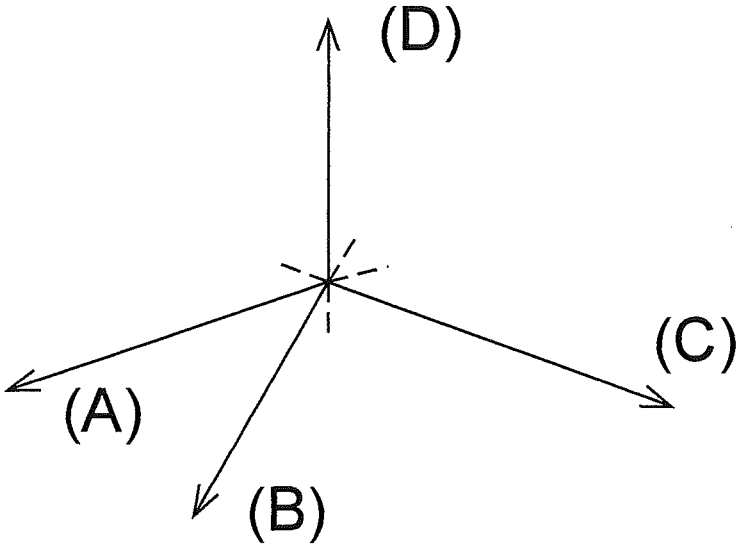

C

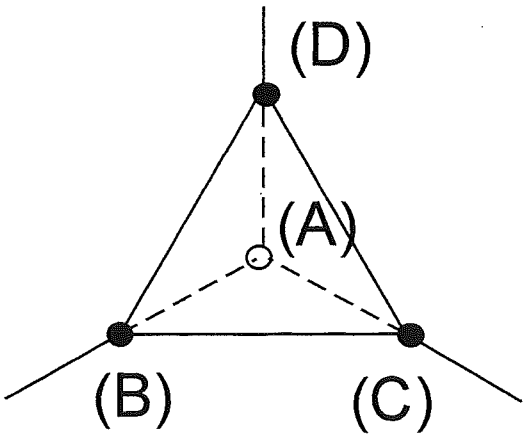

Fig. 11

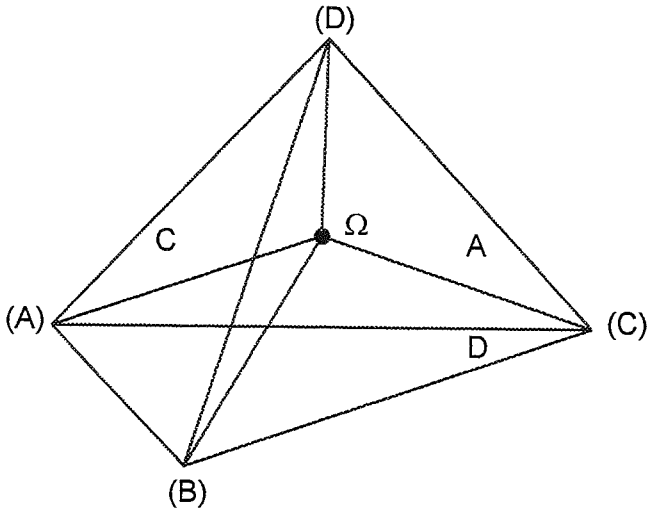

Fig. 11D

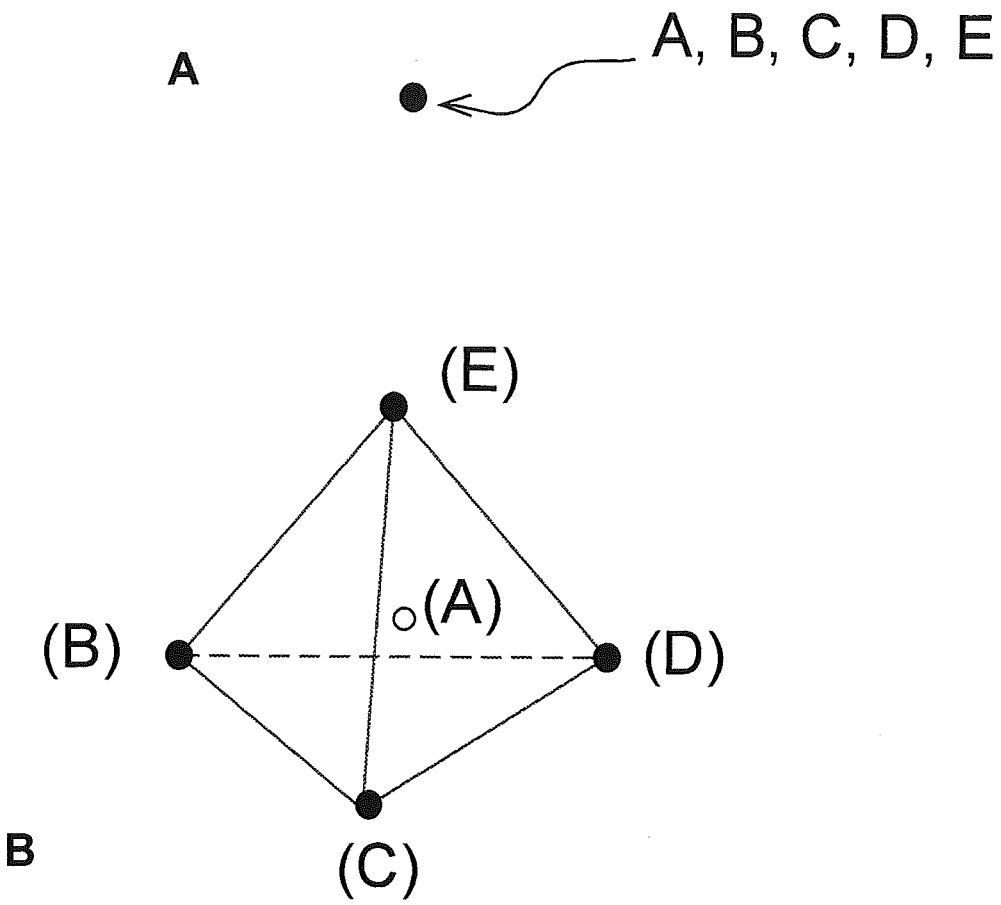

Fig. 12

A

B

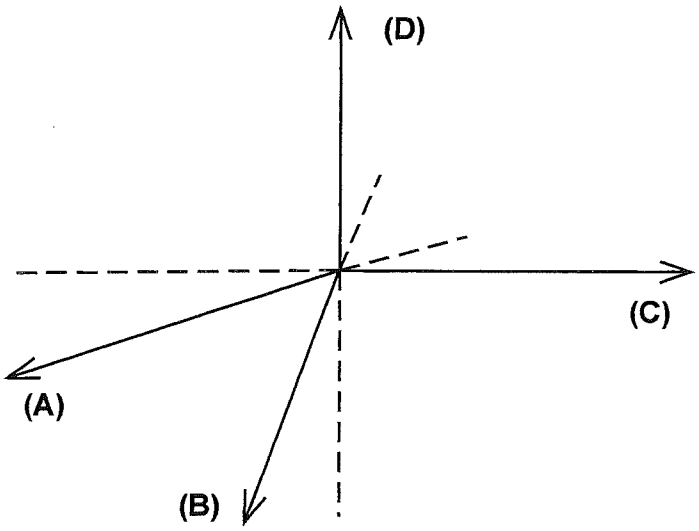

C

Fig. 13

A

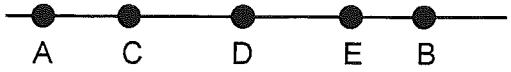

B

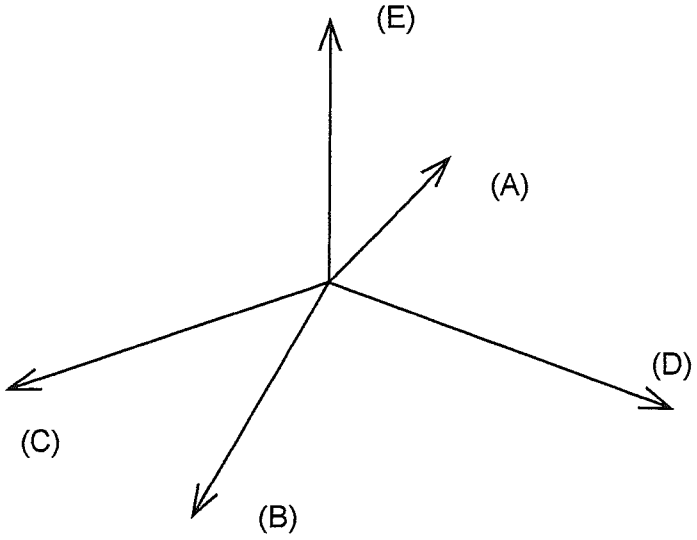

C

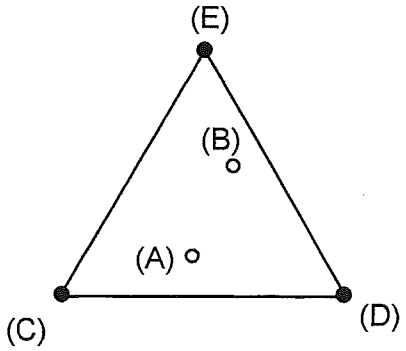

Fig. 14

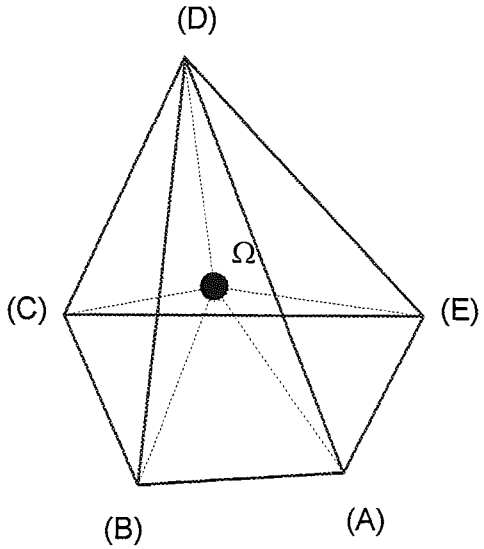

Fig. 14 D

A

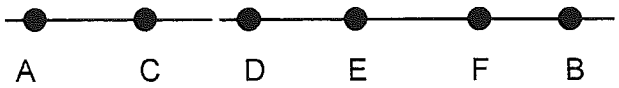

B

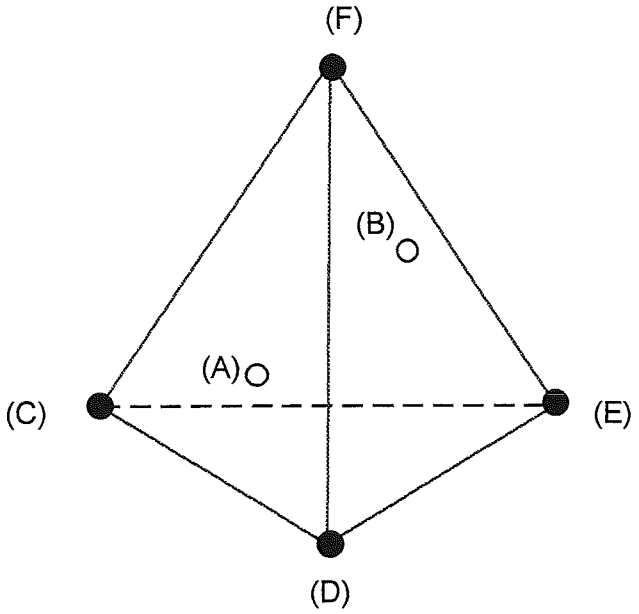

Fig. 15

B

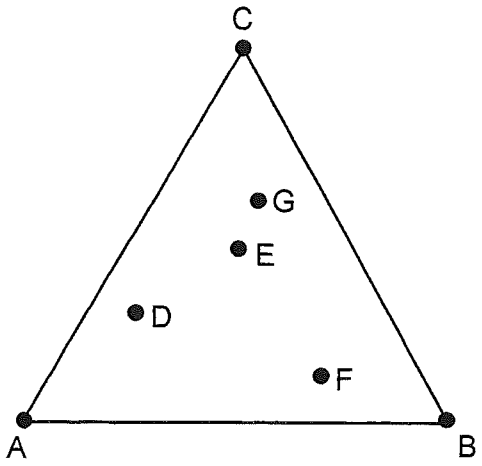

A

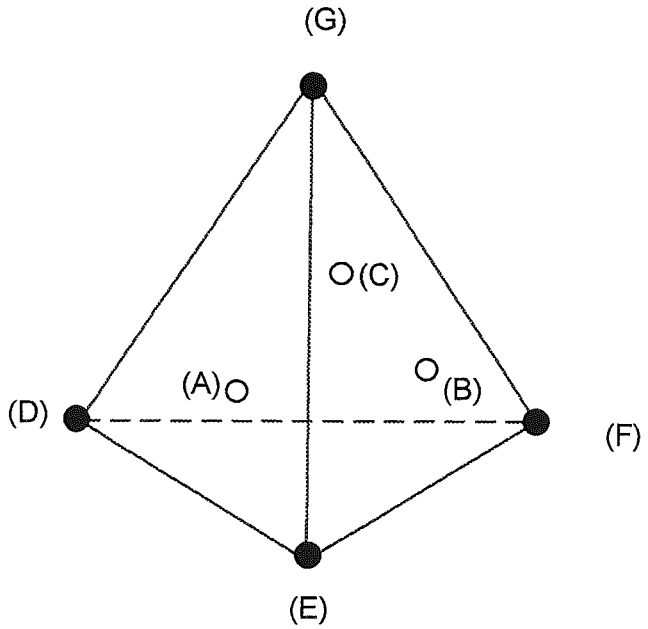

Fig. 16

A

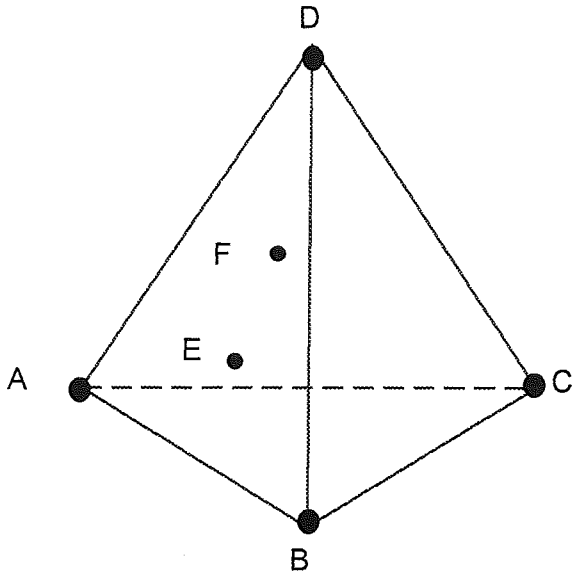

B

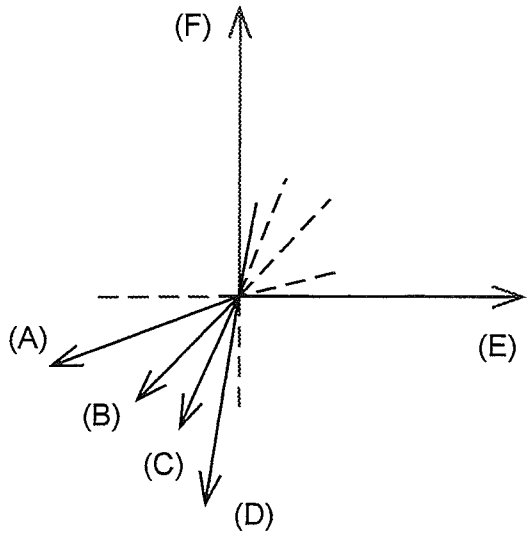

C

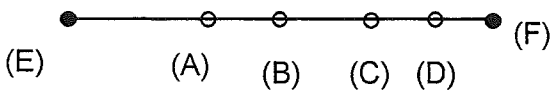

Fig. 17

A

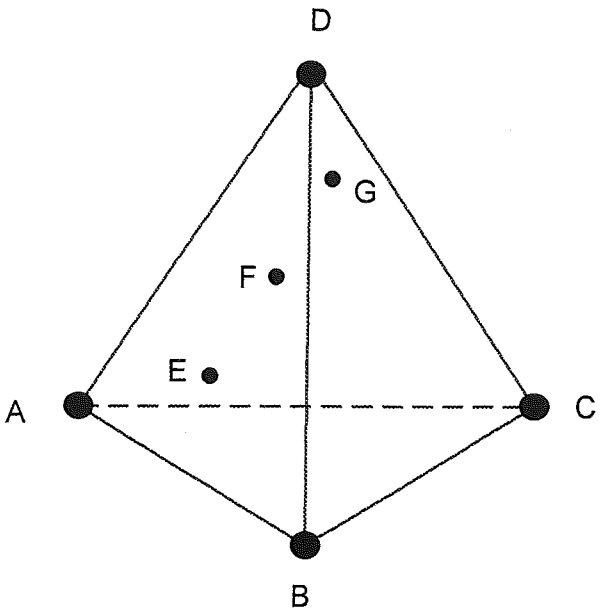

B

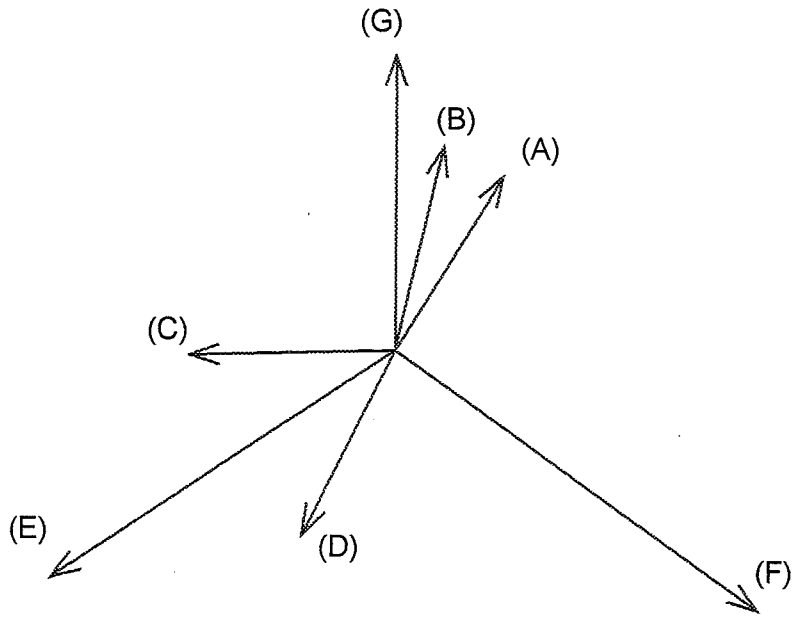

C

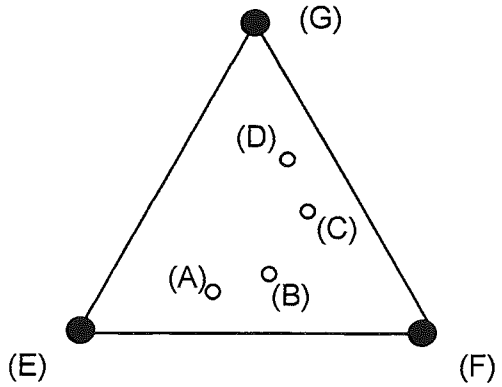

Fig. 18

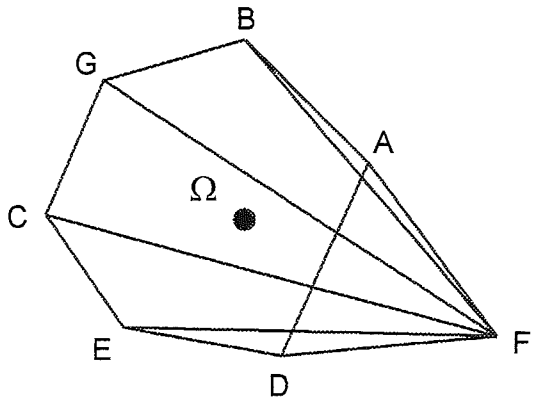

Fig. 18 D

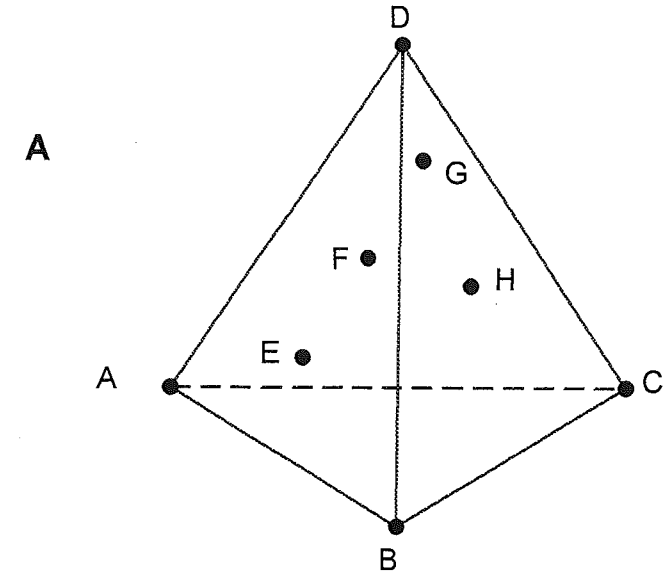

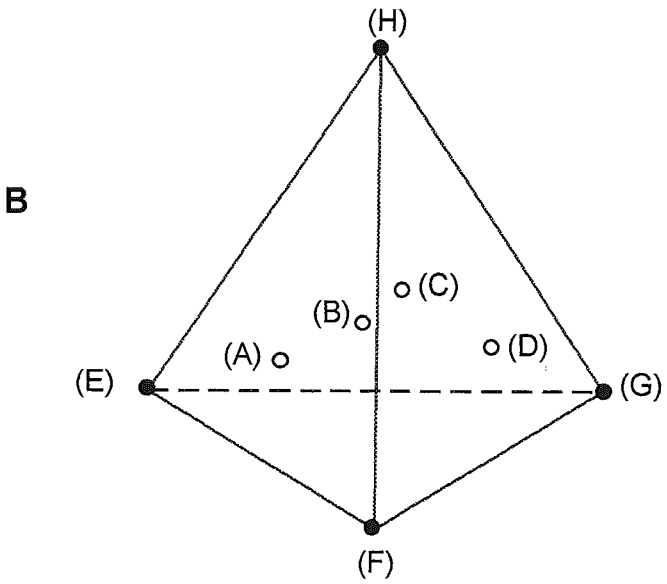

Fig. 19

A

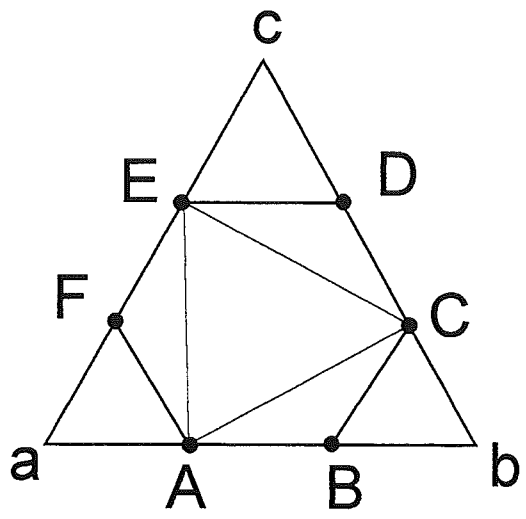

B

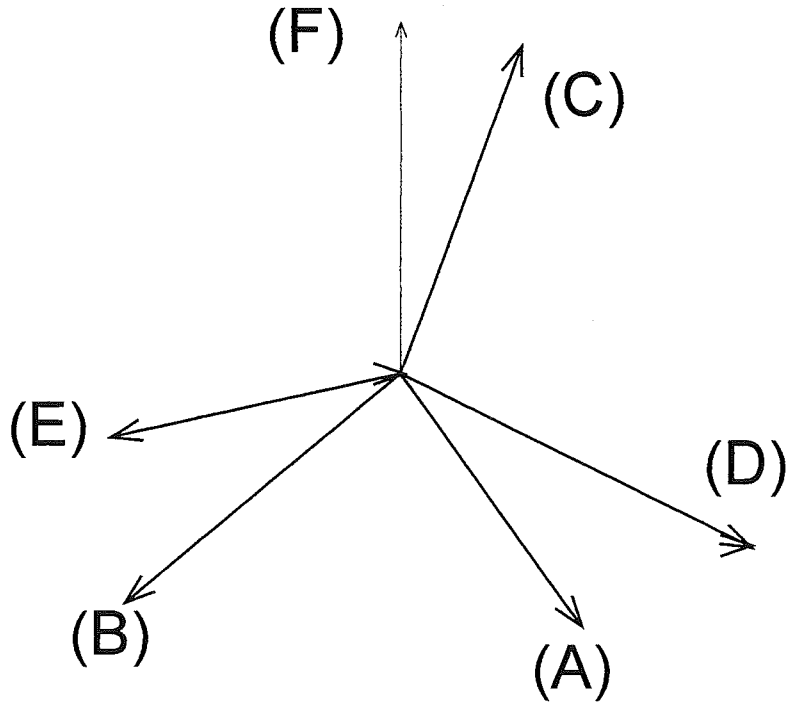

C

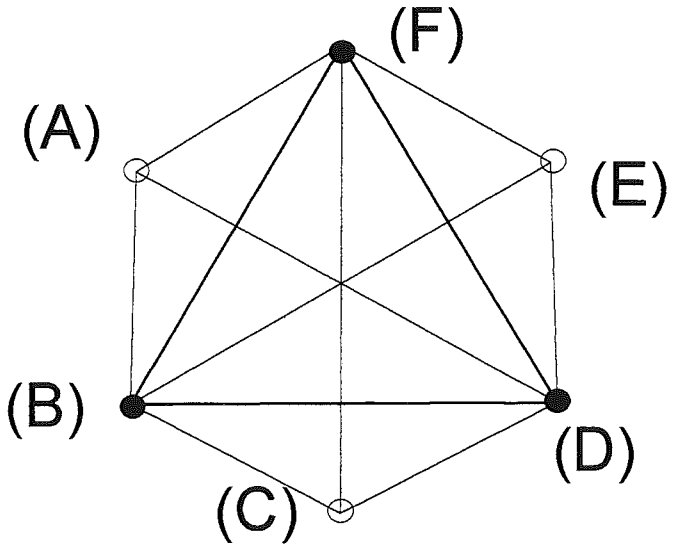

Fig. 20

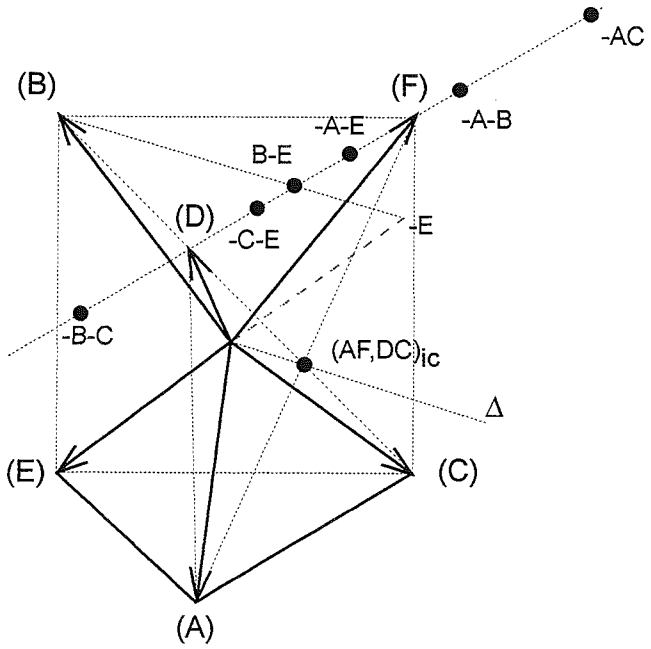

Fig. 20 D

A

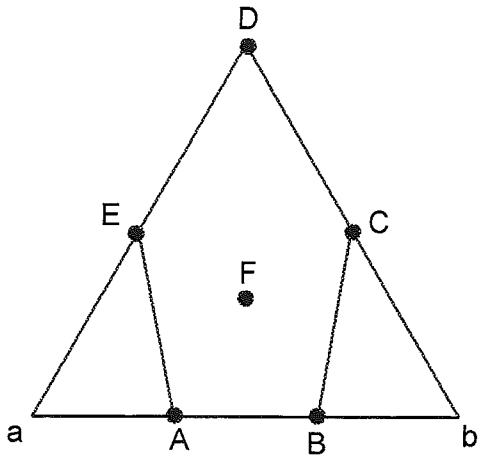

B

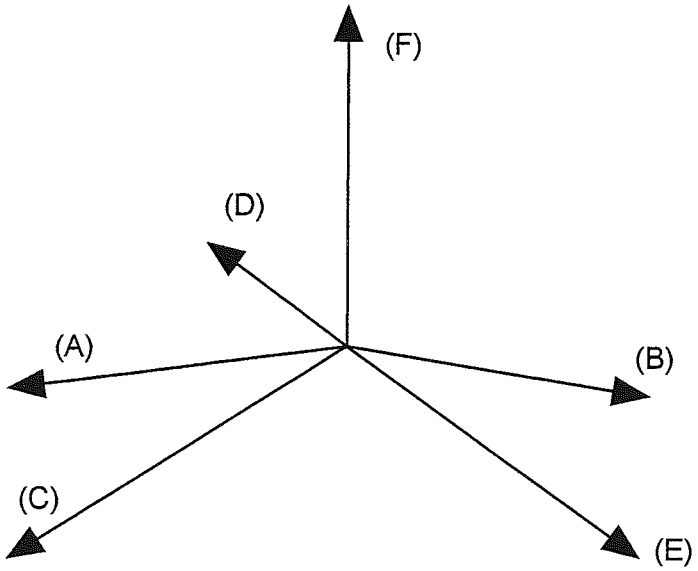

C

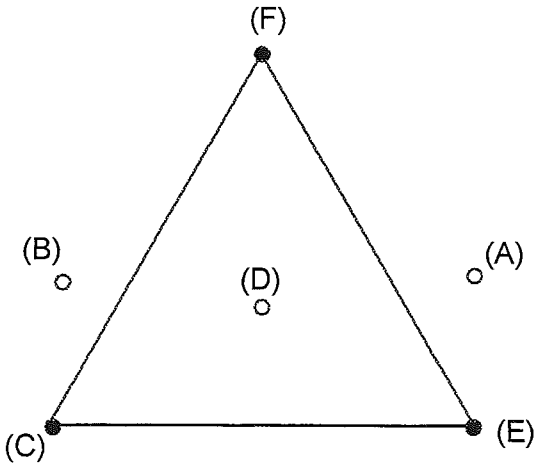

Fig. 21

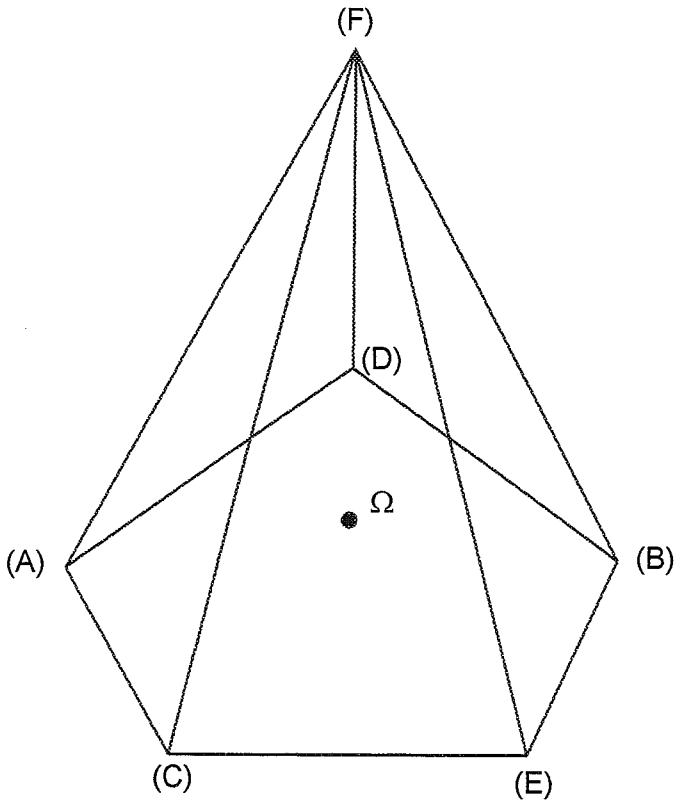

Fig. 21 D

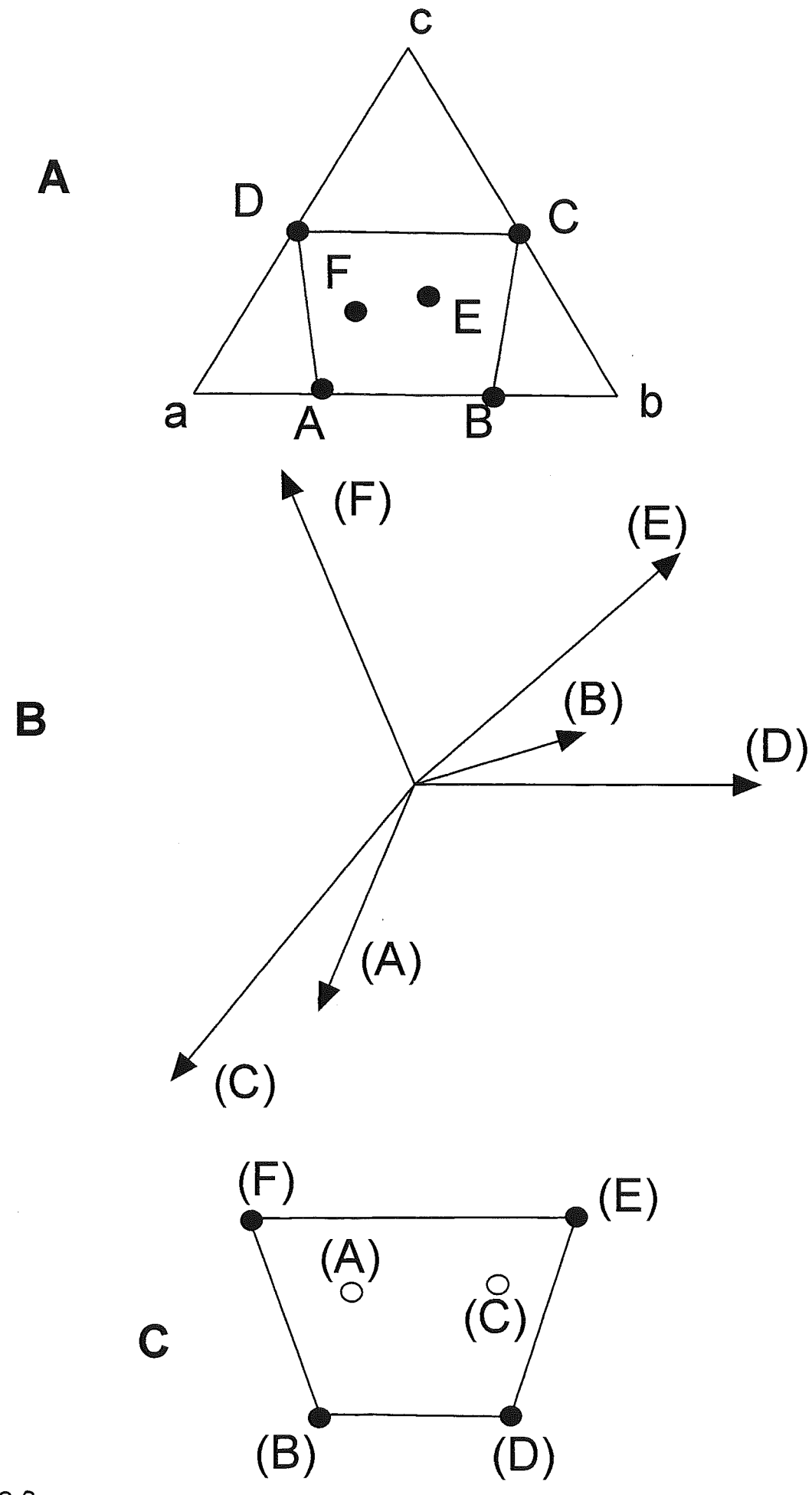

Fig. 22

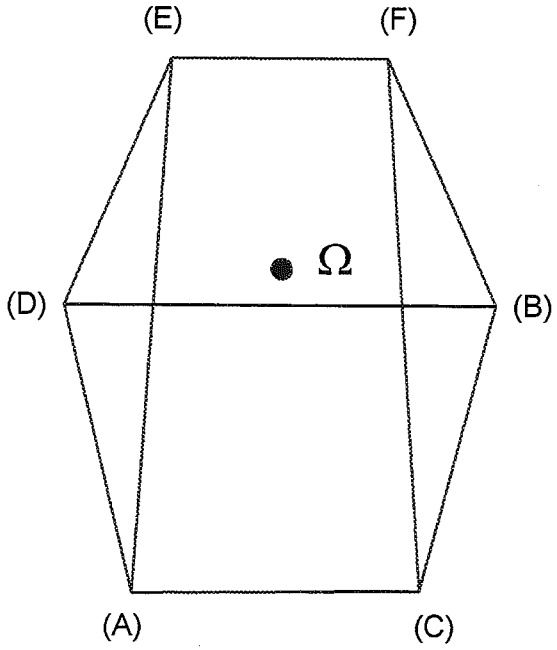

Fig. 22D

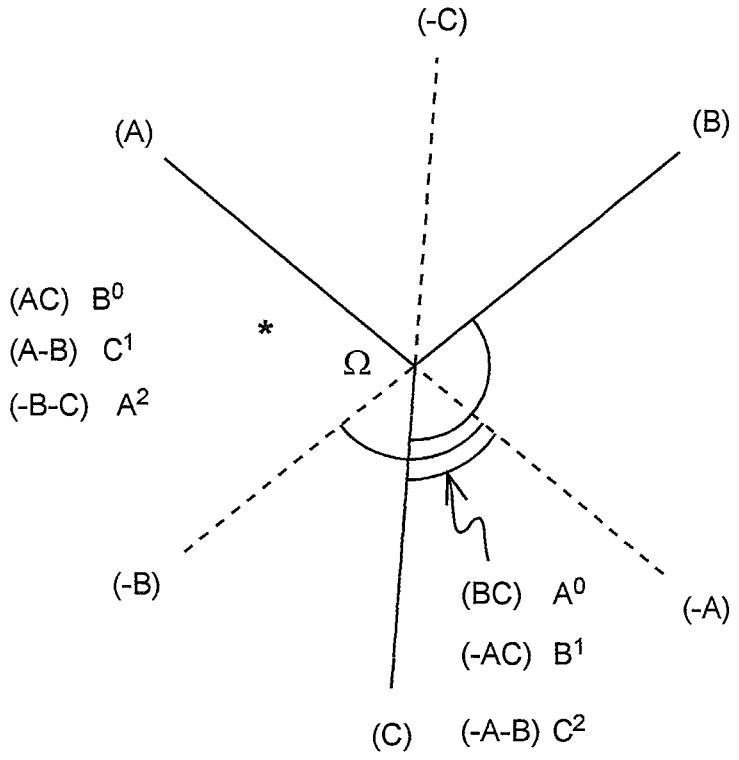
(-C)
(A)
(B)
(AC) B^0
(A-B) C^1
(-B-C) A^2
*
Ω
(-B)
(BC) A^0
(-AC) B^1
(-A)
(C)
(-A-B) C^2

FIG. 23

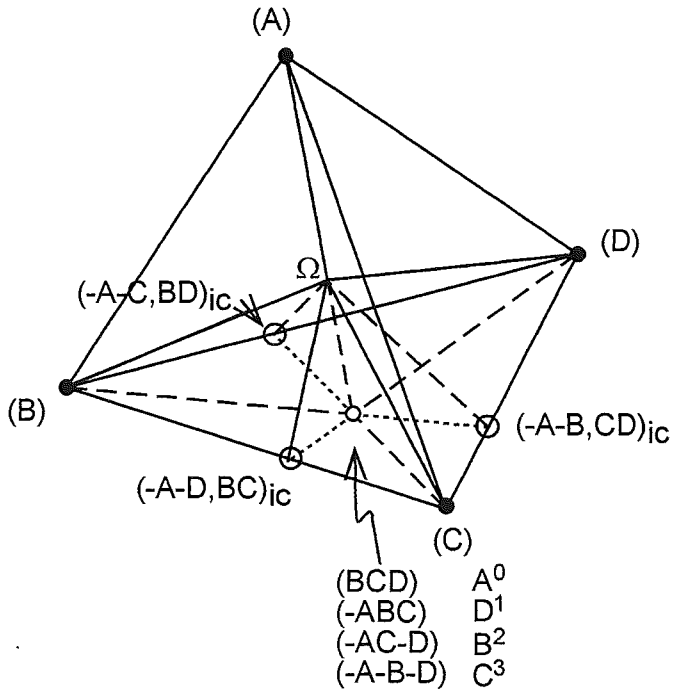
(A)
(D)
Ω
$(-A\text{-}C,BD)_{ic}$
(B)
$(-A\text{-}B,CD)_{ic}$
$(-A\text{-}D,BC)_{ic}$
(C)
(BCD) A^0
(-ABC) D^1
(-AC-D) B^2
(-A-B-D) C^3

FIG. 24

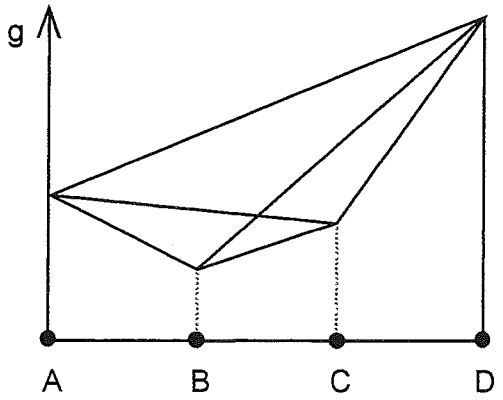

FIG. 25 A

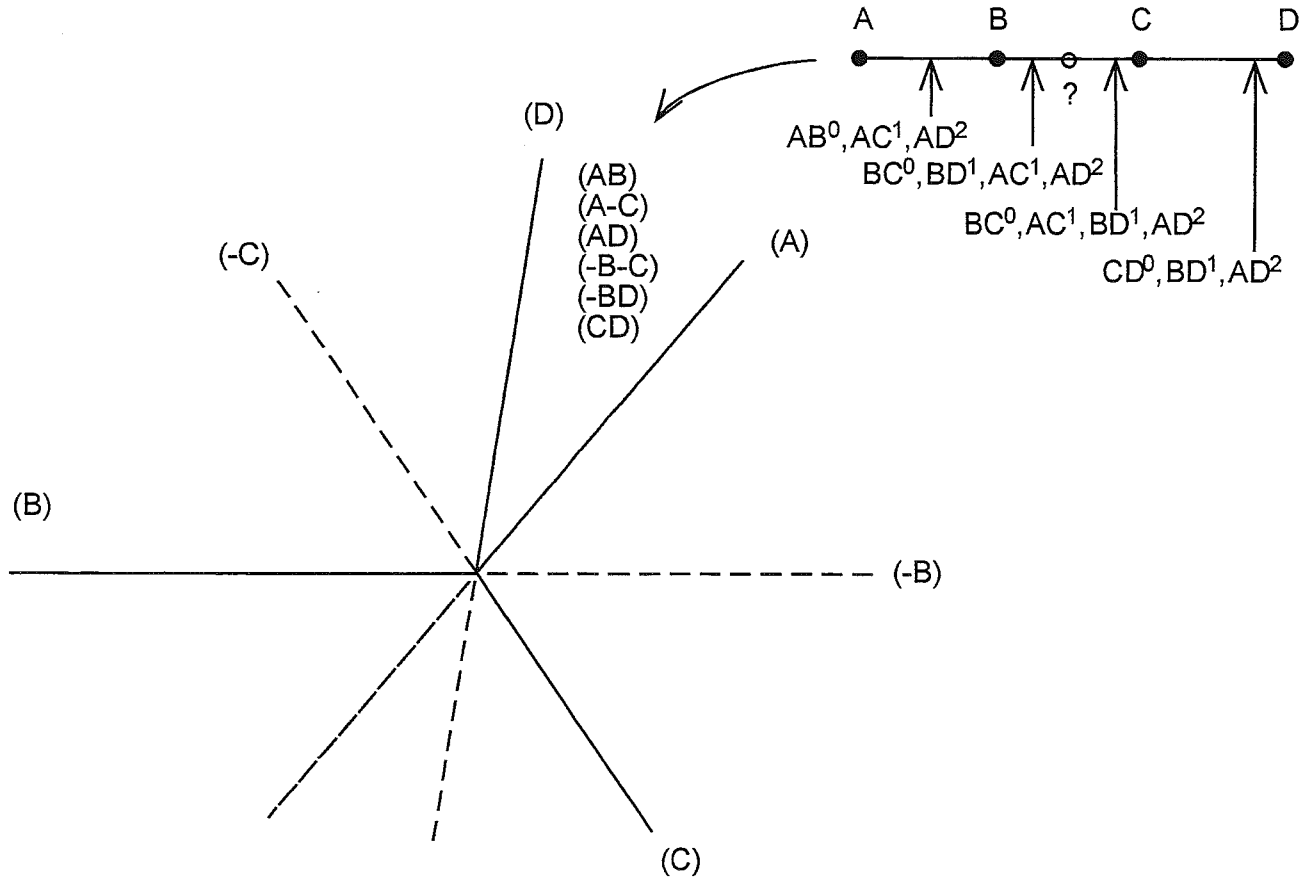

FIG. 25 B

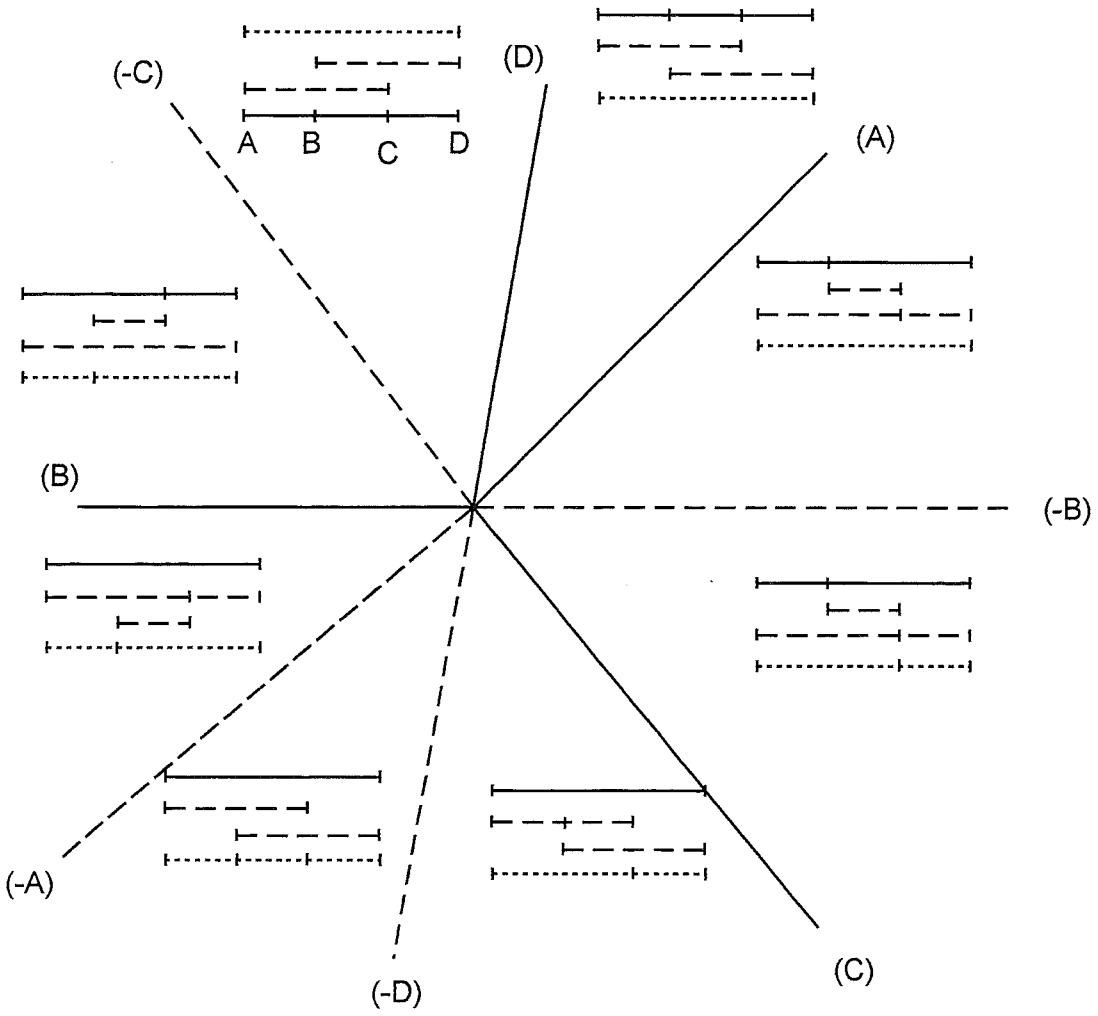

Fig. 25 C

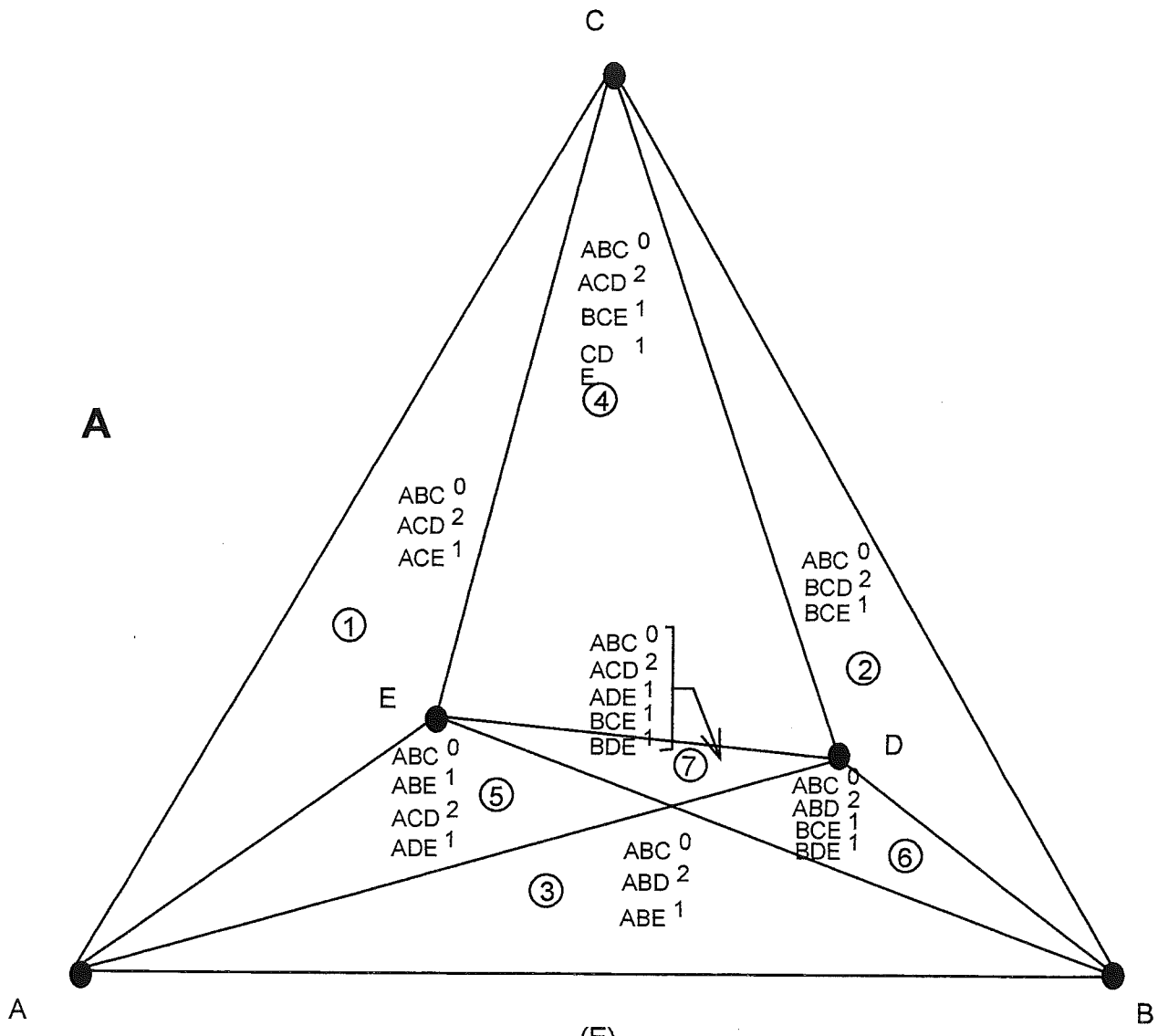
A
C
ABC 0
ACD 2
BCE 1
CD 1
E
4
ABC 0
ACD 2
ACE 1
1
ABC 0
BCD 2
BCE 1
2
ABC 0
ACD 2
ADE 1
BCE 1
BDE 1
7
E
D
ABC 0
ABE 1
ACD 2
ADE 1
5
ABC 0
ABD 2
BCE 1
BDE 1
6
ABC 0
ABD 2
ABE 1
3
A
B

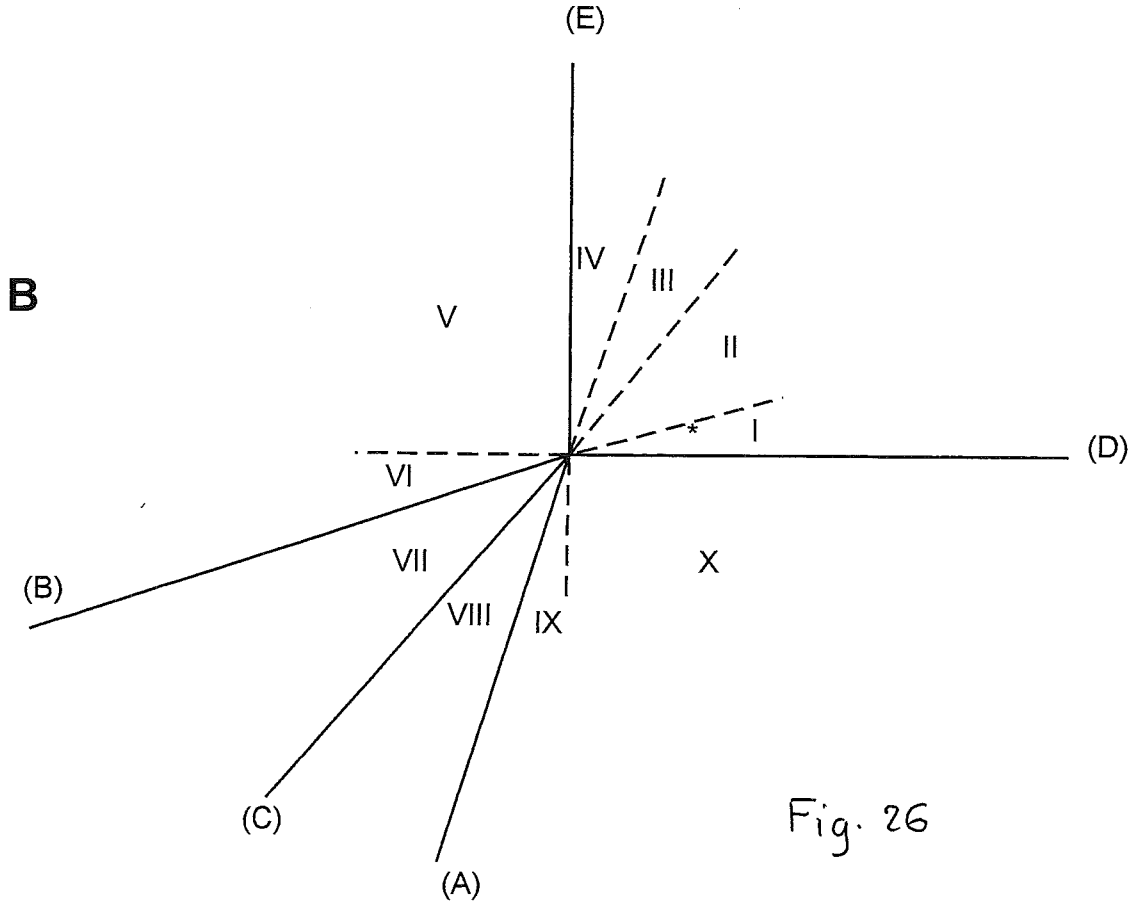
B
(E)
IV
III
V
II
I
(D)
VI
(B)
VII
X
VIII
IX
(C)
(A)

Fig. 26

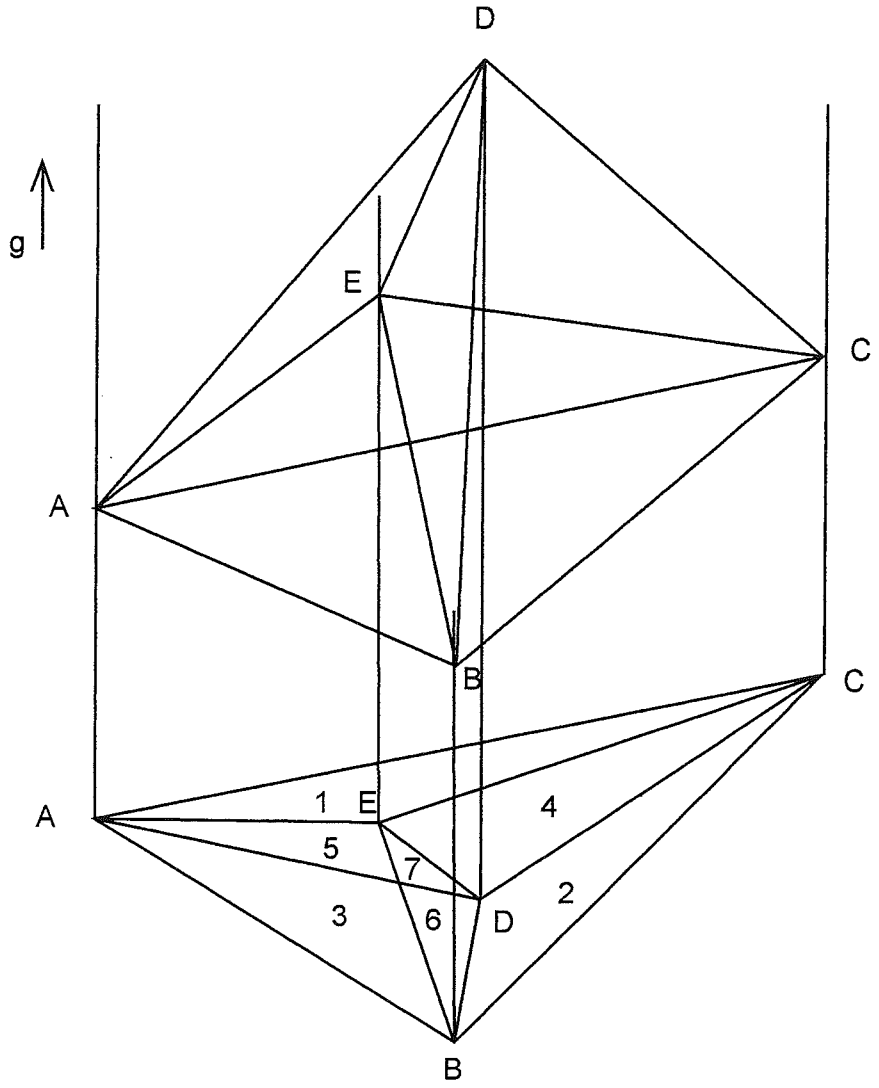

FIG. 26 C

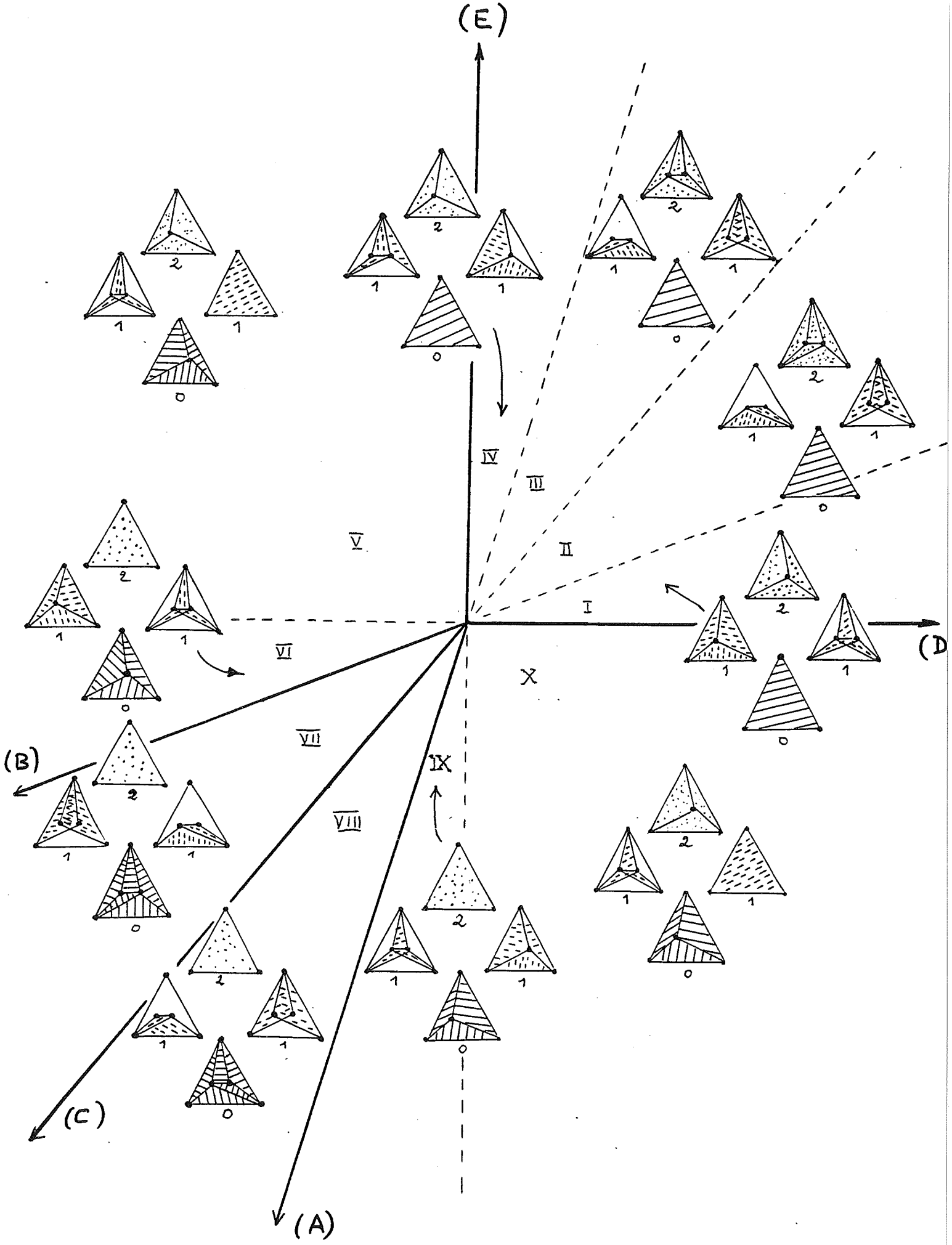

Fig. 27

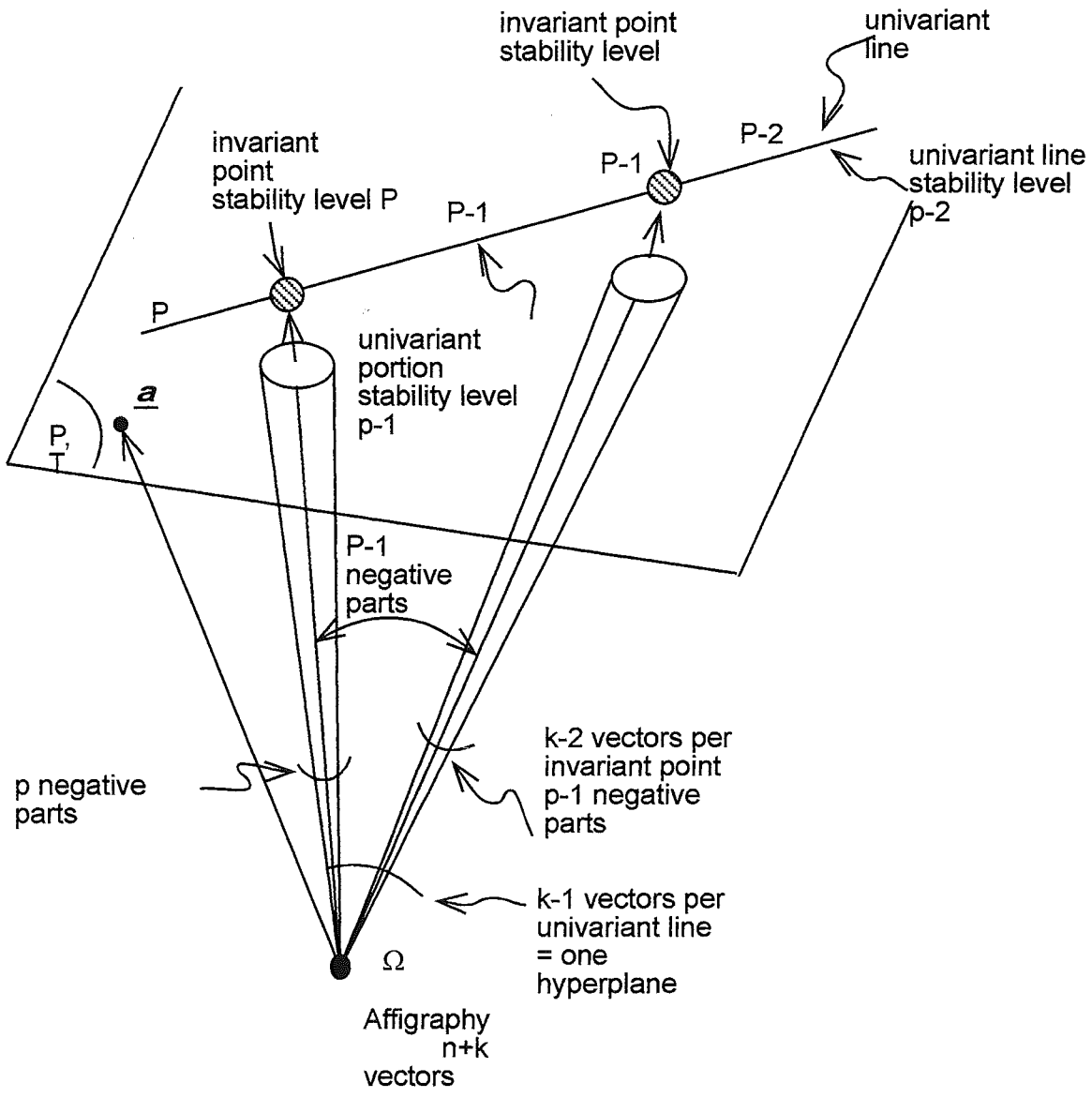
invariant point stability level
univariant line
invariant point stability level P
P-1
P-2
univariant line stability level p-2
P-1
P
univariant portion stability level p-1
a
P,
P-1 negative parts
k-2 vectors per invariant point p-1 negative parts
p negative parts
k-1 vectors per univariant line = one hyperplane
Ω
Affigraphy n+k vectors

fig.28

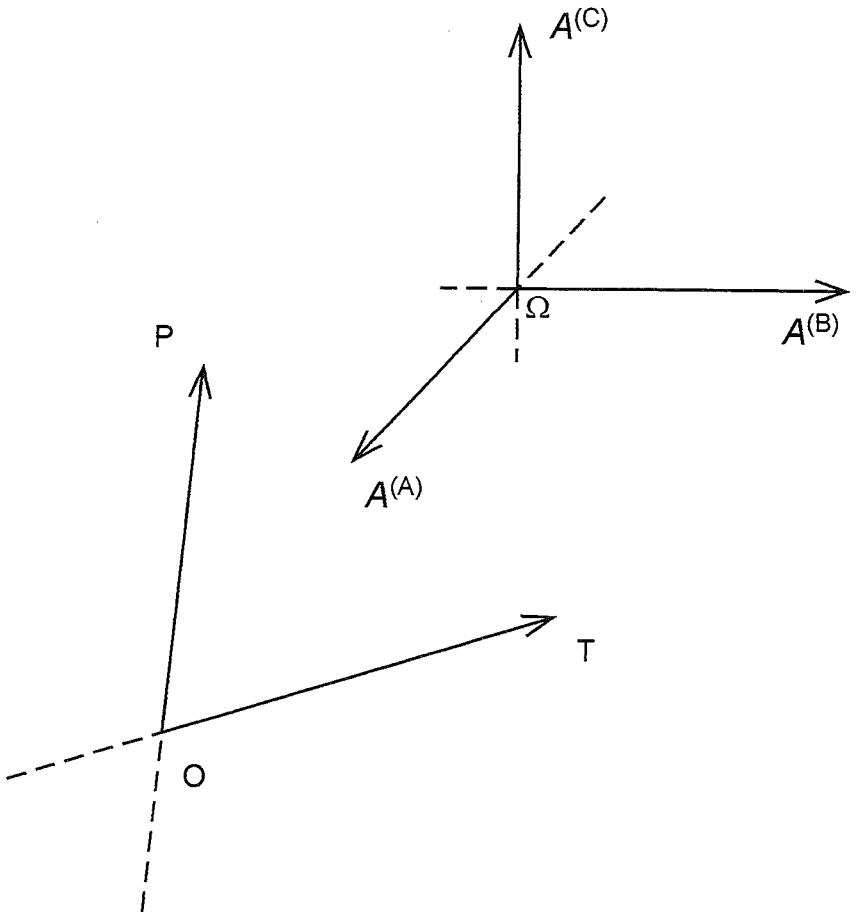

FIG. 29 A

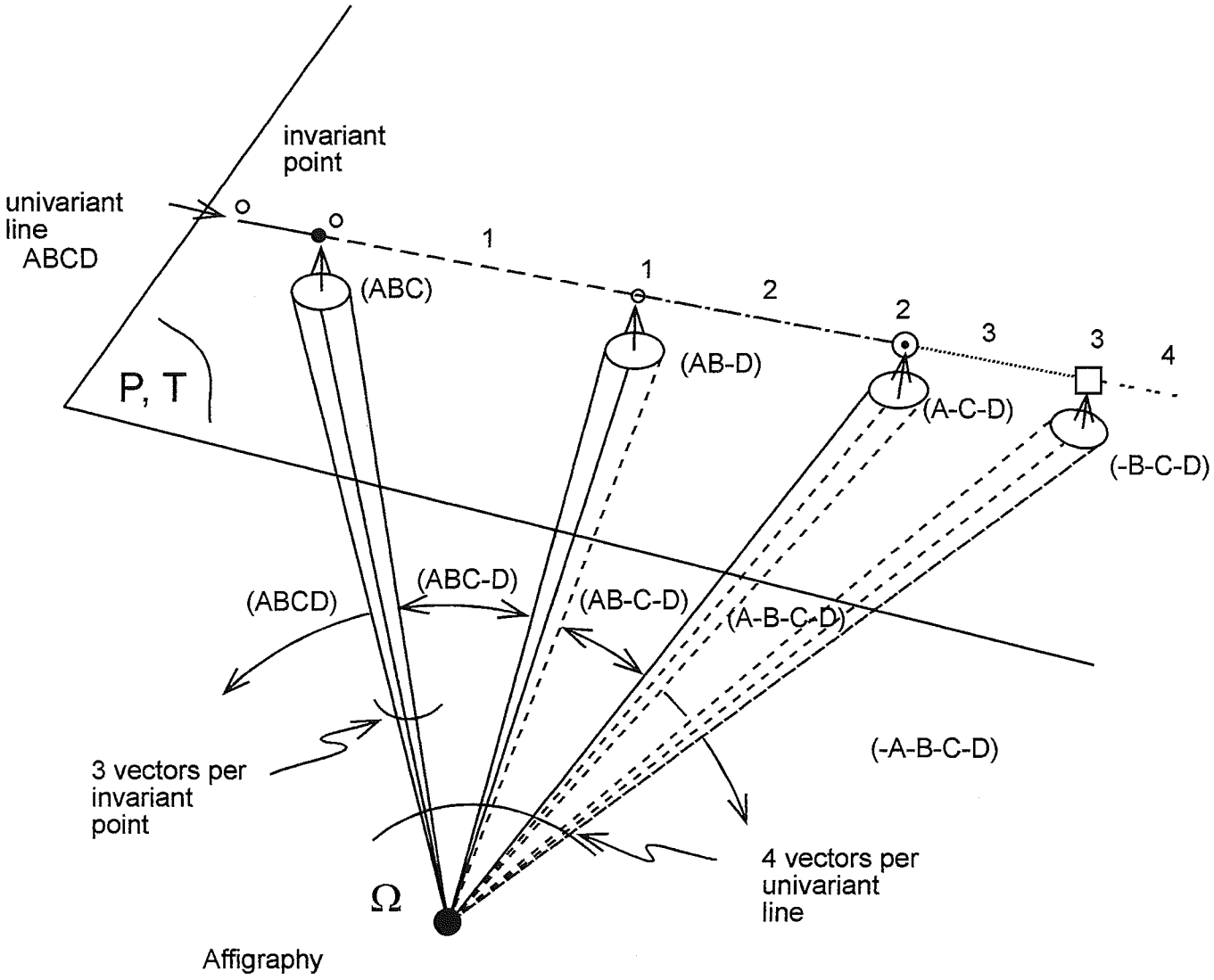
invariant
point
univariant
line
ABCD
1
(ABC)
1
2
(AB-D)
2
3
(A-C-D)
3
4
(-B-C-D)
P, T
(ABCD)
(ABC-D)
(AB-C-D)
(A-B-C-D)
(-A-B-C-D)
3 vectors per
invariant
point
4 vectors per
univariant
line
Ω
Affigraphy

Fig. 29 B

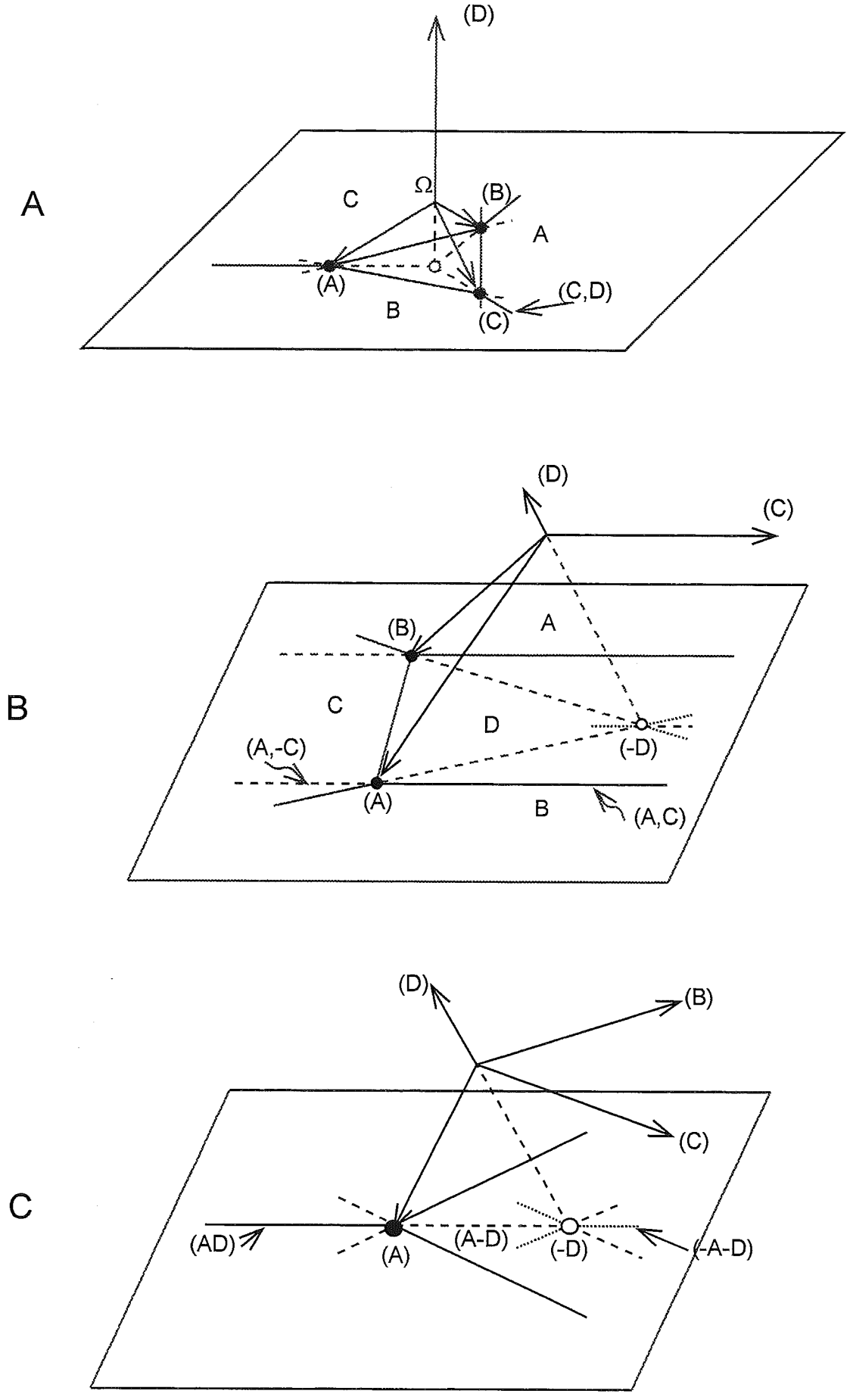

FIG. 30

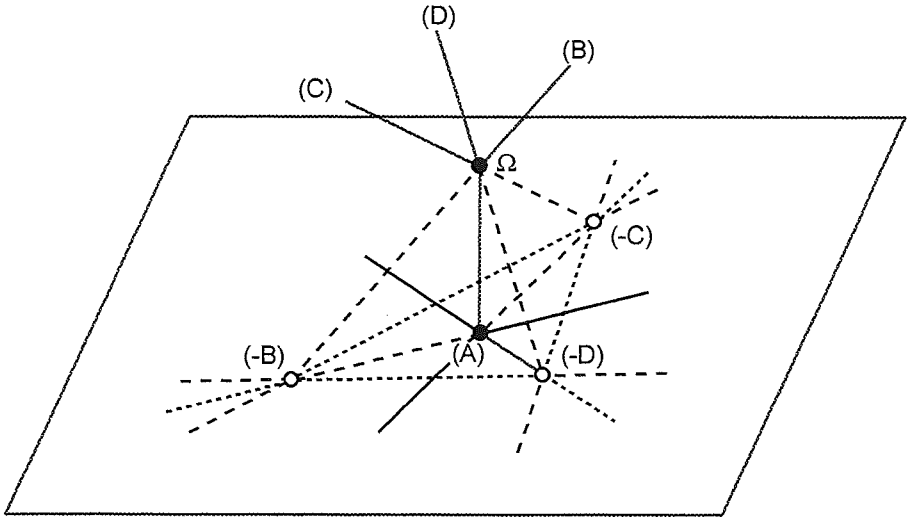

30 D

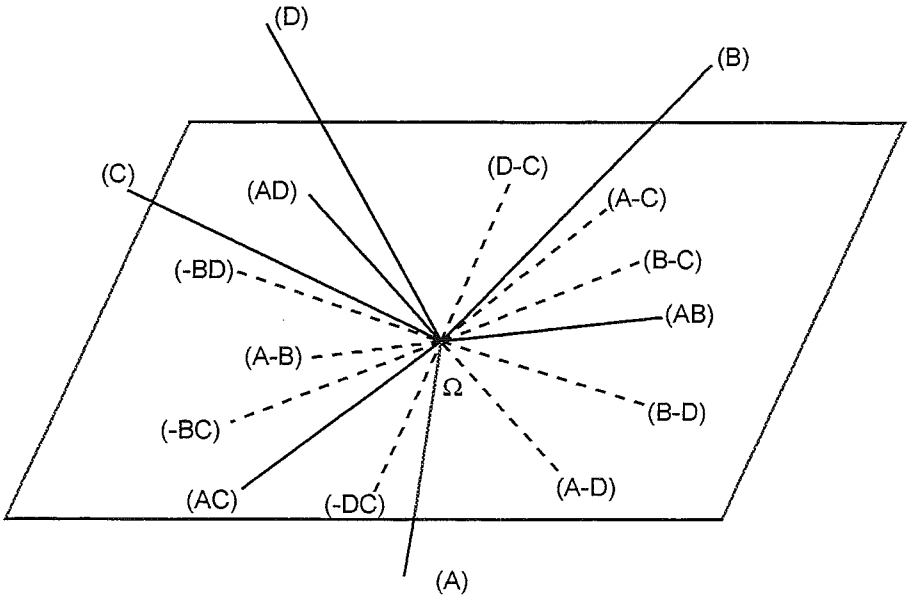

30 E

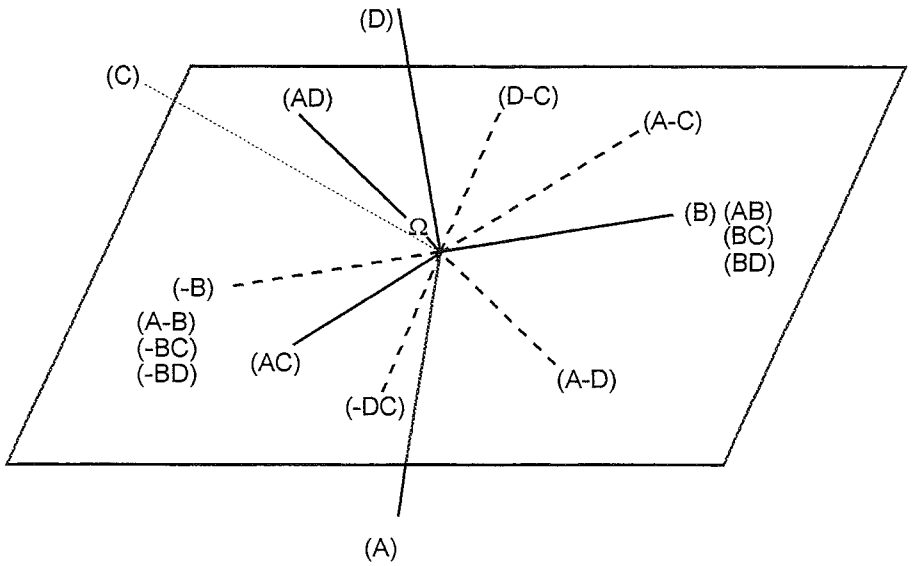

30 F

Fig. 30

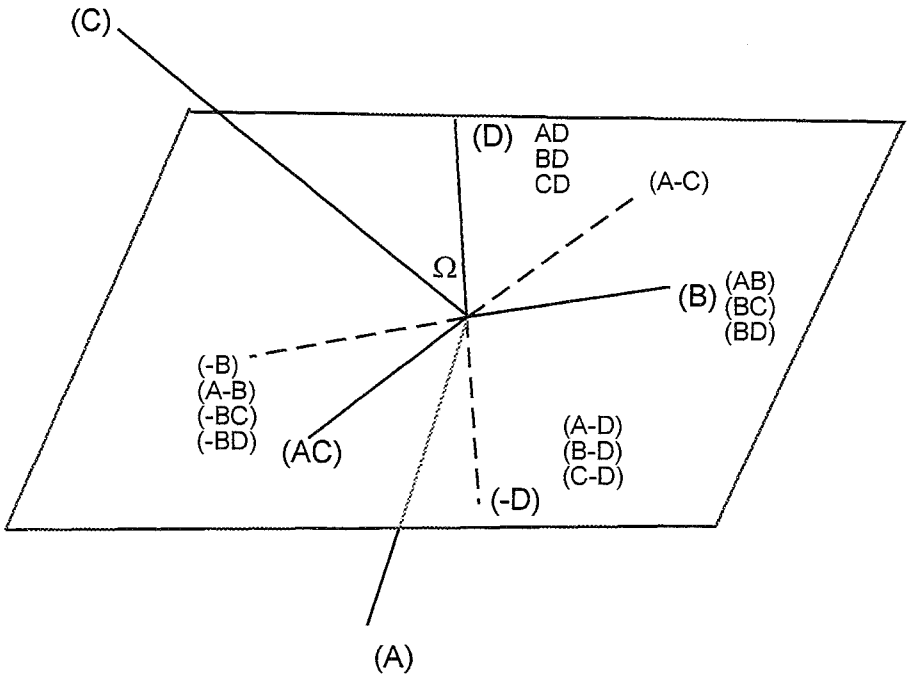

Fig. 30 G

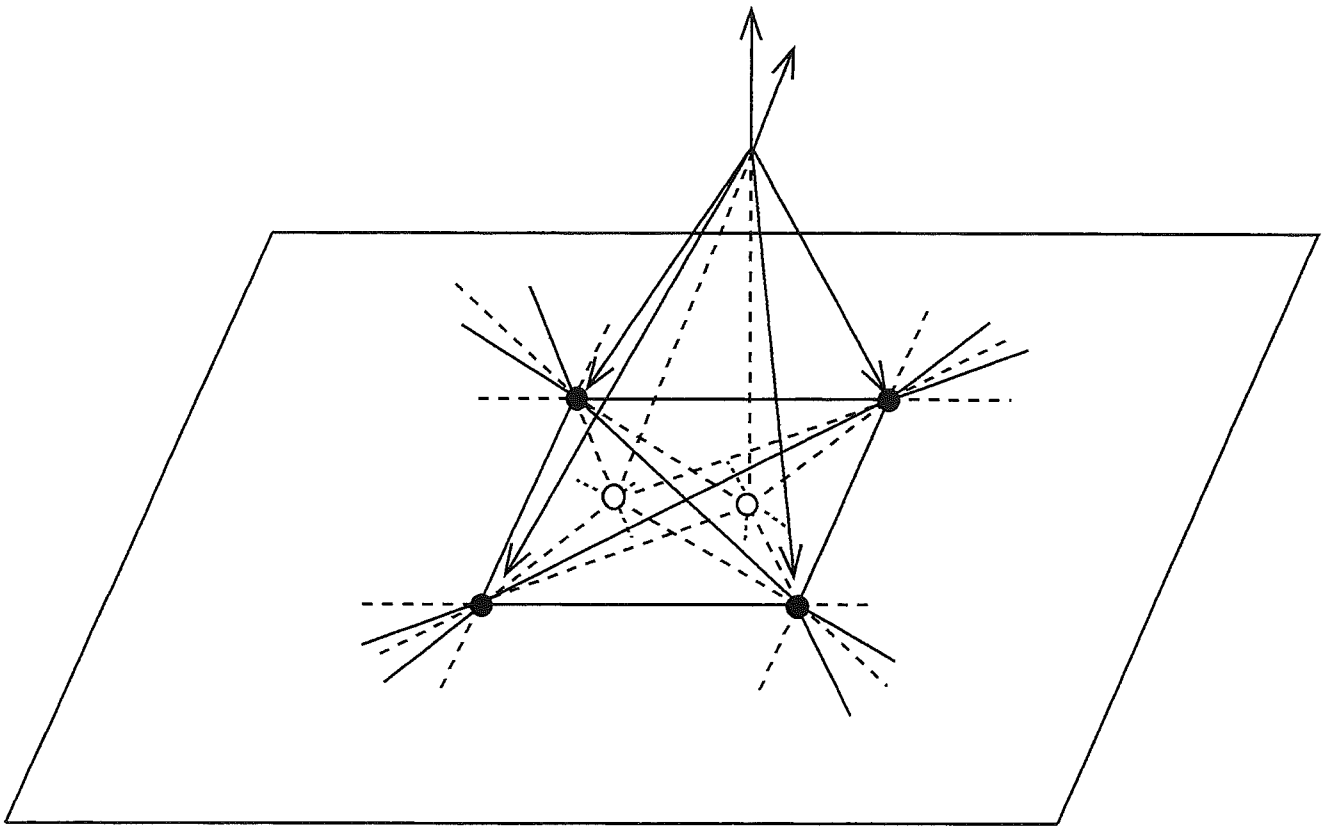

Fig. 31

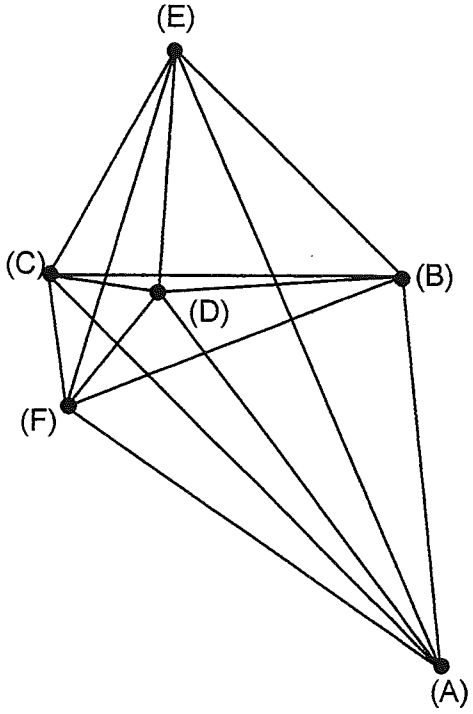

Fig. 32

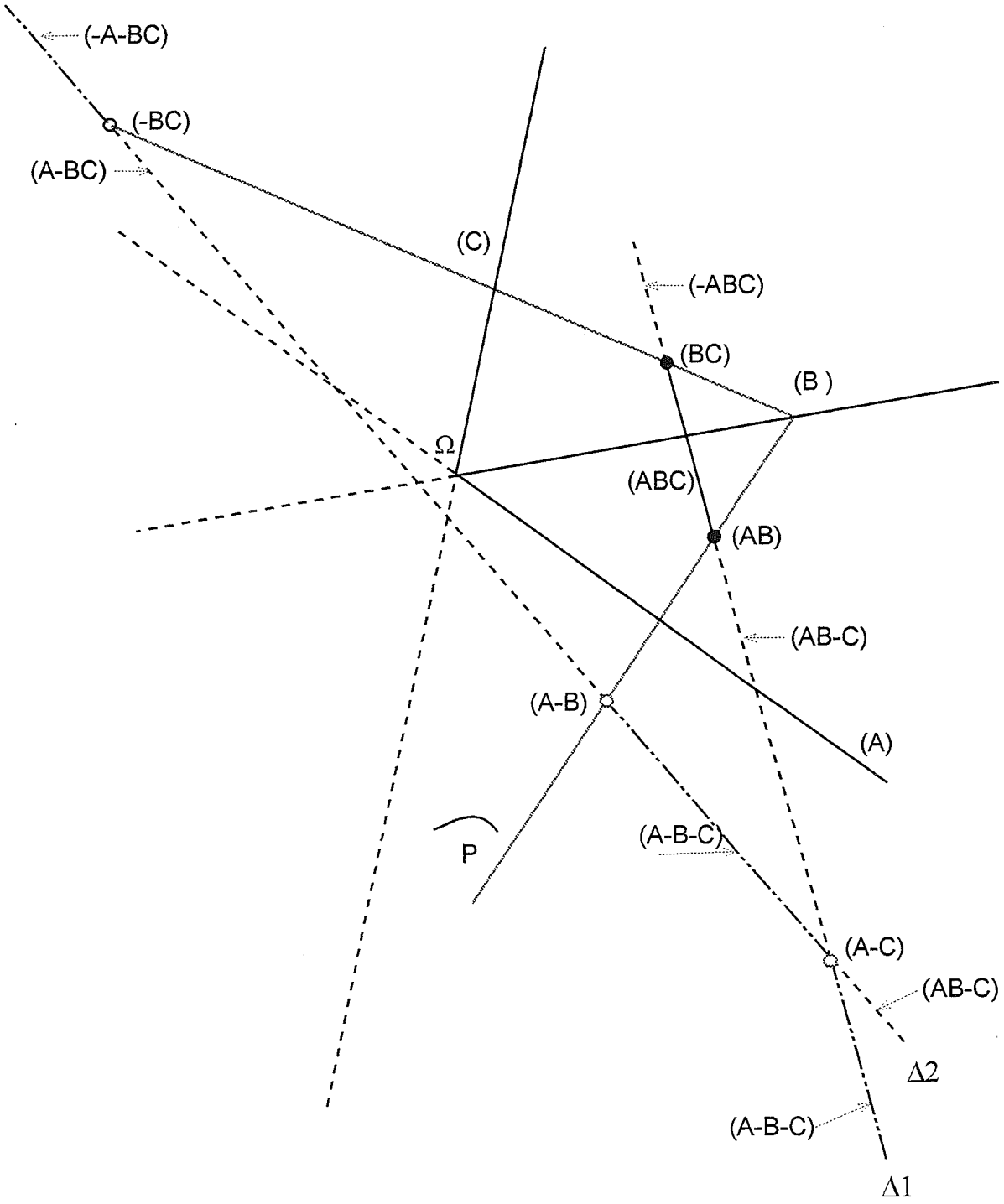

FIG.33 A

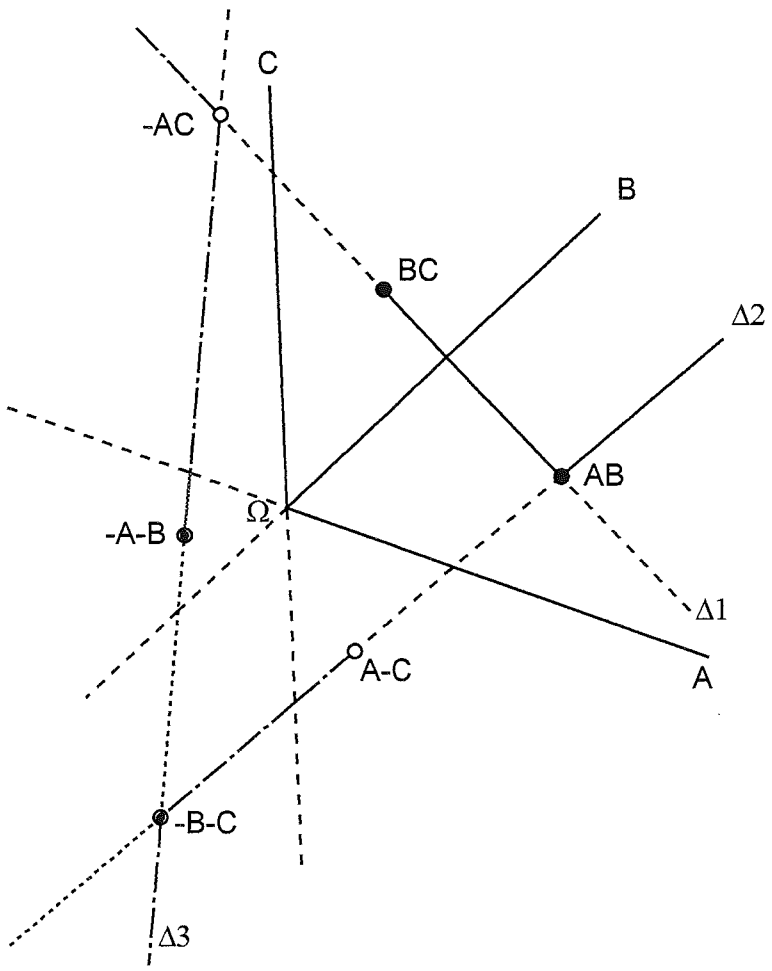

FIG. 33 B

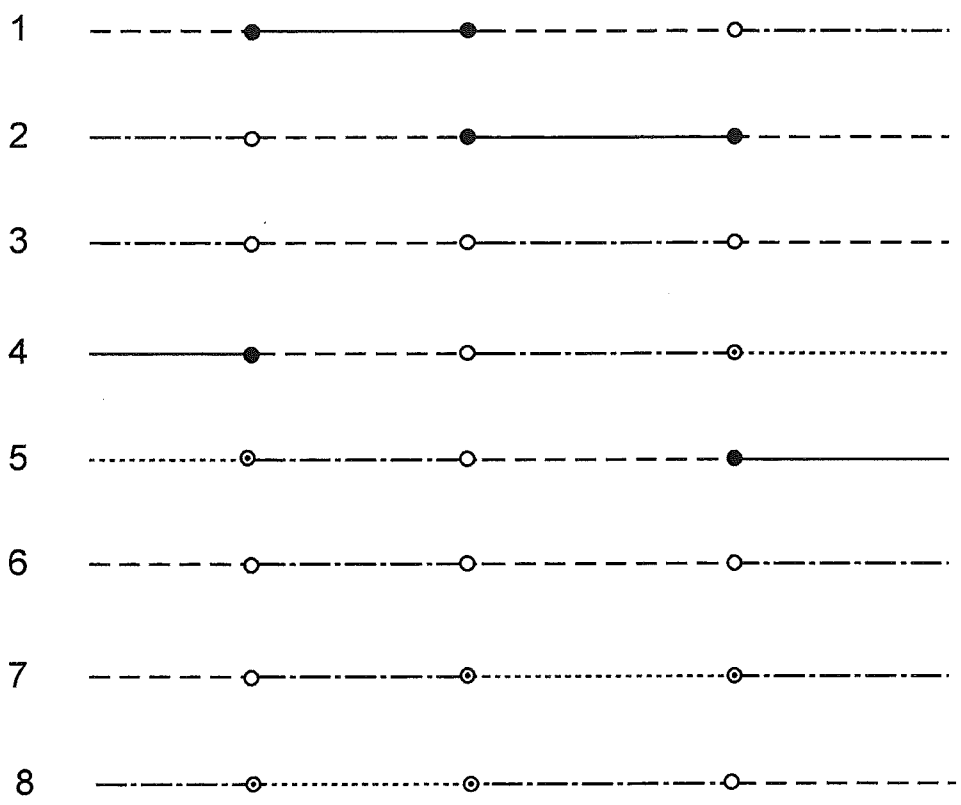

Points:

- stable
- singly metastable
- doubly metastable

Lines:

- stable
- singly metastable
- doubly metastable
- triply metastable

FIG. 34

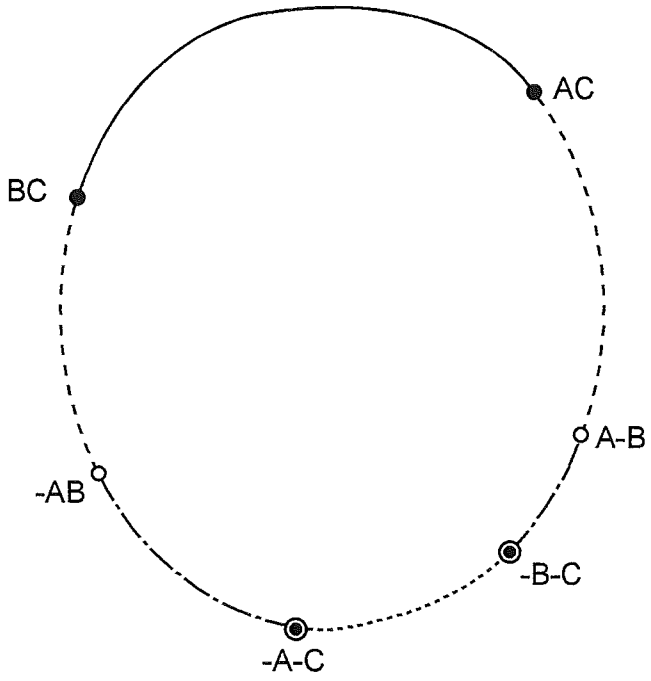

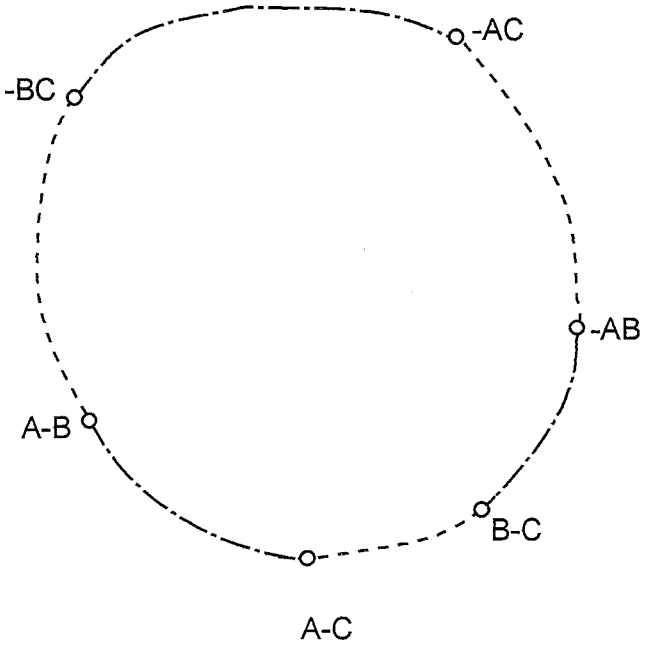

FIG. 35

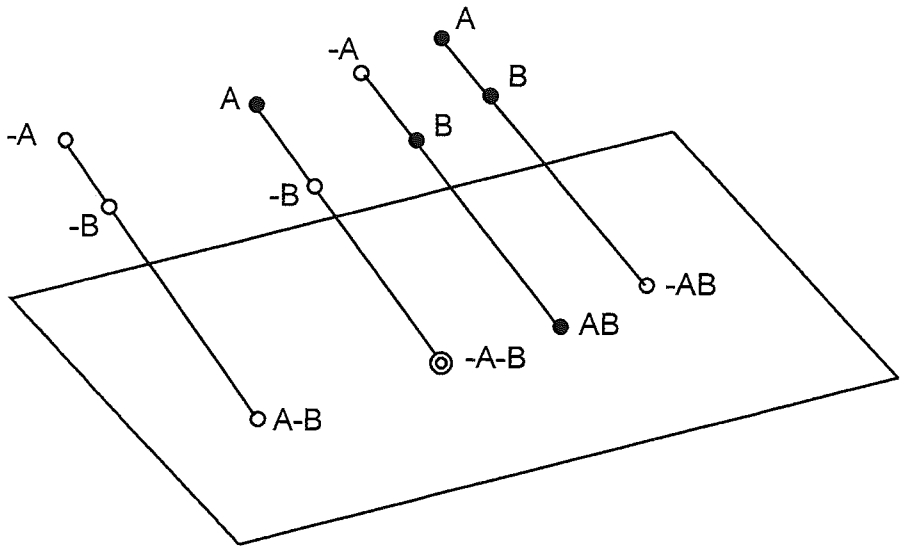

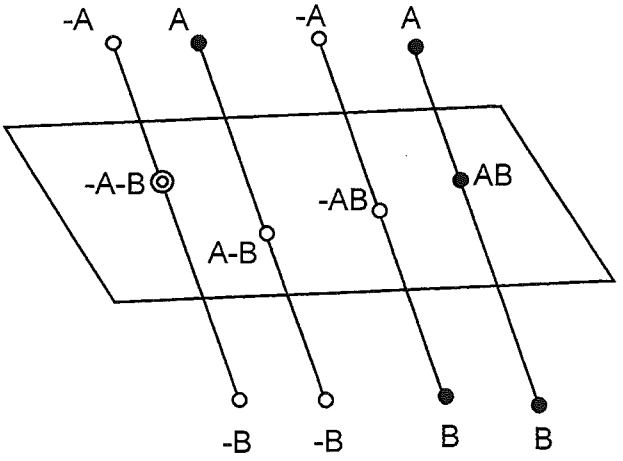

FIG. 36

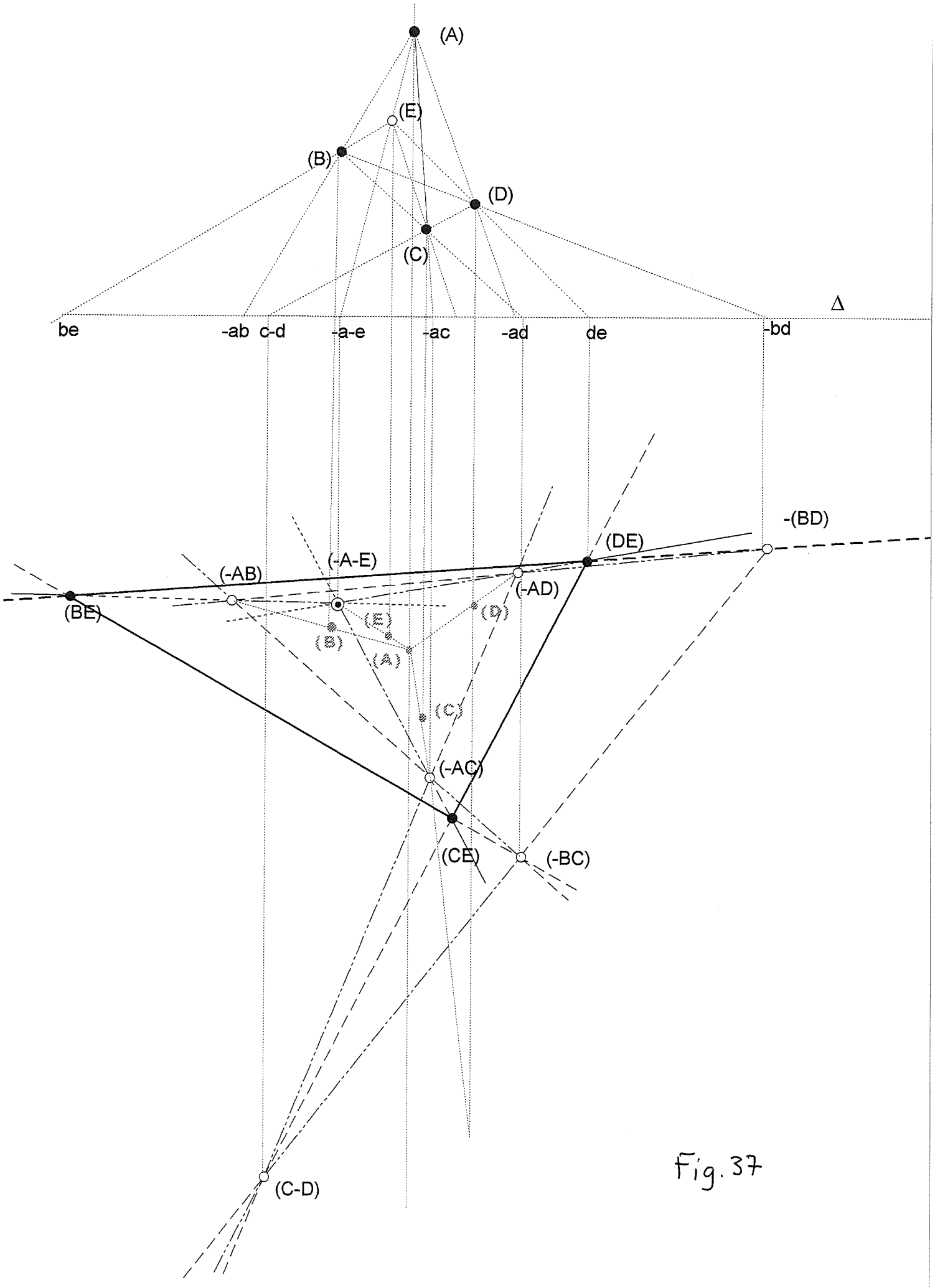

Fig. 37

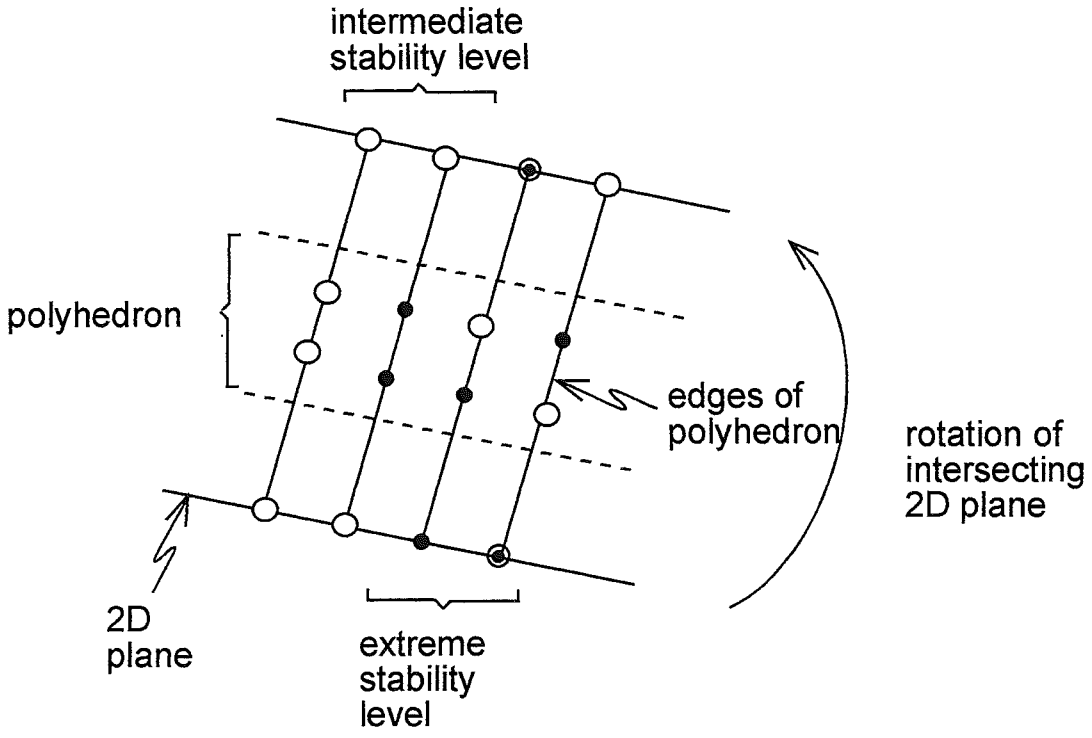

● stable

○ singly metastable

◉ doubly metastable

FIG. 38

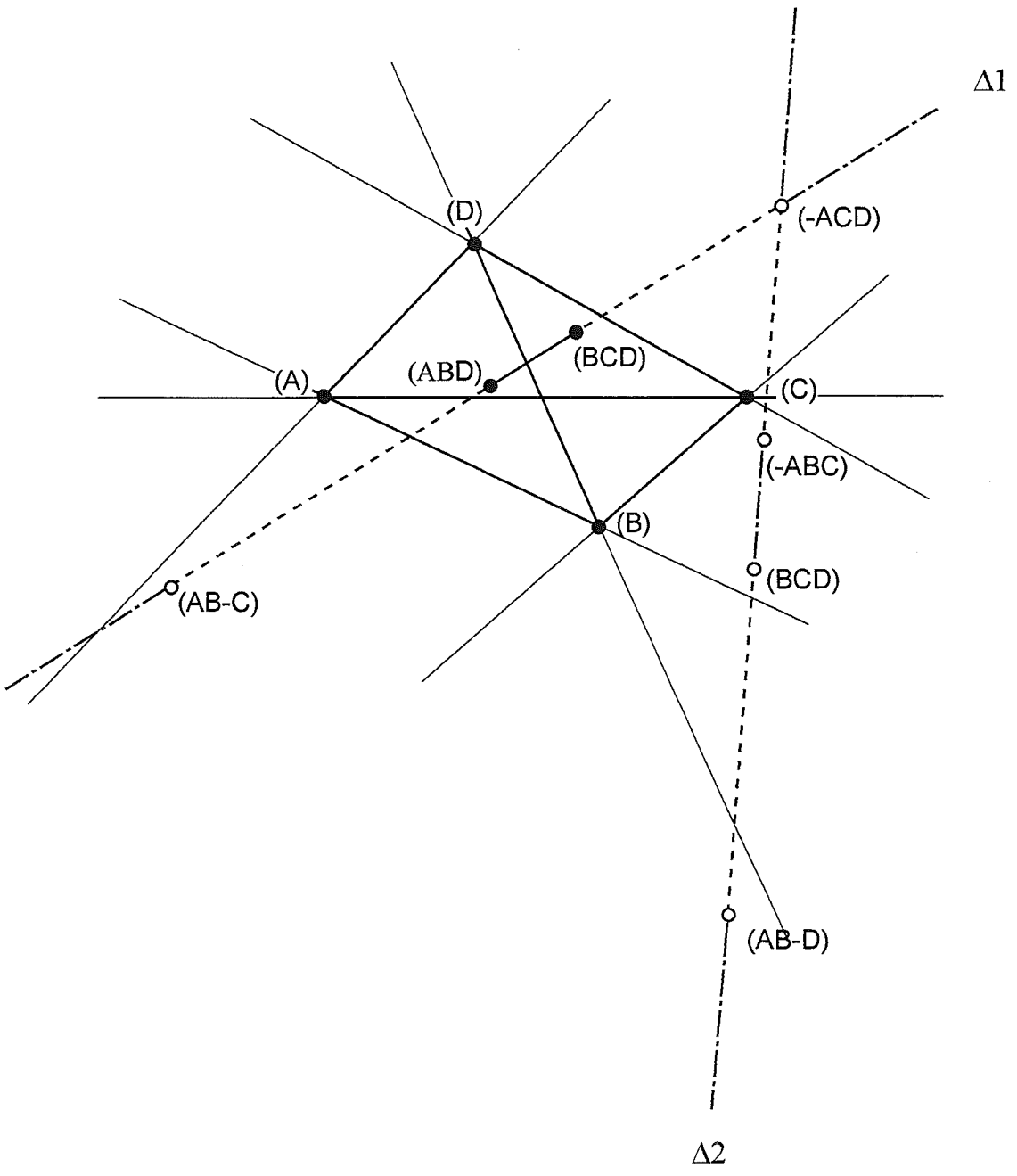

FIG. 39 A

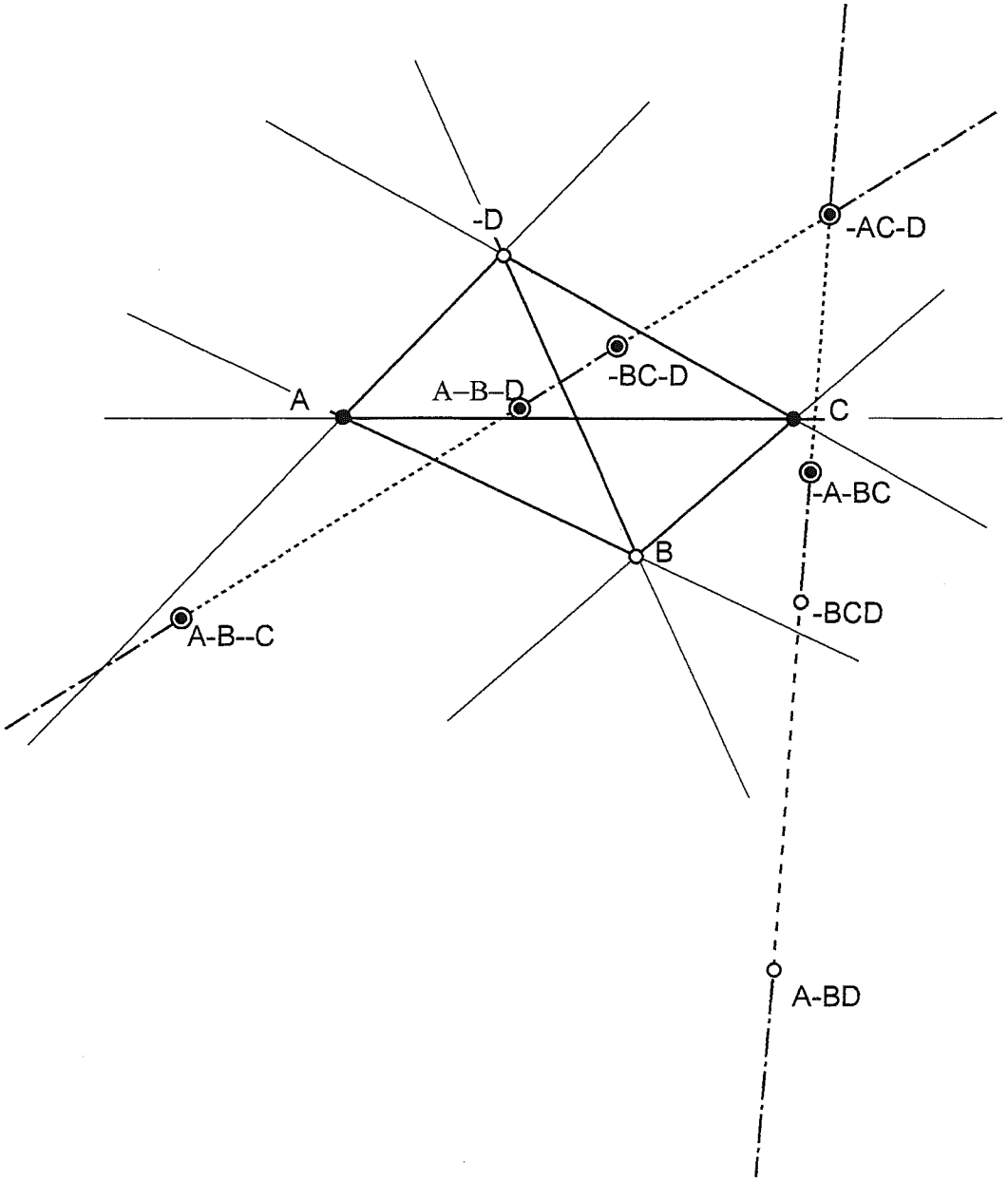

FIG. 39 B

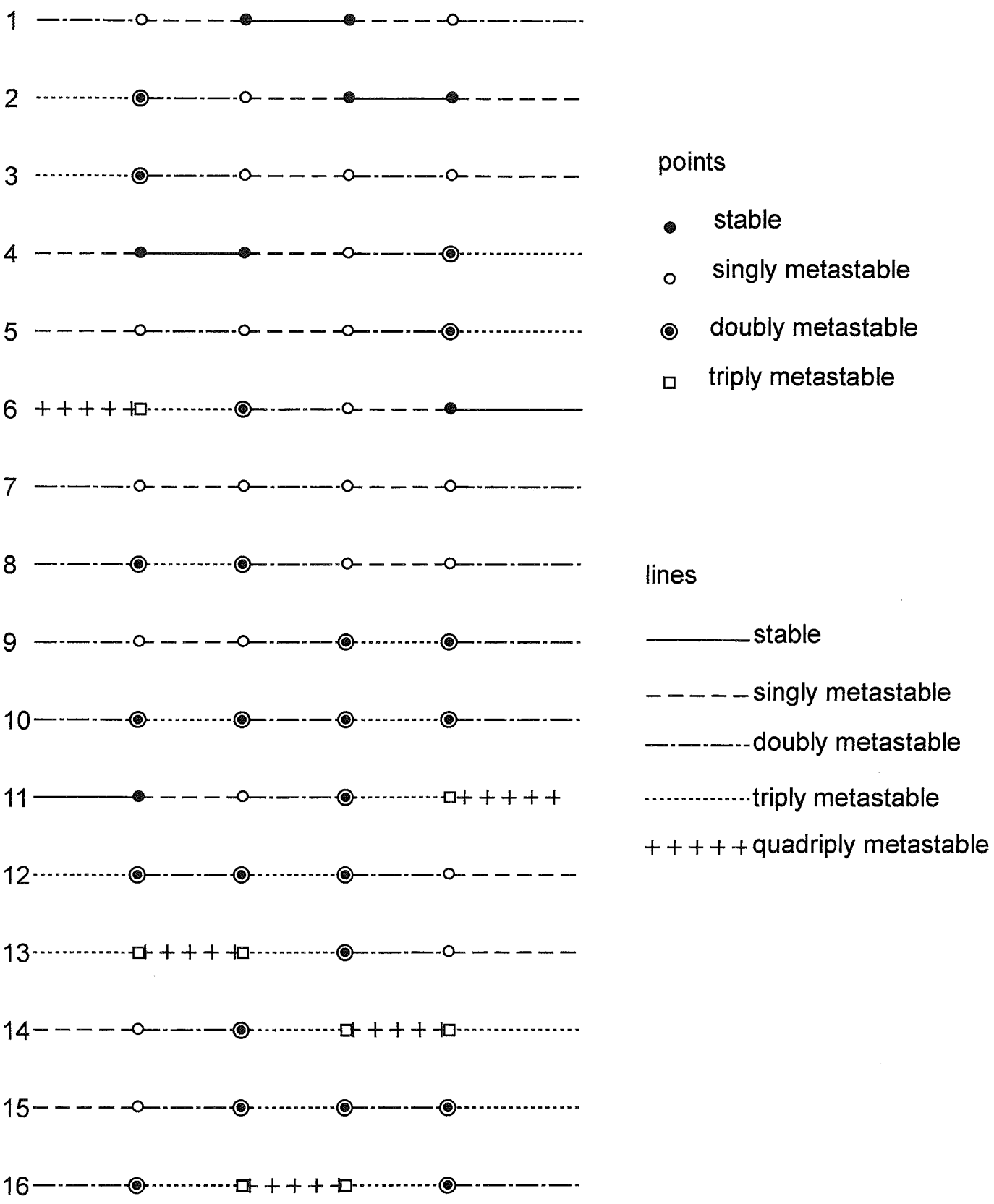
1
2
3
4
5
6
7
8
9
10
11
12
13
14
15
16
points
stable
singly metastable
doubly metastable
triply metastable
lines
stable
singly metastable
doubly metastable
triply metastable
quadriply metastable

FIG. 40

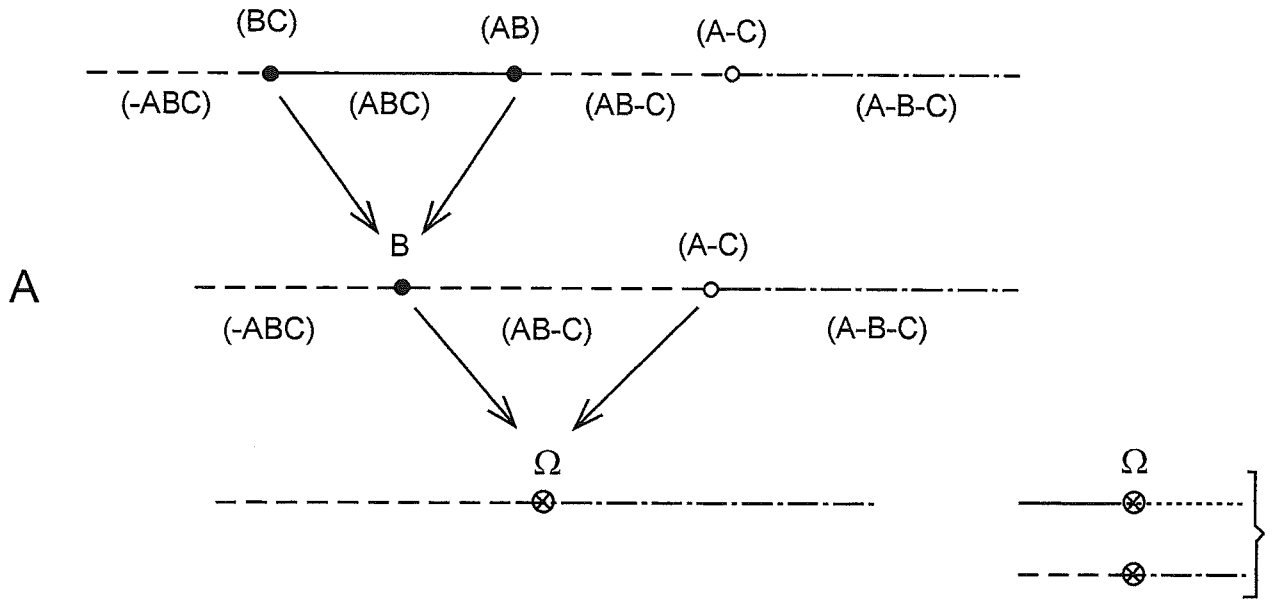
A
(BC)
(AB)
(A-C)
(-ABC)
(ABC)
(AB-C)
(A-B-C)
B
(A-C)
(-ABC)
(AB-C)
(A-B-C)
Ω
Ω

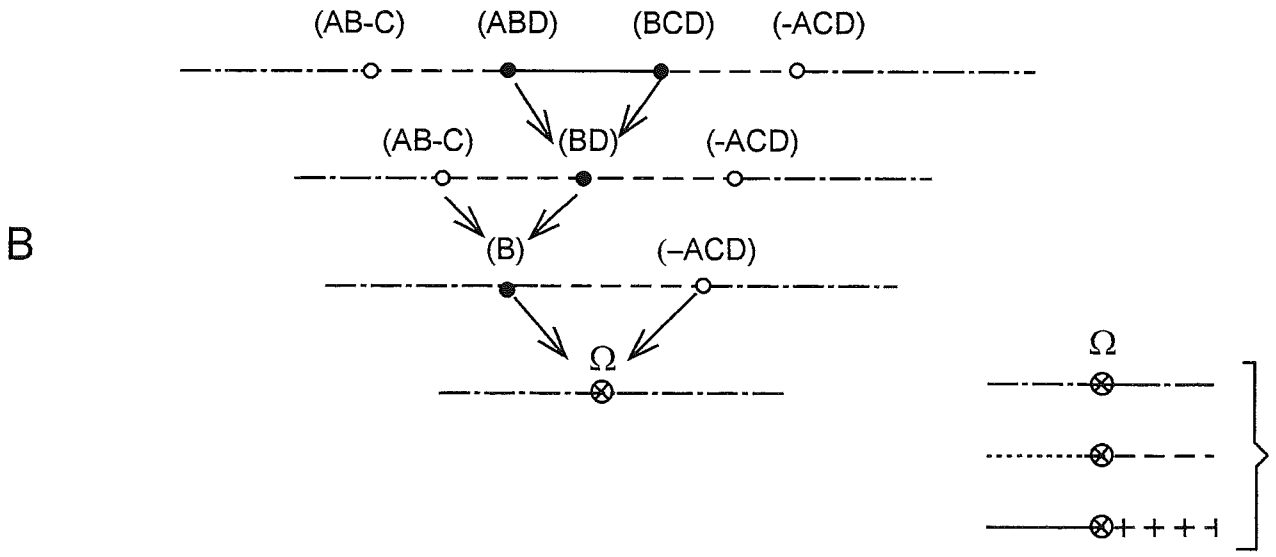
B
(AB-C)
(ABD)
(BCD)
(-ACD)
(AB-C)
(BD)
(-ACD)
(B)
(–ACD)
Ω
Ω

FIG. 41

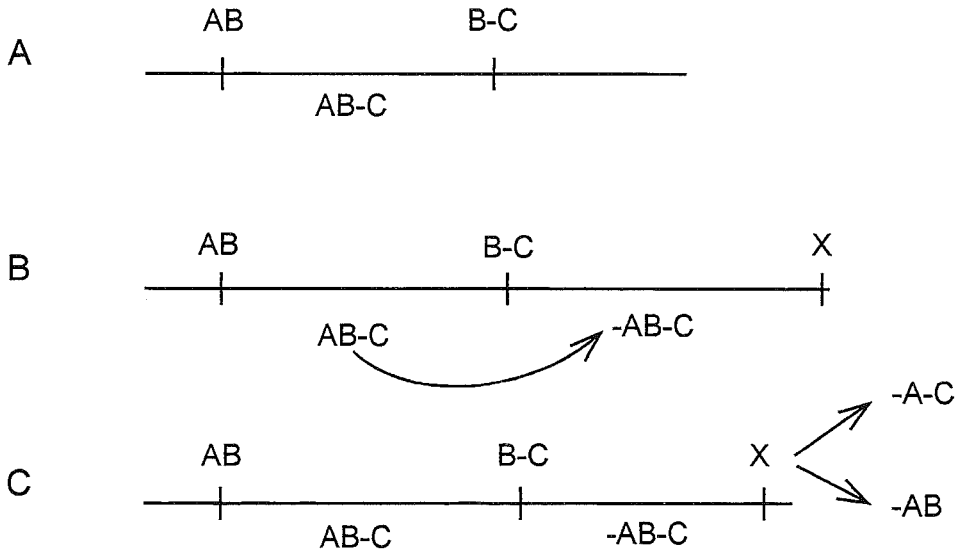

FIG. 42

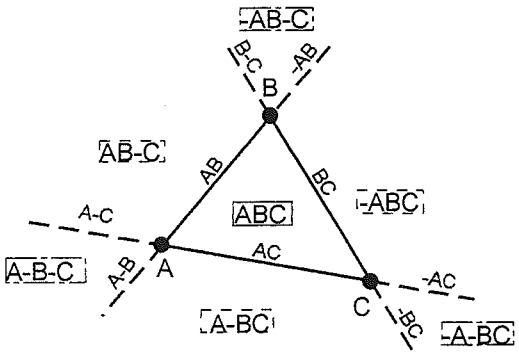
-AB-C
-BC
-AB
B
AB-C
AB
BC
-ABC
A-C
ABC
A-B-C
-AB
A
AC
-AC
C
-A-BC
-BC
-A-BC

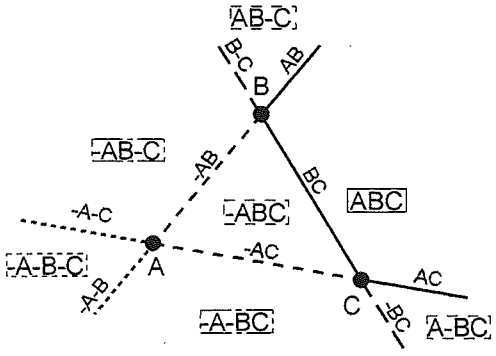
AB-C
-BC
AB
B
-AB-C
-AB
BC
ABC
-A-C
-ABC
-A-B-C
A
-AC
AC
-A-B
C
-BC
-A-BC
A-BC

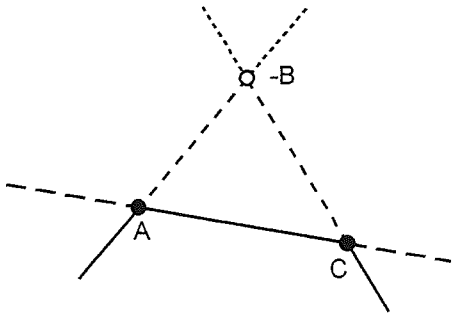
-B
A
C

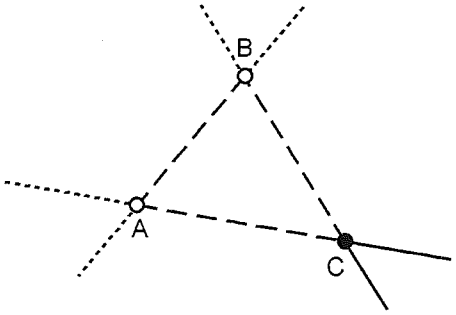
B
A
C

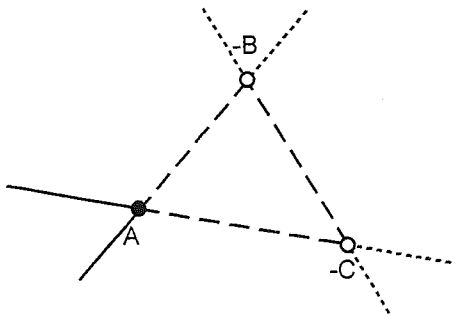
-B
A
-C

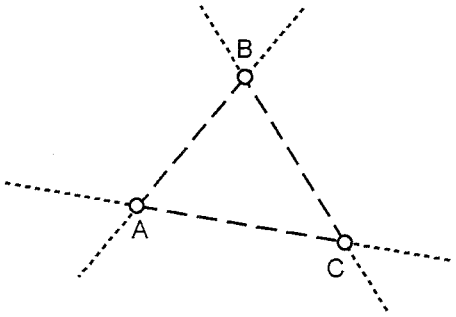
B
A
C

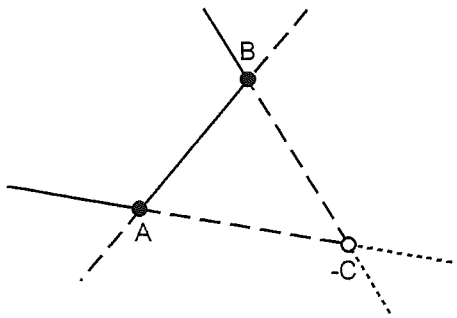
B
A
-C

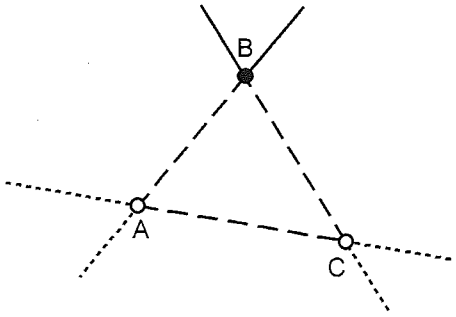
B
A
C

FIG. 43

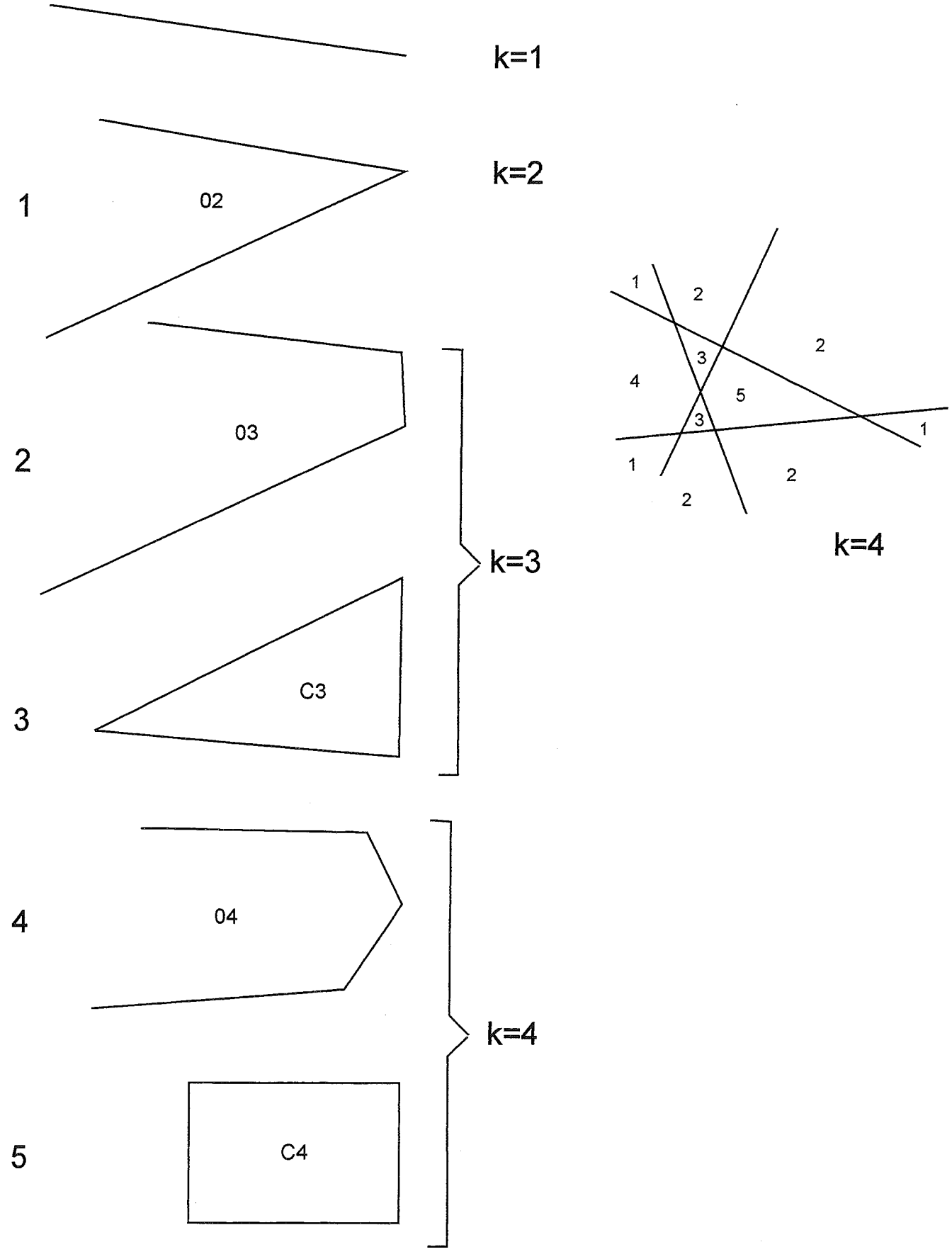

FIG. 44A

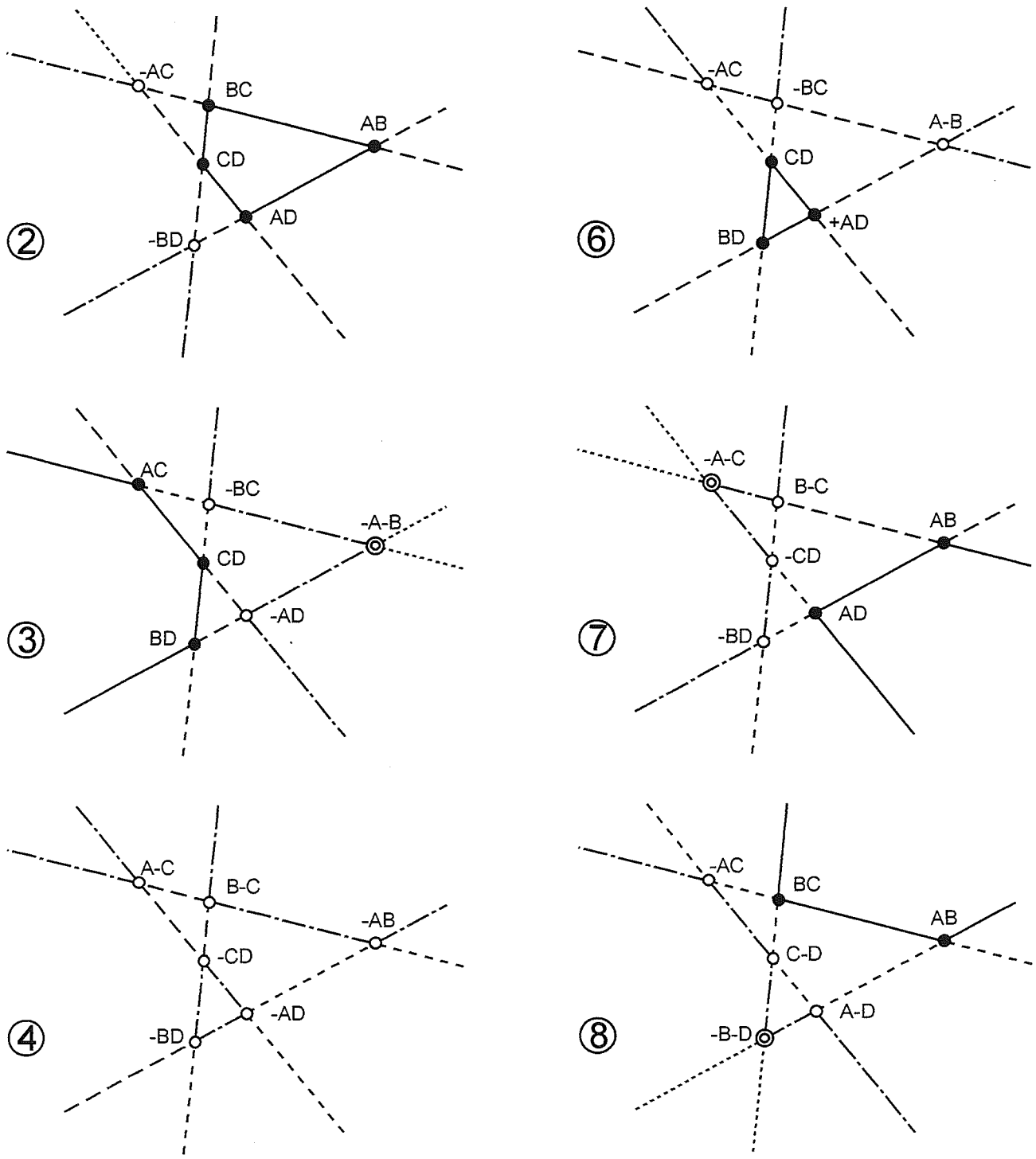
②
-AC
BC
AB
CD
AD
-BD
⑥
-AC
-BC
A-B
CD
+AD
BD
③
AC
-BC
-A-B
CD
-AD
BD
⑦
-A-C
B-C
AB
-CD
AD
-BD
④
A-C
B-C
-AB
-CD
-AD
-BD
⑧
-AC
BC
AB
C-D
A-D
-B-D

Fig. 44 B1

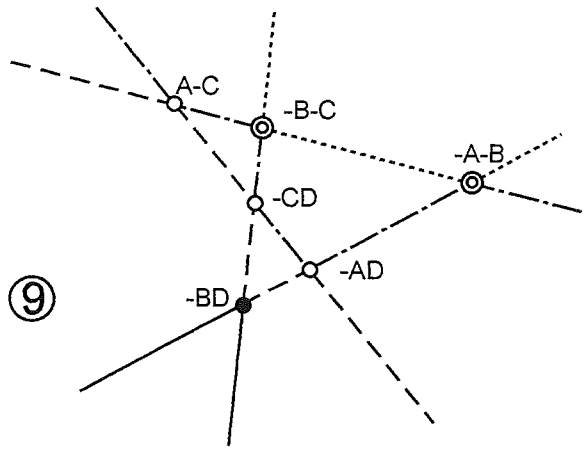

9

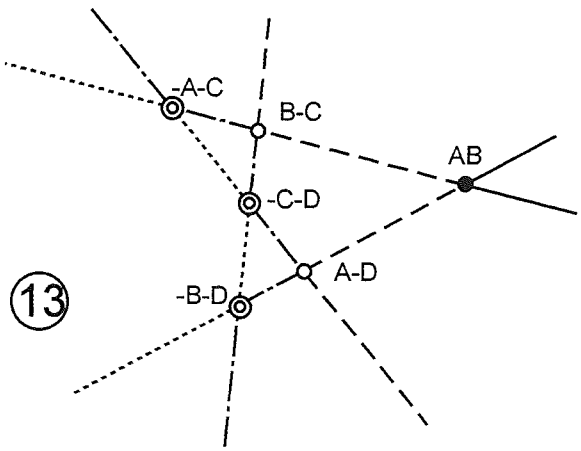

13

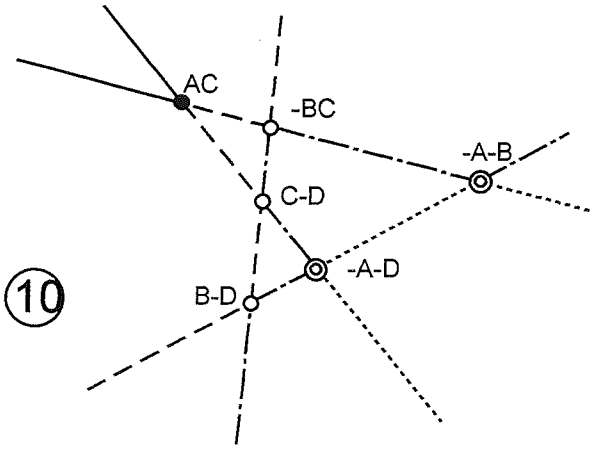

10

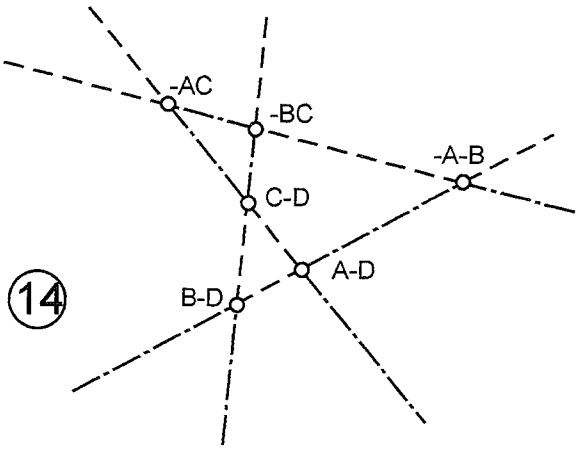

14

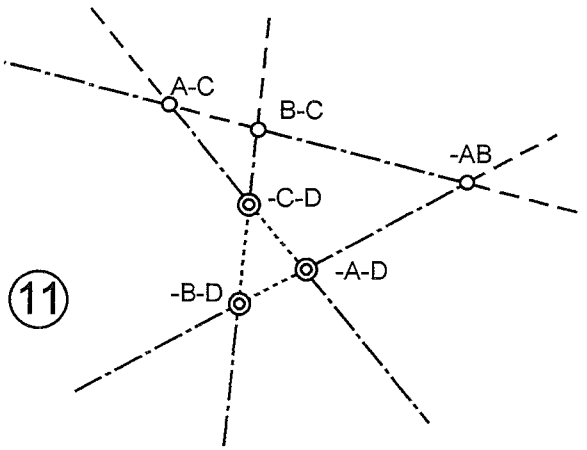

11

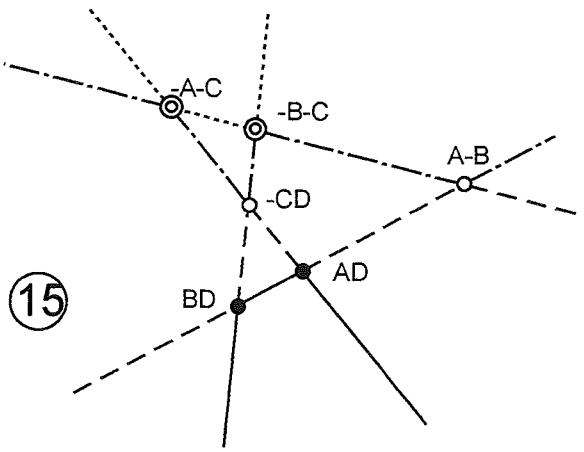

15

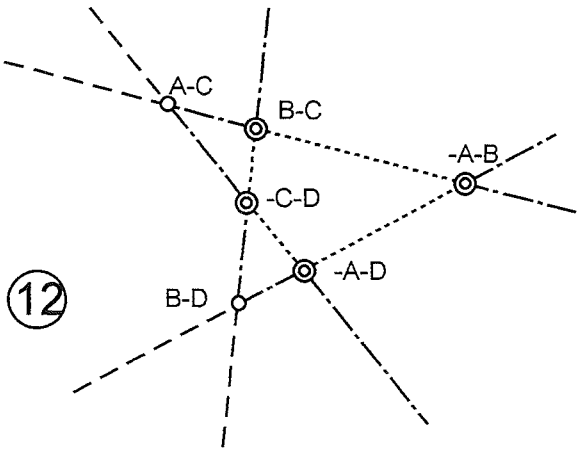

12

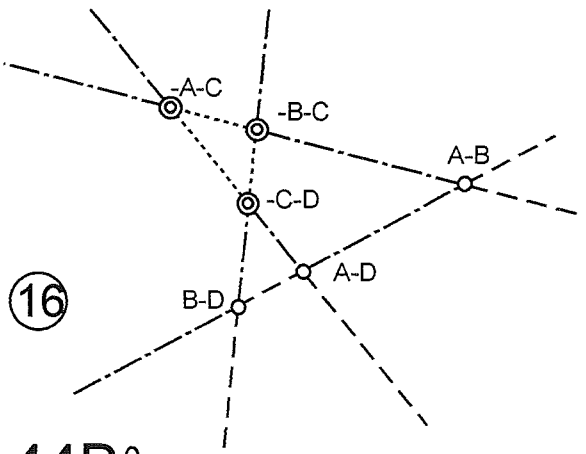

16

FIG. 44B2

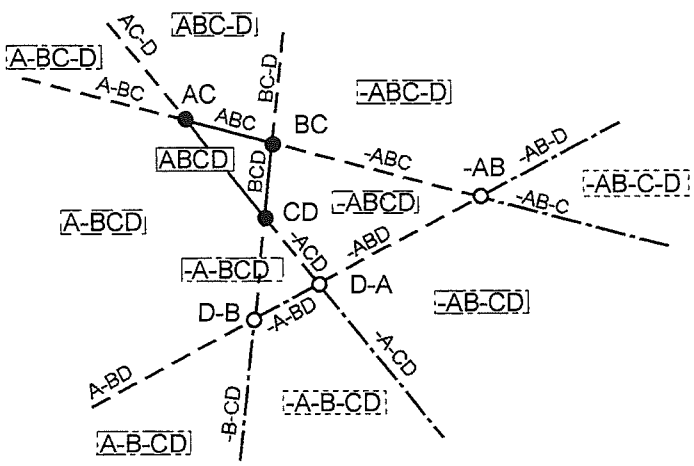

①

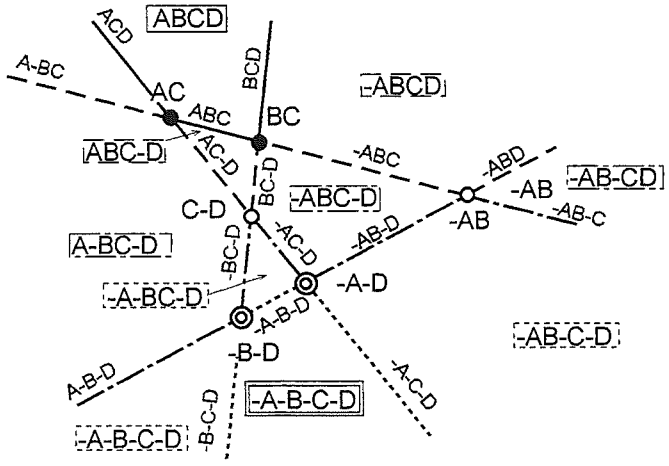

⑤

Points:

- AB
- A-B
- -A-B

Lines:

- ABC
- A-BC
- -A-BC
- -A-B-C

2D-domains:

- ABCD
- ABC-D
- AB-C-D
- A-B-C-D
- -A-B-C-D

FIG. 44B 3

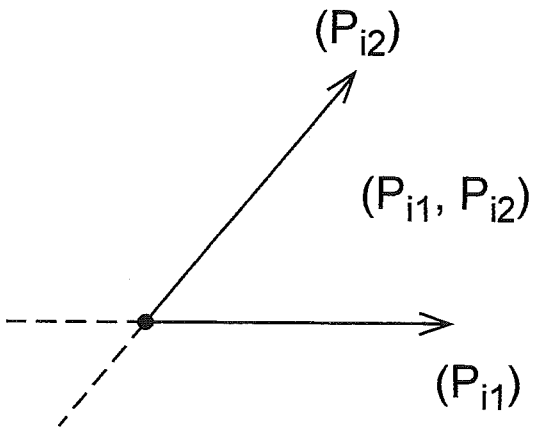

FIG.45

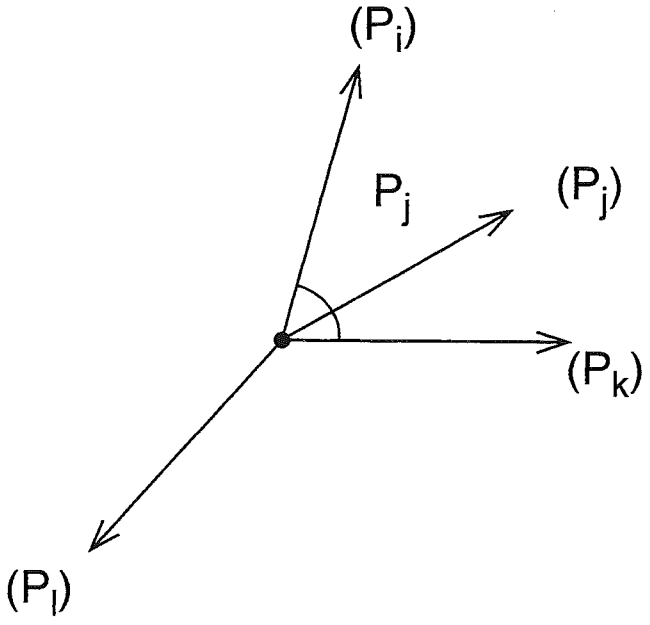

FIG. 46

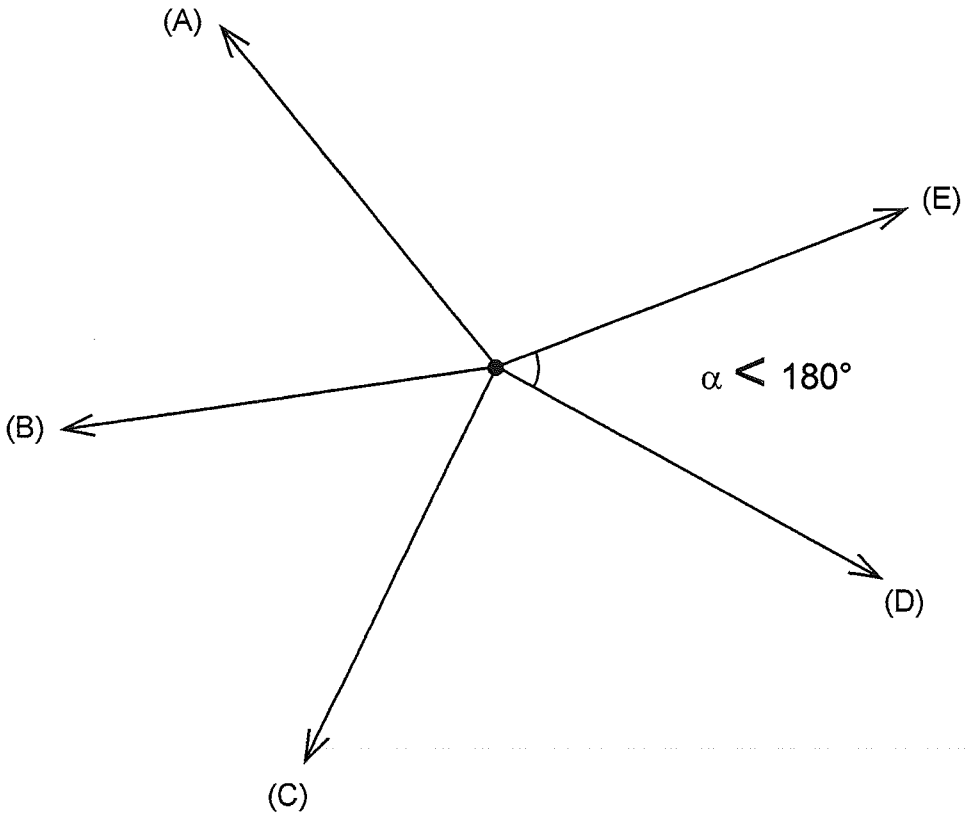

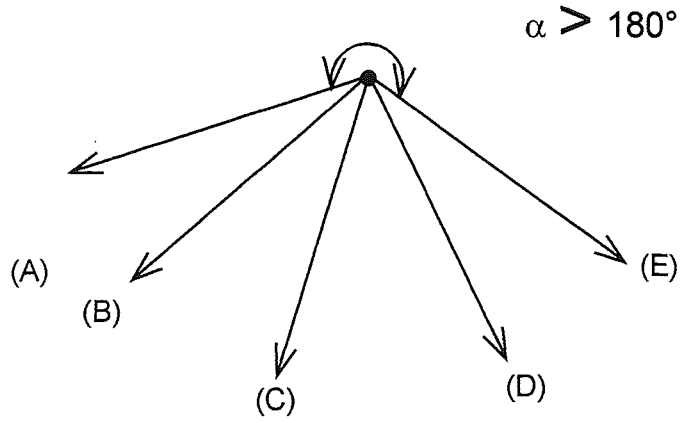

FIG.47

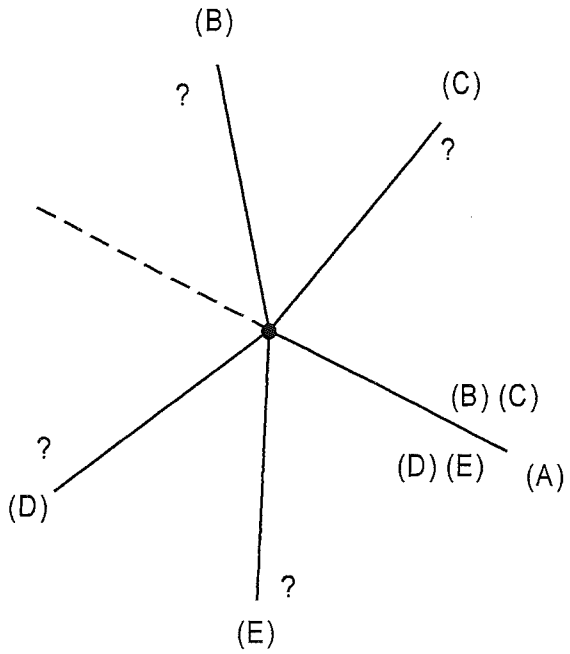

FIG. 48A

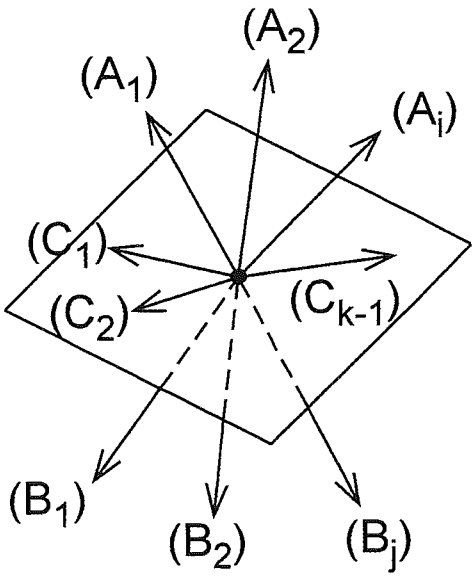

FIG. 48B

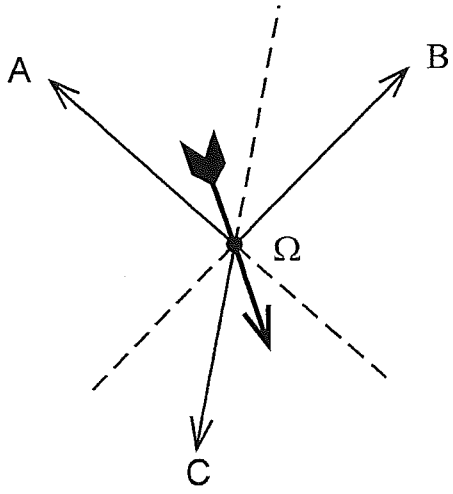

A B → -A-B
A-C → -A C
-B-C → B C

FIG. 49

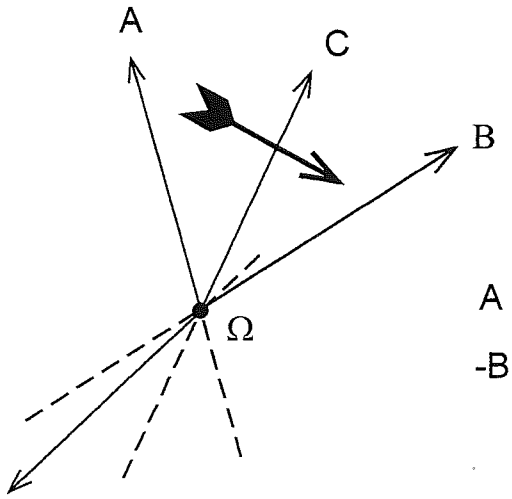

A C → B C
-B C → -A C

FIG. 50

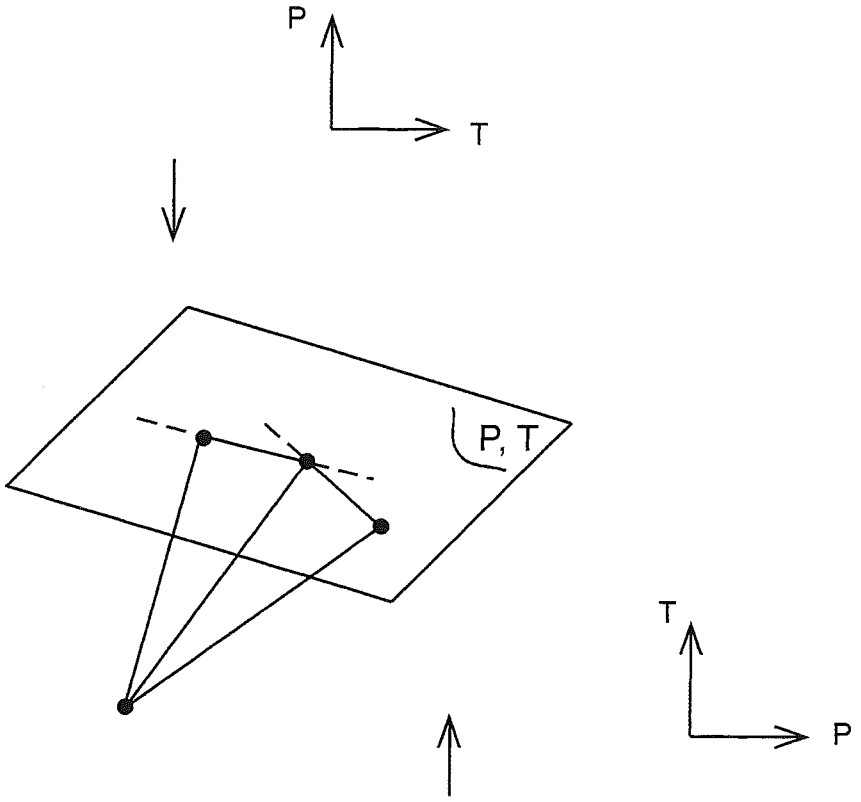

FIG. 51 A

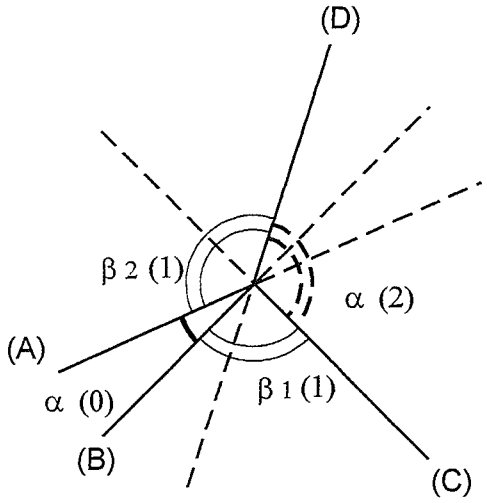

FIG. 51B

A

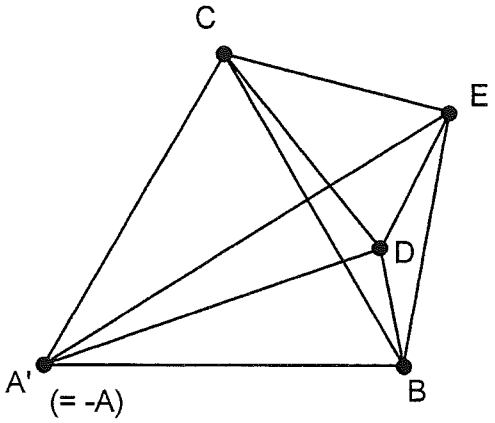

B

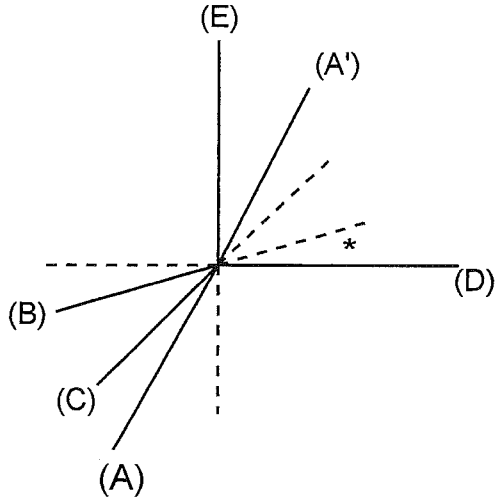

FIG. 52

A

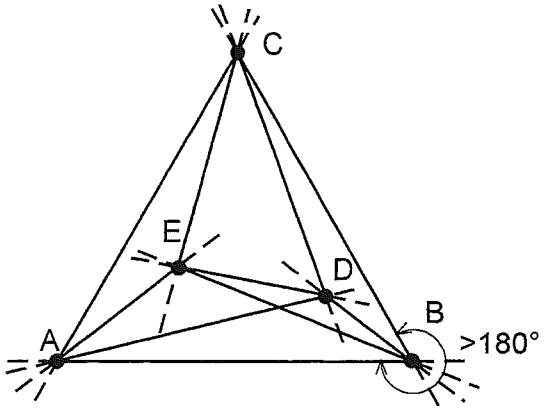

FIG. 53A

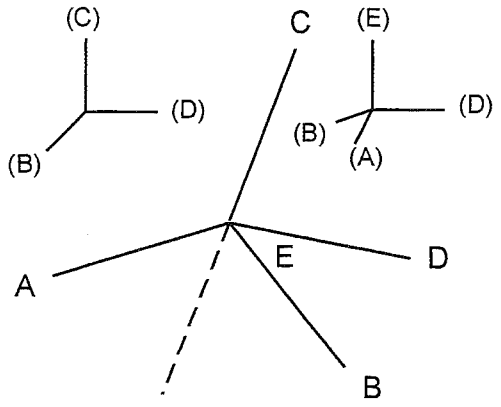

(A) = (B) + (D)
CE

chemography

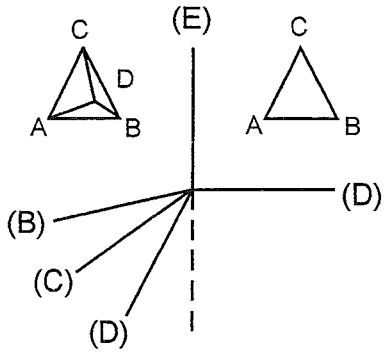

A + B +C = D
(E)

affigraphy

FIG. 53 B

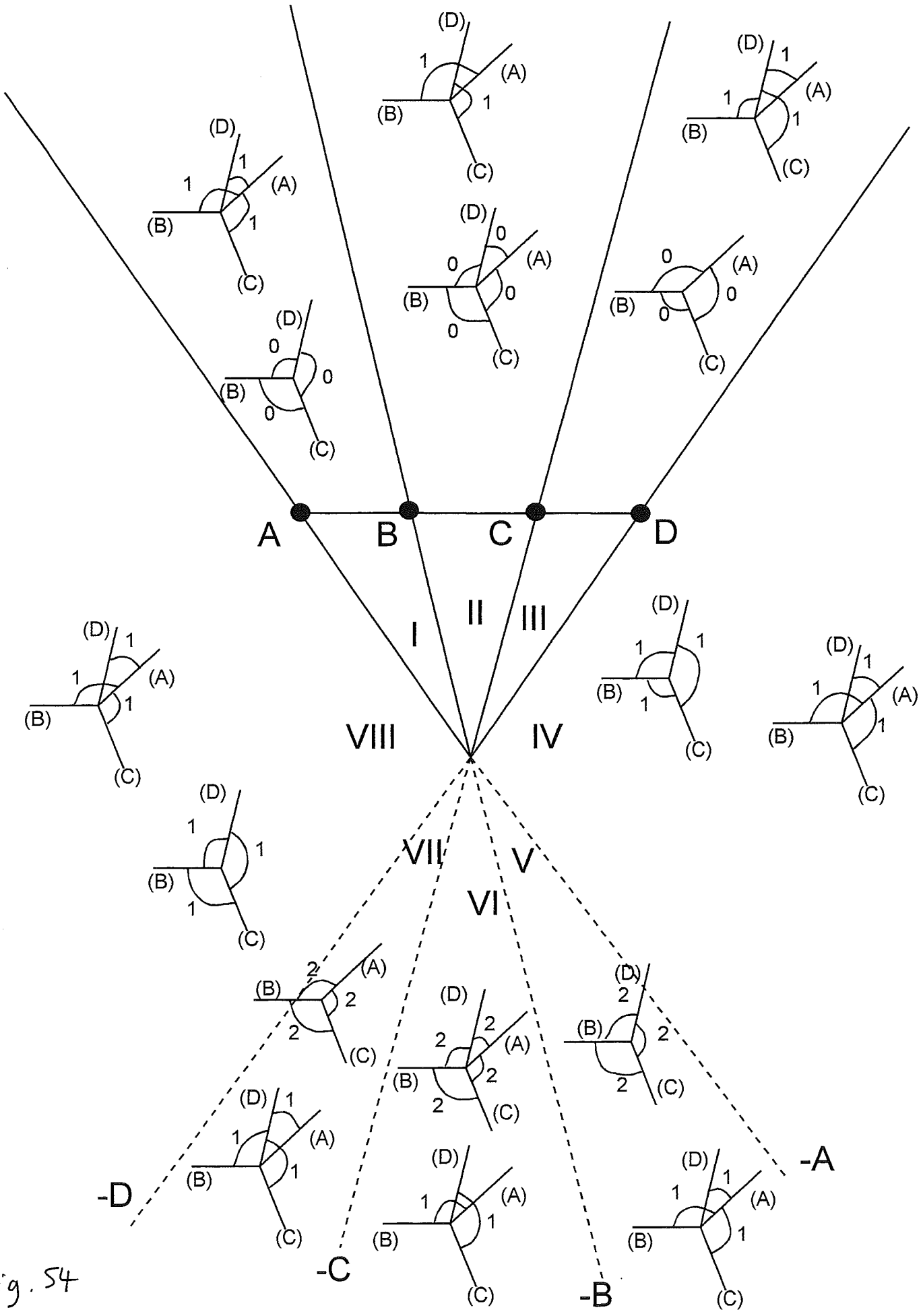

Fig. 54

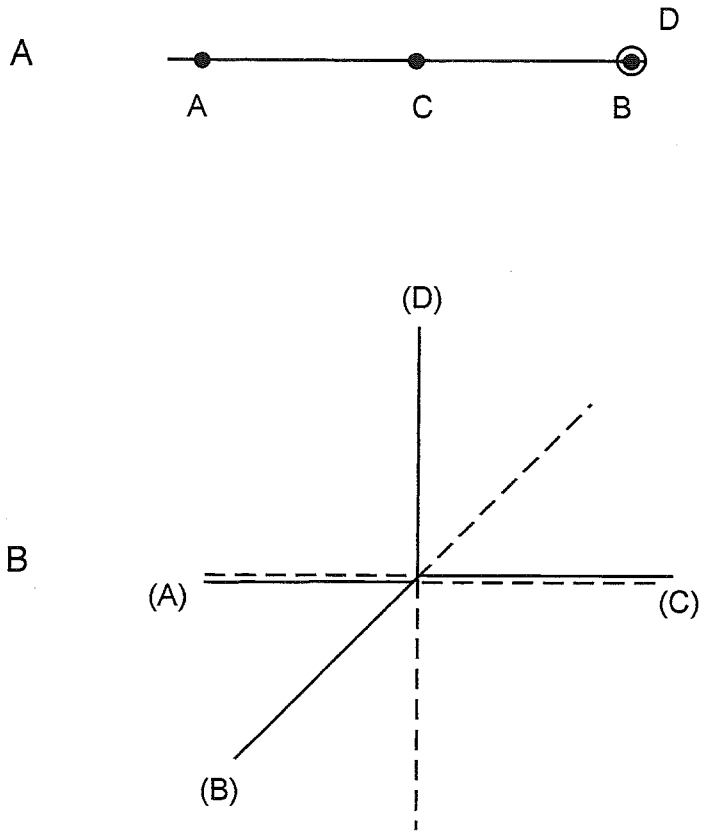

FIG. 55

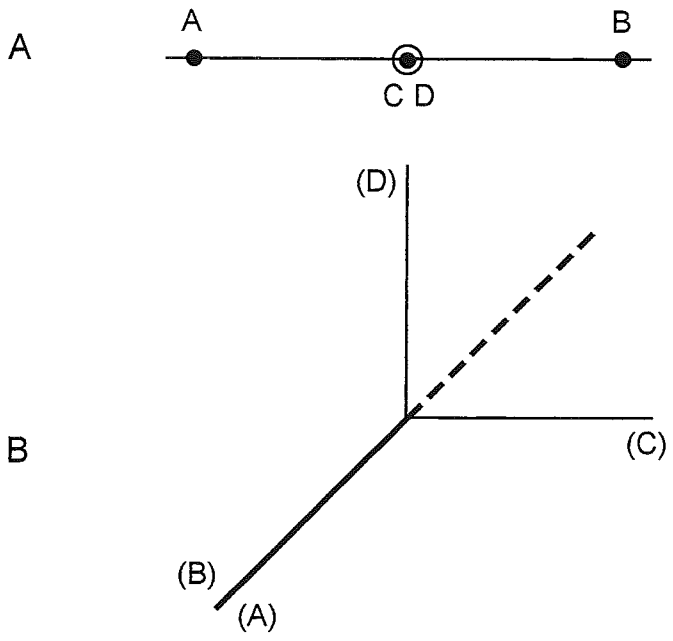

FIG. 56

A

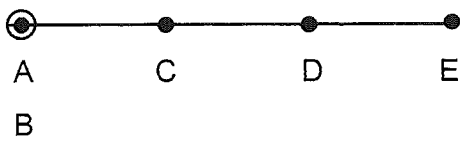

B

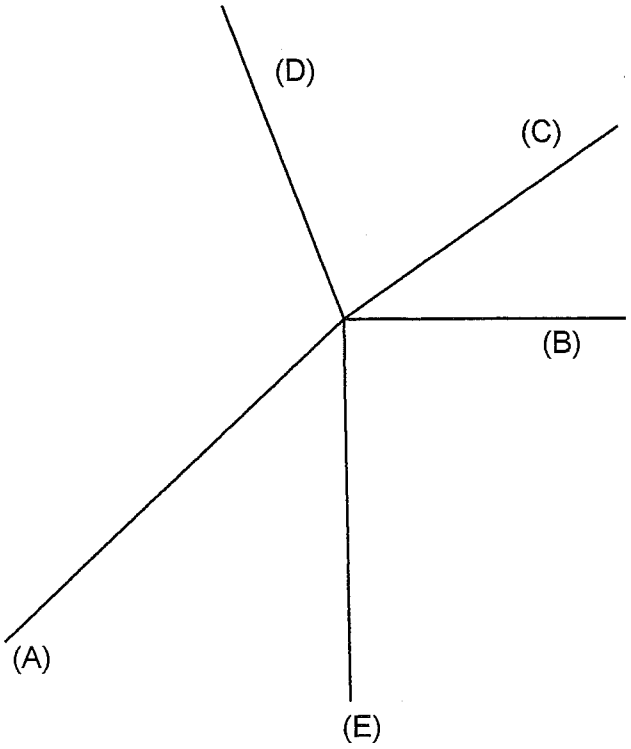

FIG. 57

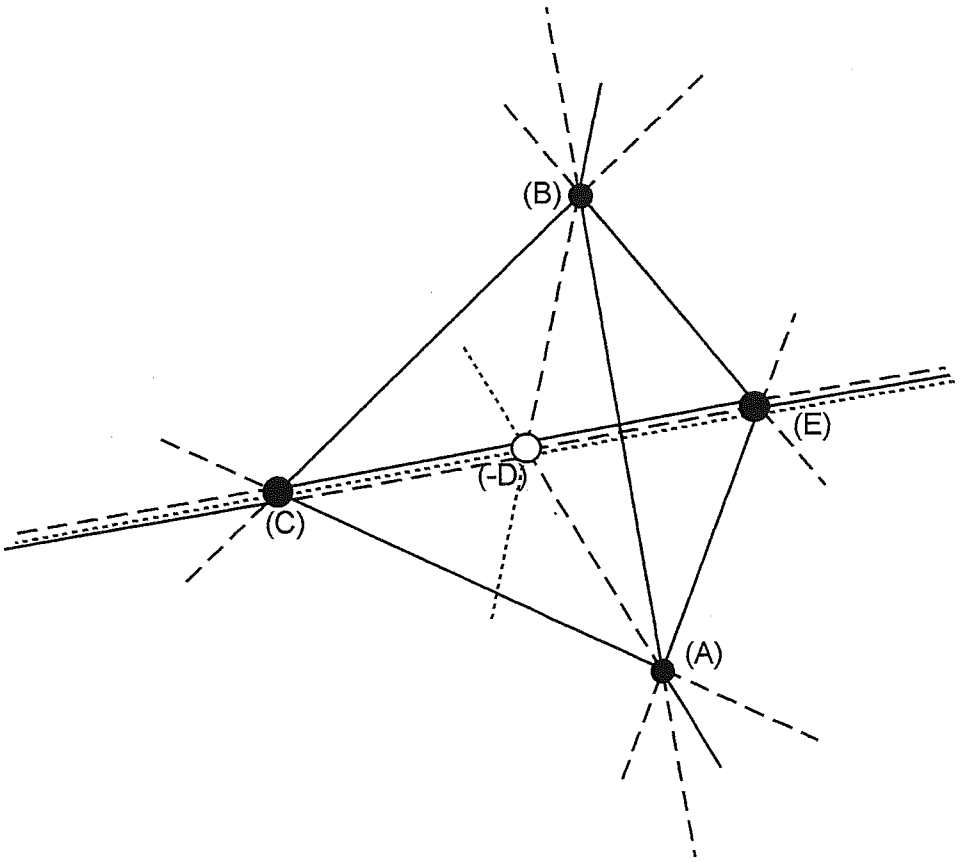

FIG. 57C

A

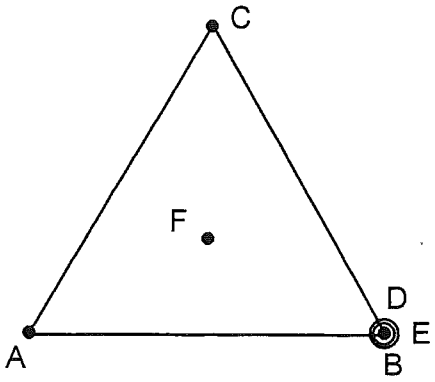

B

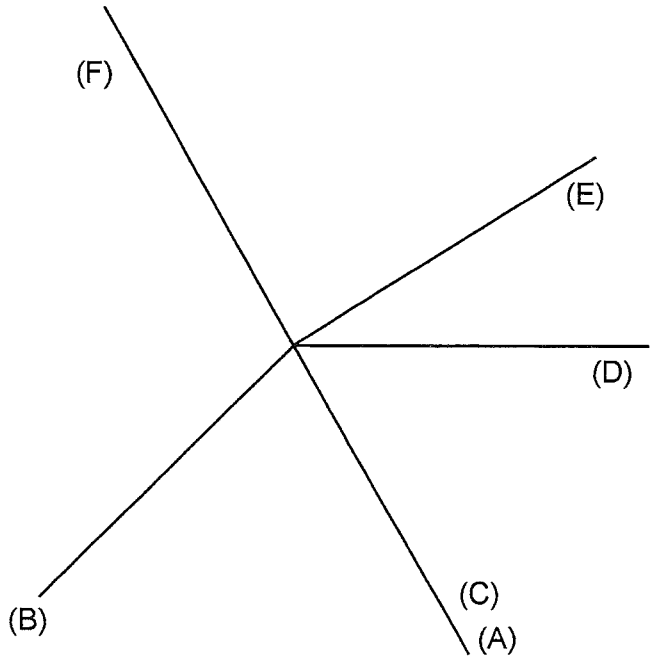

FIG. 58

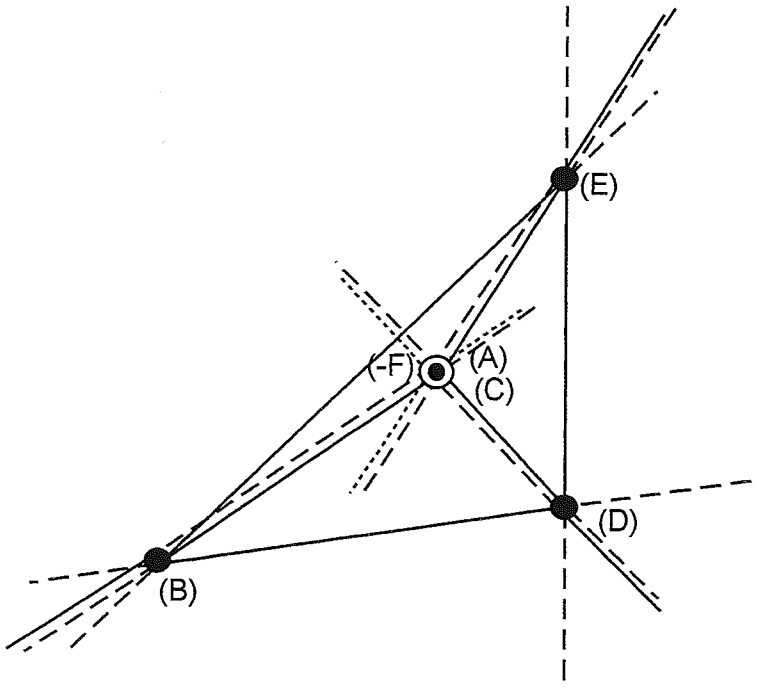

FIG. 58 C

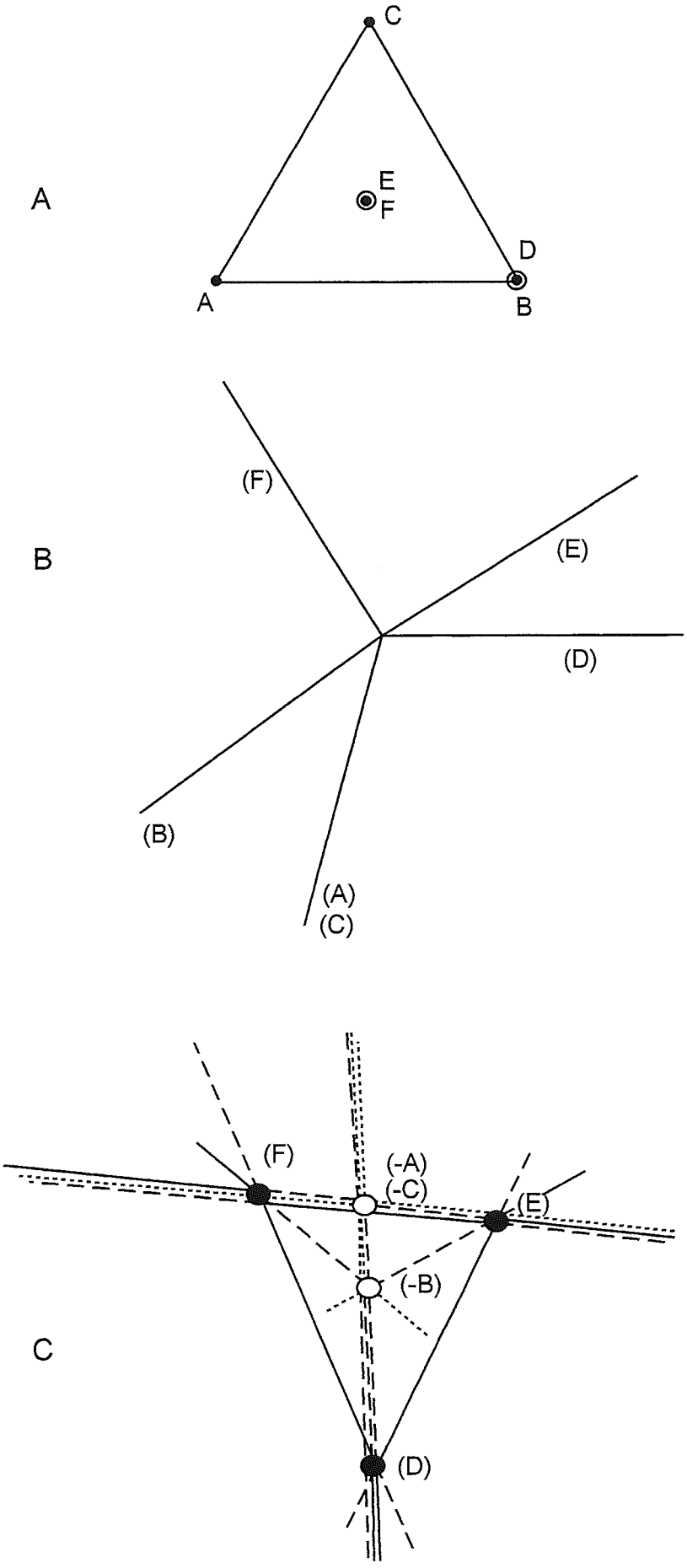

FIG. 59

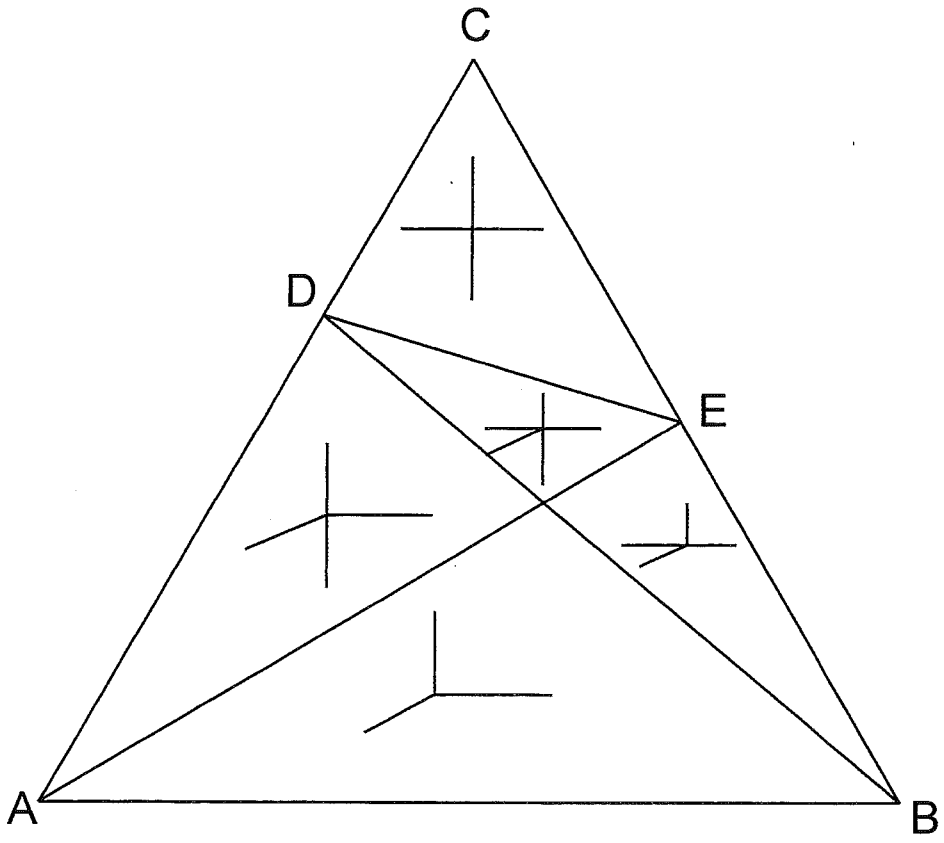

FIG. 60 A

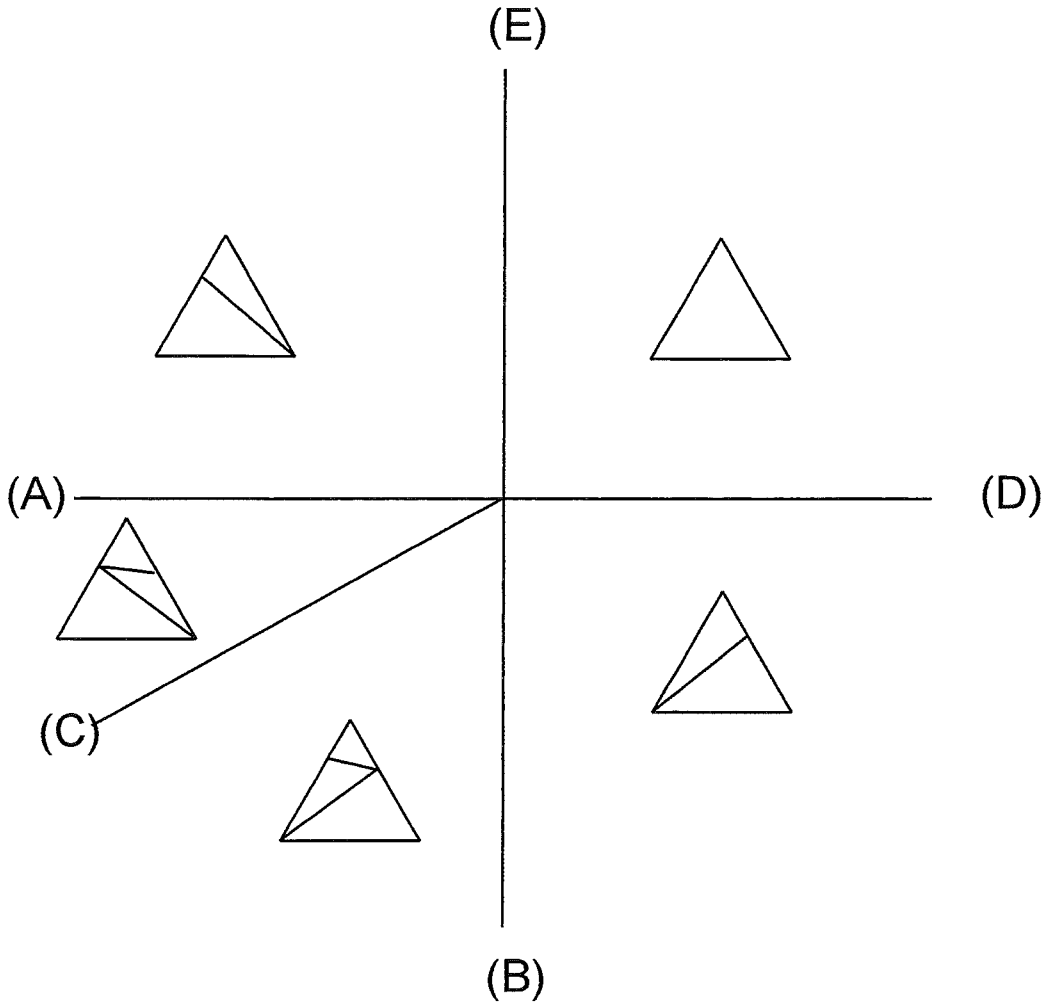

FIG. 60 B

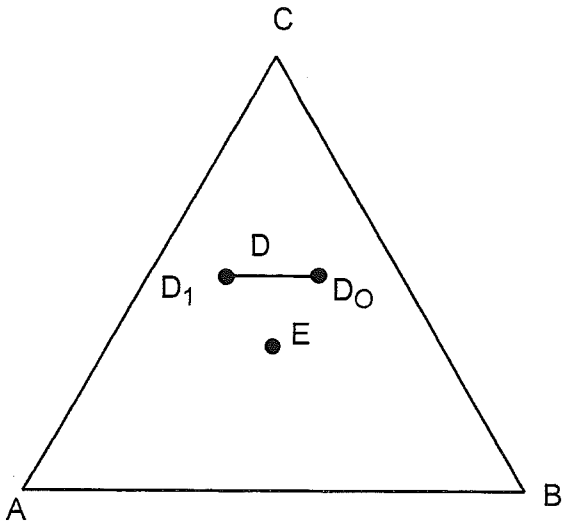

FIG. 61 A

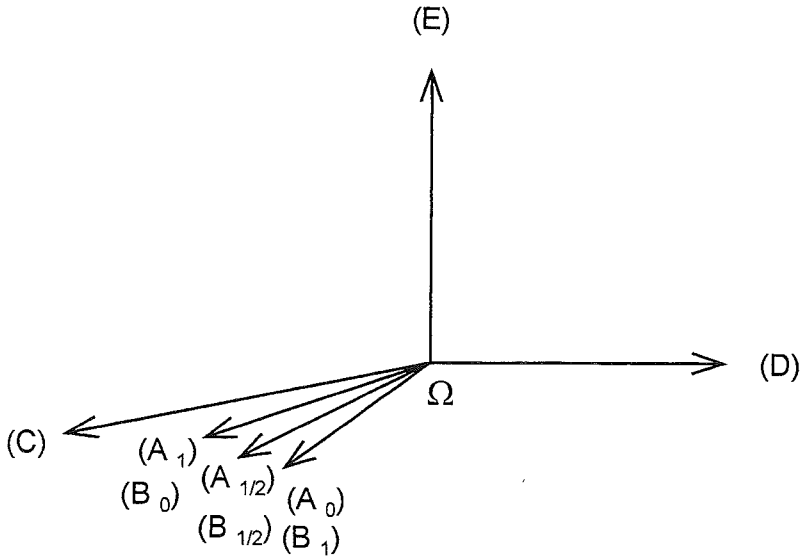

FIG. 61 B

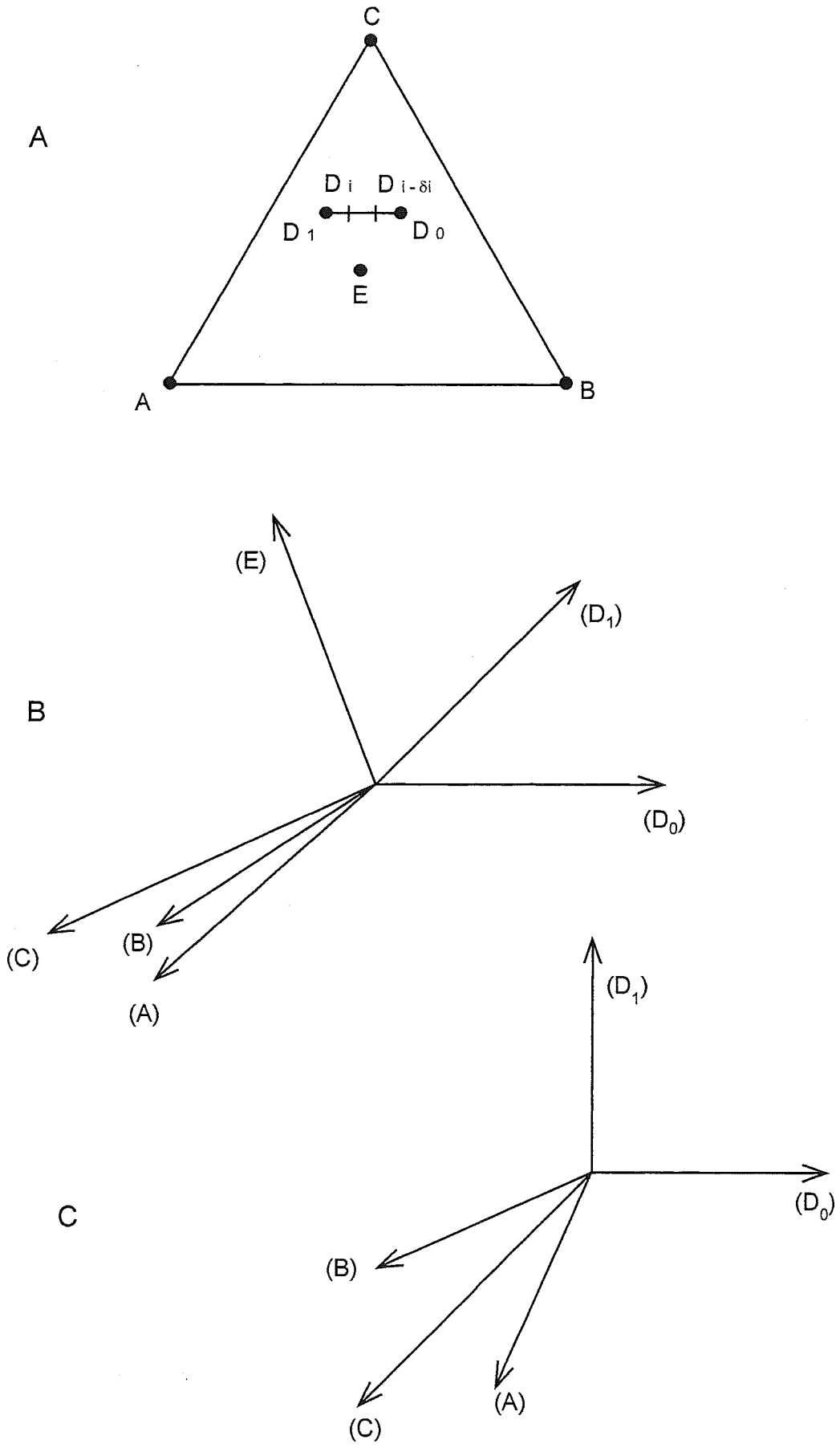

FIG. 62

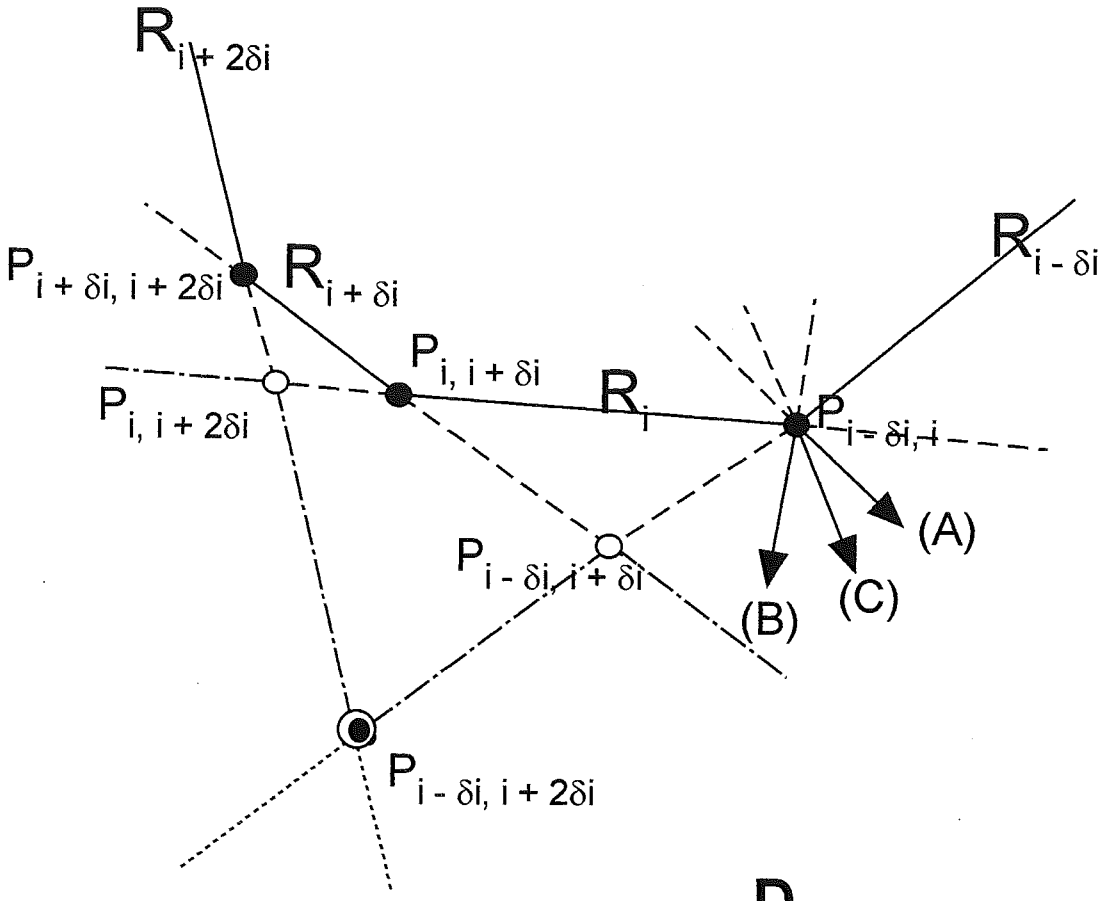
R i + 2δi
P i + δi, i + 2δi
R i + δi
R i - δi
P i, i + δi
P i, i + 2δi
R i
P i - δi, i
(A)
P i - δi, i + δi
(B)
(C)
P i - δi, i + 2δi
D

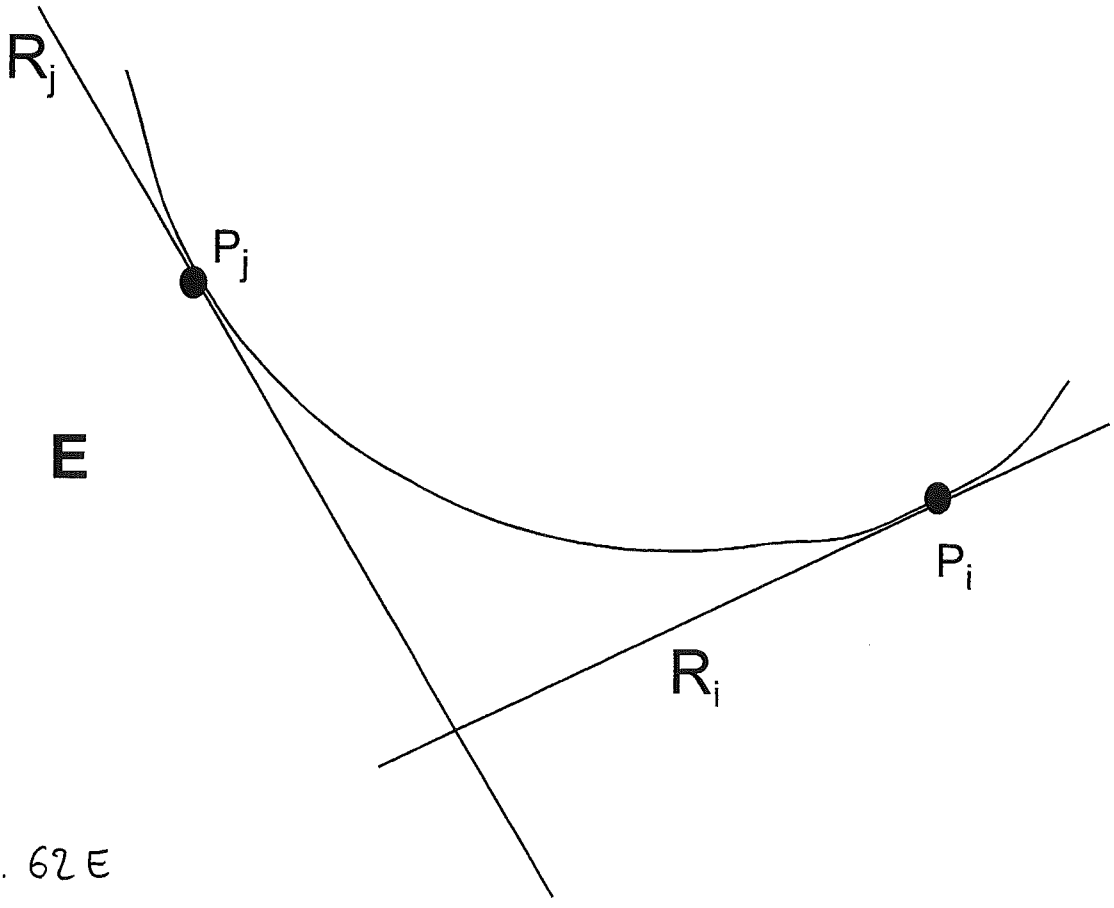
R j
P j
E
P i
R i

Fig. 62E

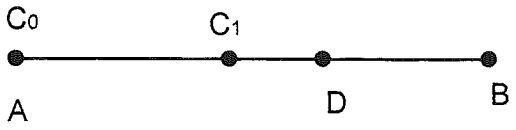

FIG. 63 A

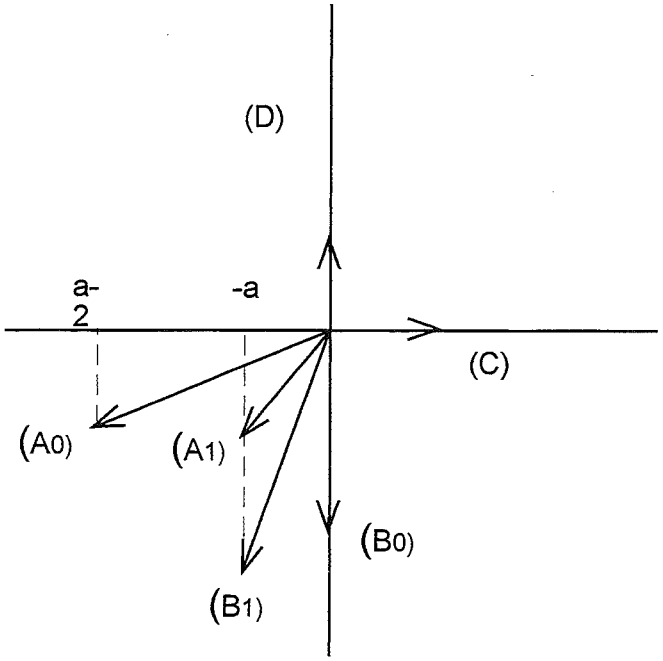

FIG. 63B

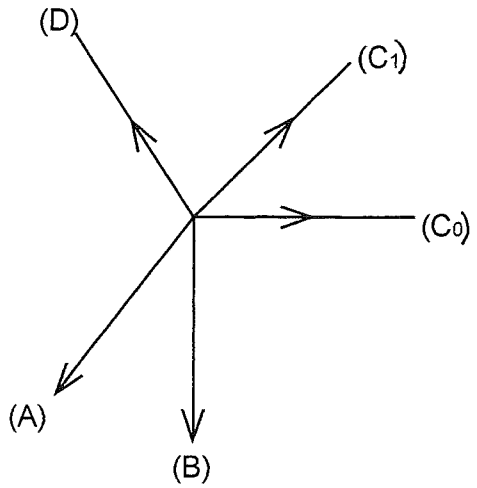

FIG. 63C

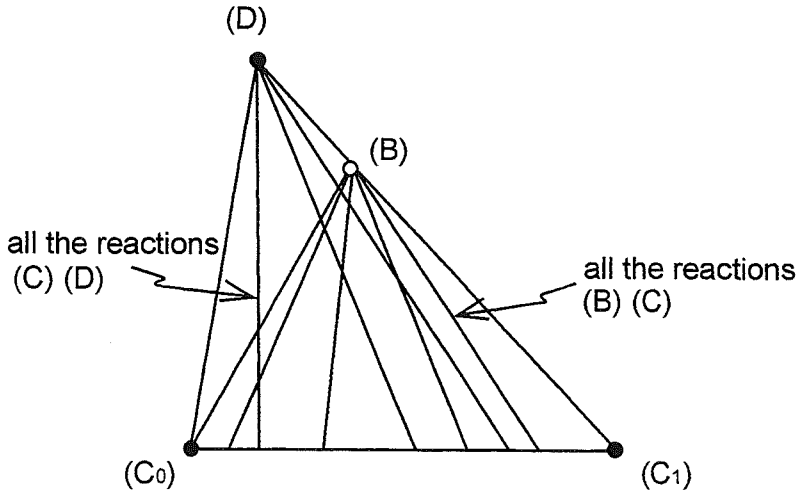

FIG. 63 D

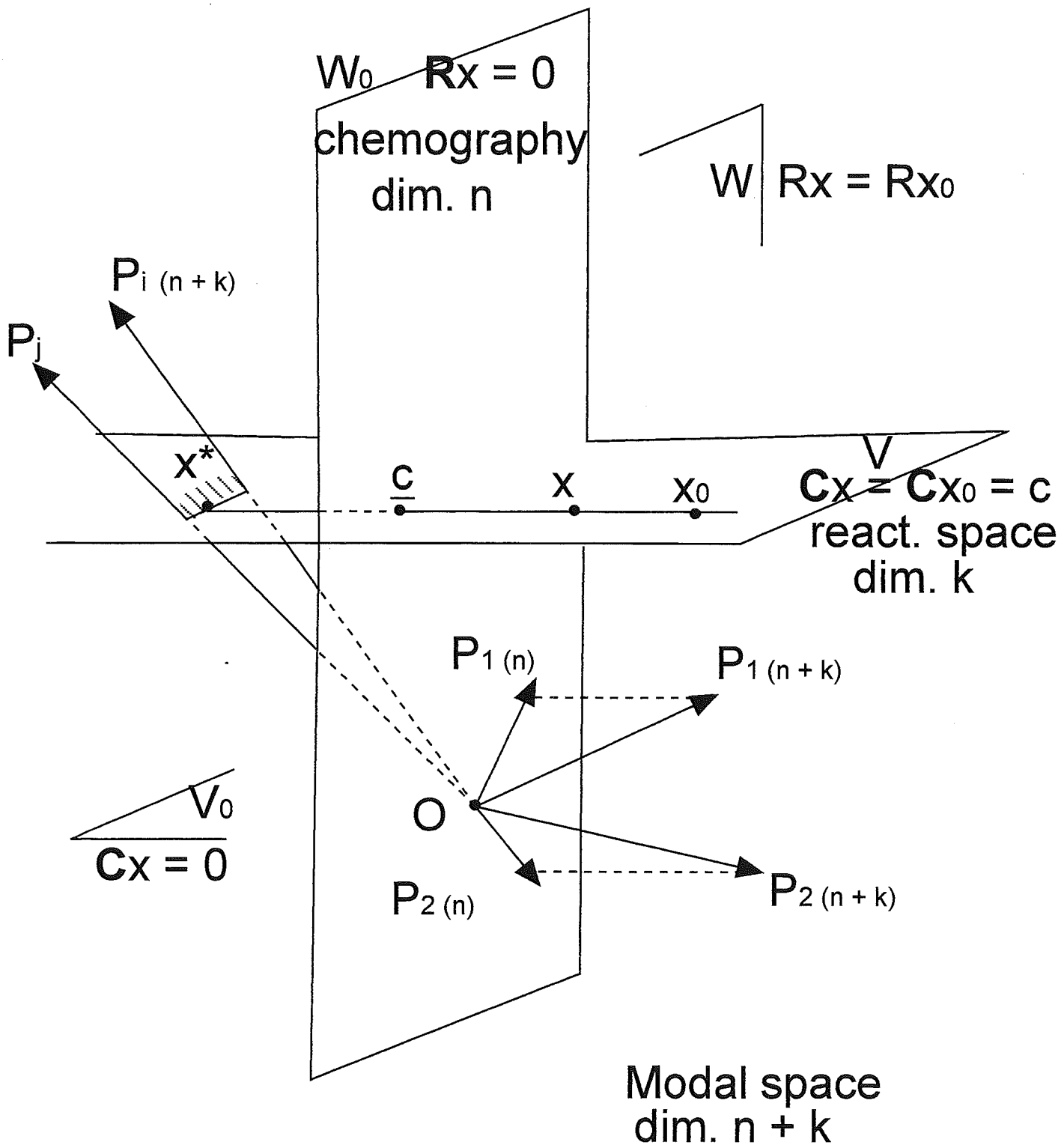
W0 Rx = 0
chemography
dim. n
W Rx = Rx0
Pi (n + k)
Pj
x*
c
x
x0
V
Cx = Cx0 = c
react. space
dim. k
P1 (n)
P1 (n + k)
V0
Cx = 0
O
P2 (n)
P2 (n + k)
Modal space
dim. n + k

Fig. 64A

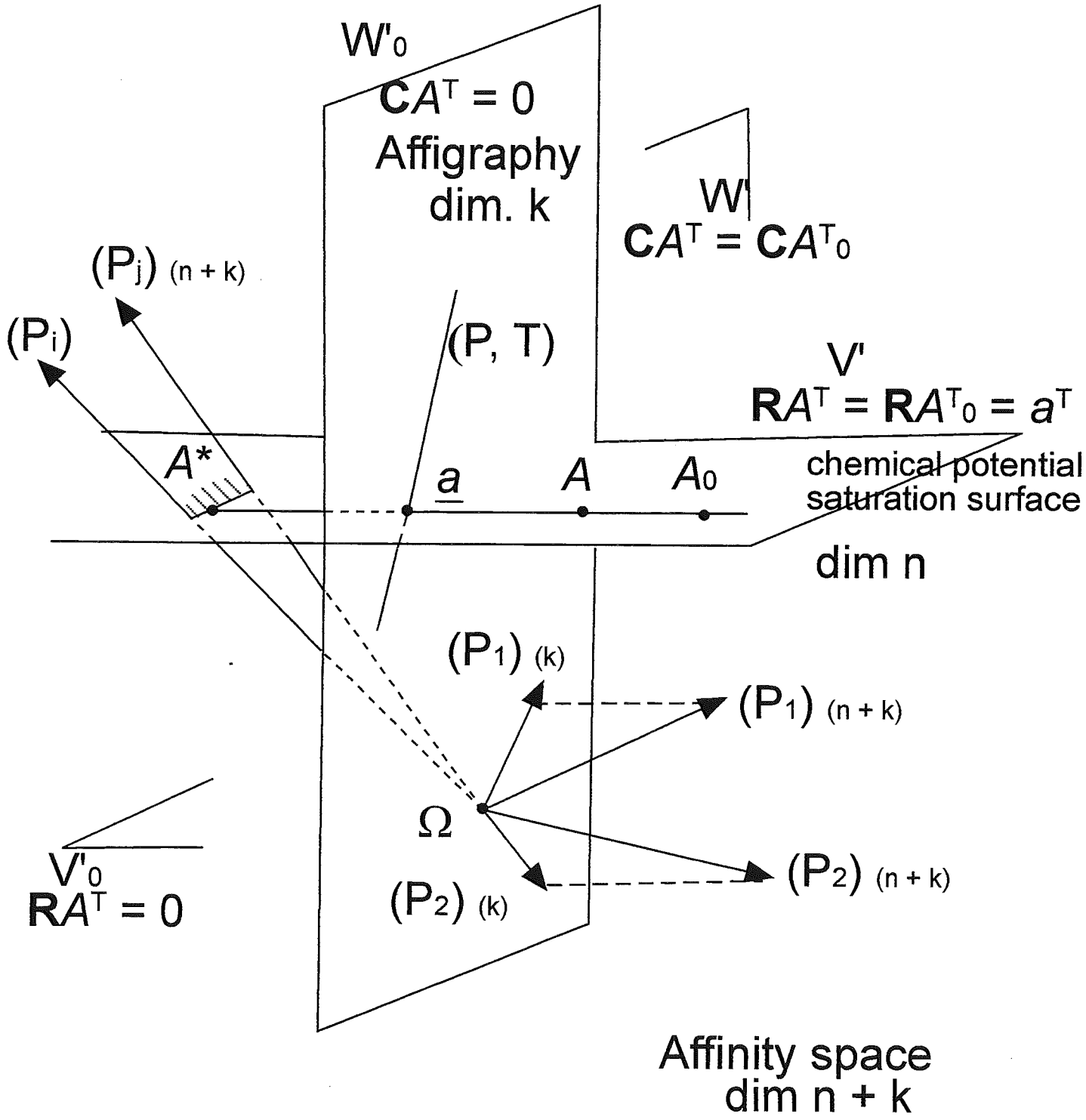
W'0
$CA^T = 0$
Affigraphy
dim. k
W'
$CA^T = CA^T_0$
$(P_j)_{(n+k)}$
(P_i)
(P, T)
V'
$RA^T = RA^T_0 = a^T$
A^*
a
A
A_0
chemical potential
saturation surface
dim n
$(P_1)_{(k)}$
$(P_1)_{(n+k)}$
Ω
$(P_2)_{(n+k)}$
$(P_2)_{(k)}$
V'_0
$RA^T = 0$
Affinity space
dim n + k

Fig. 64B

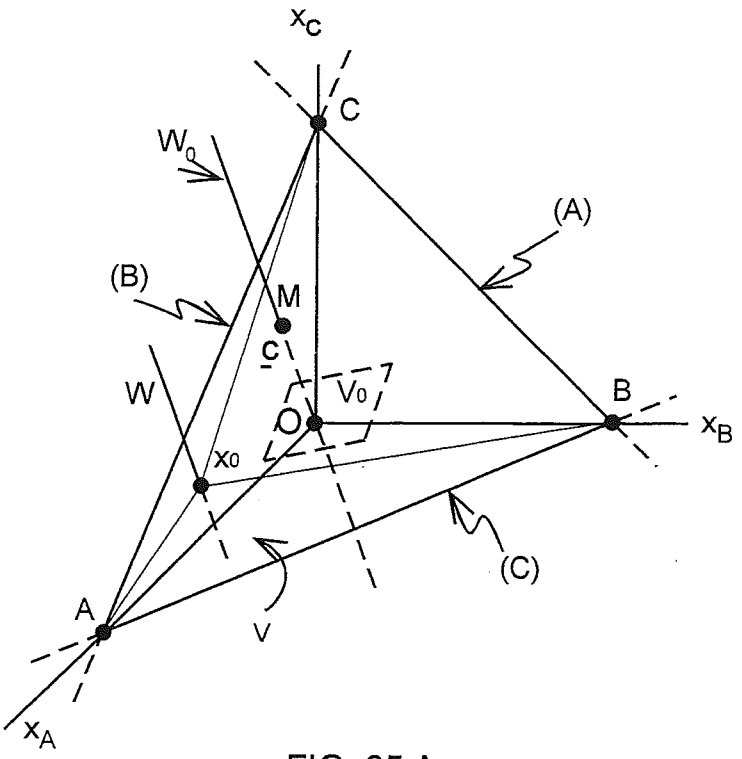

FIG. 65 A

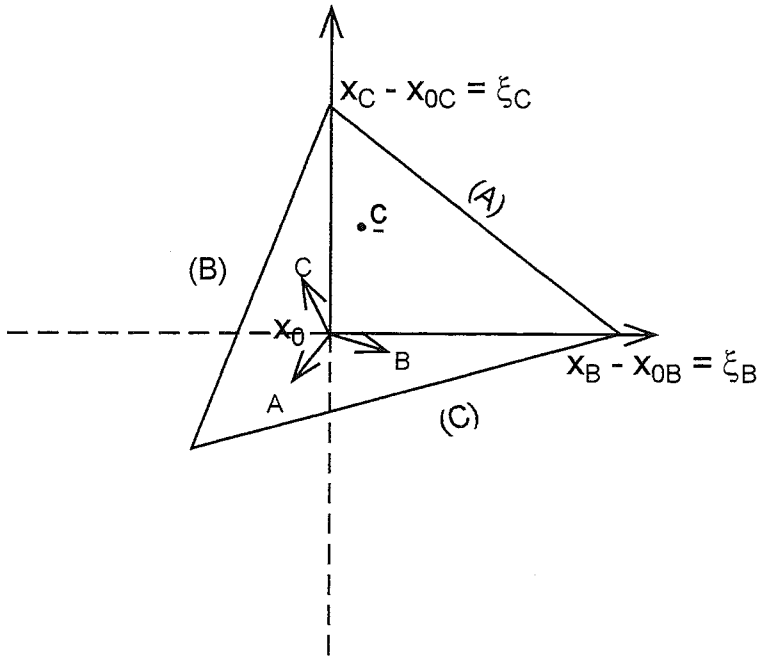

FIG. 65 B

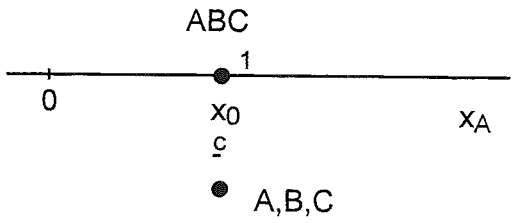

FIG. 65C

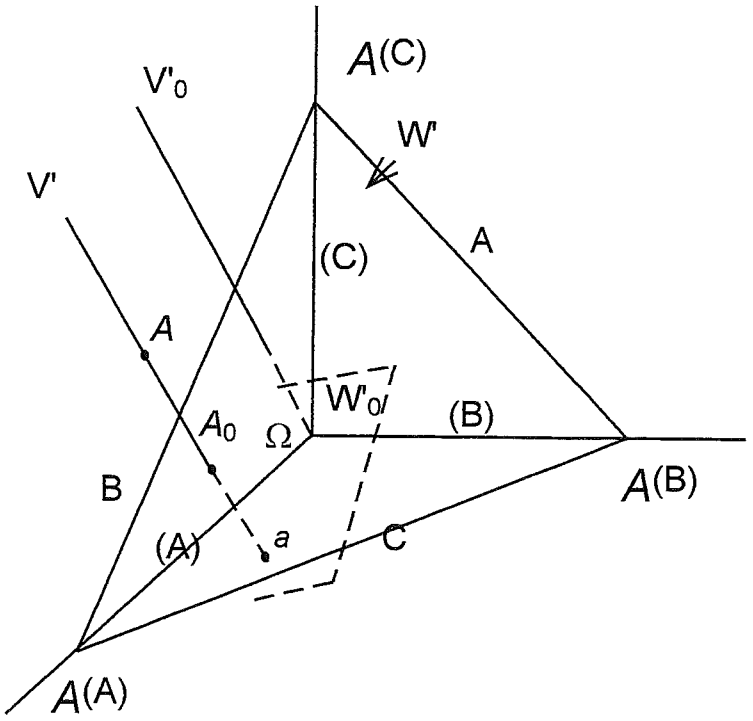

FIG. 65D

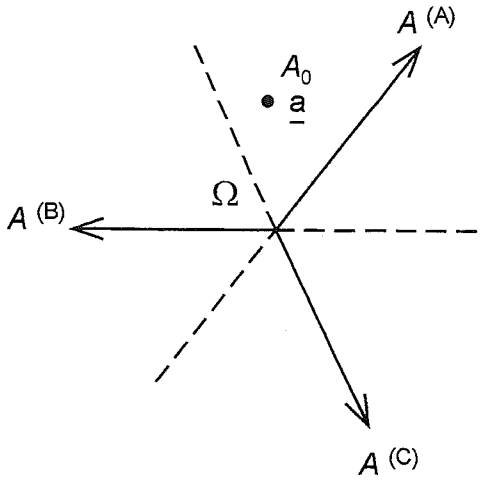

FIG. 65 E

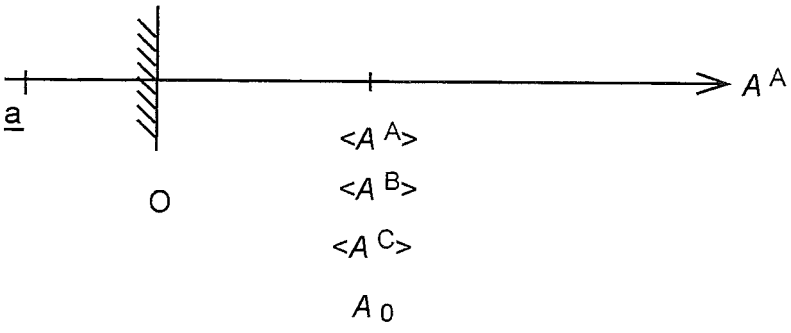

FIG. 65 F

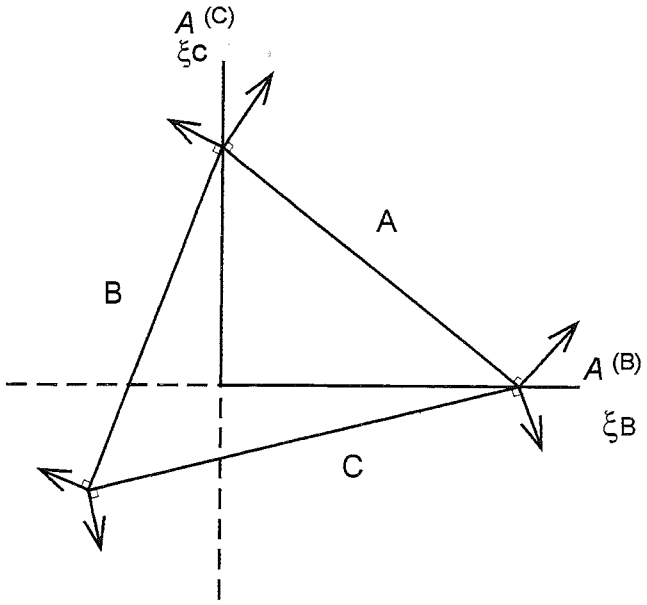

FIG. 65 G

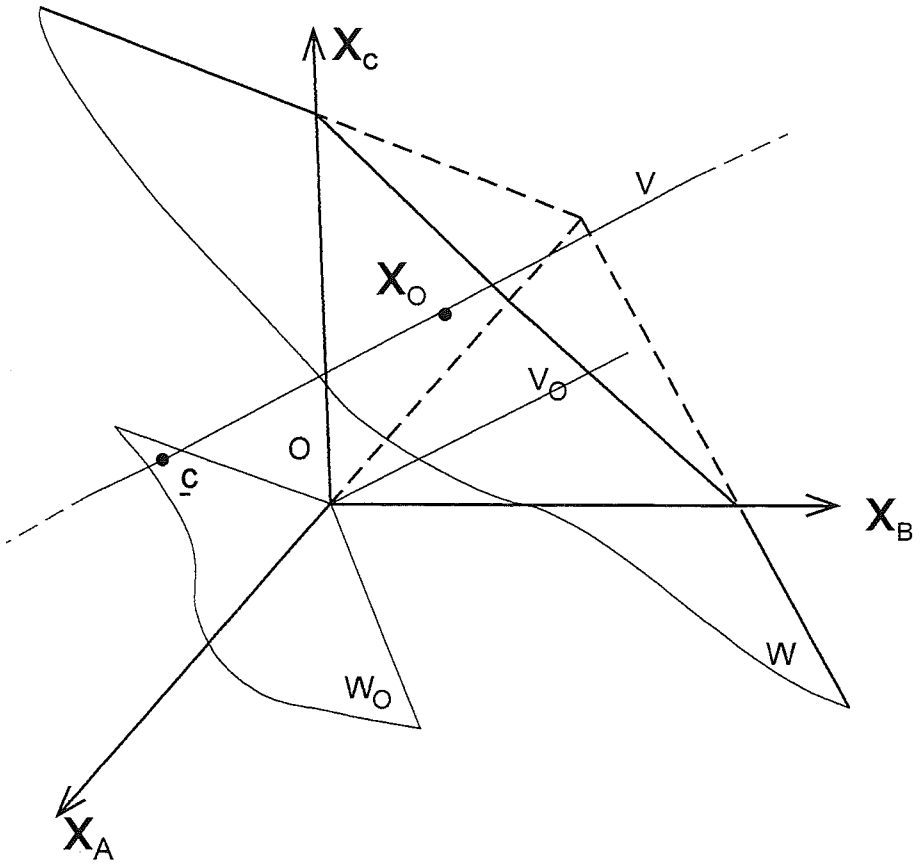

FIG. 66 A

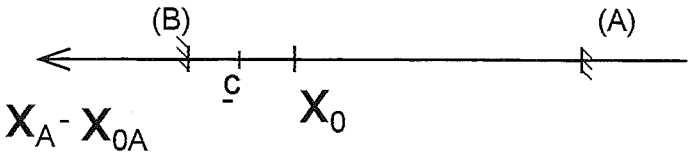

FIG. 66 B

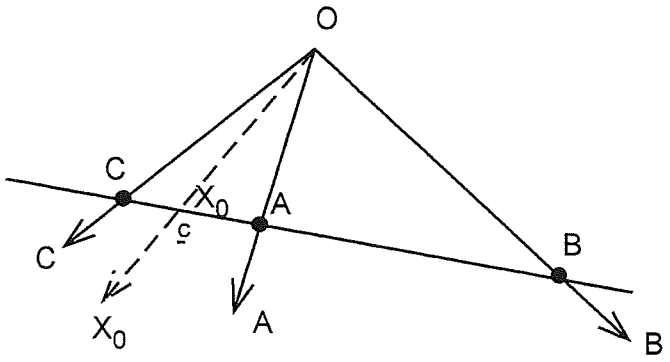

FIG. 66 C

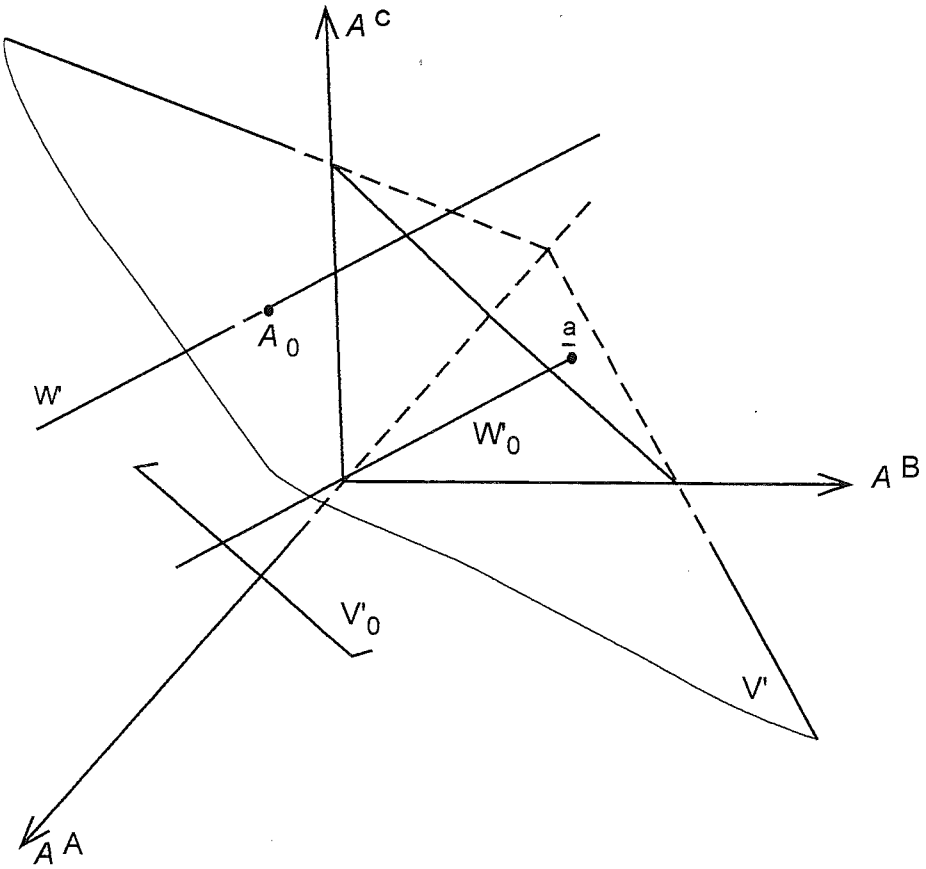

FIG. 66 D

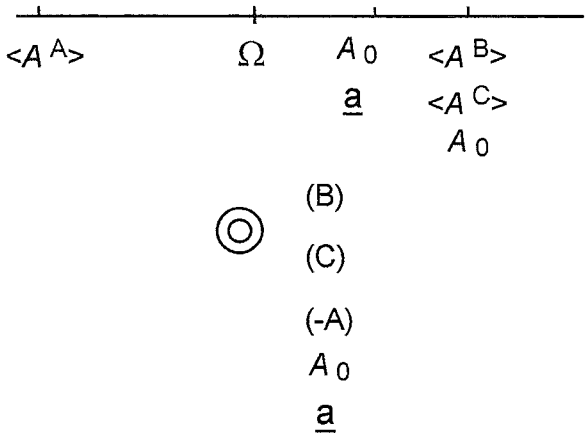

FIG. 66 E

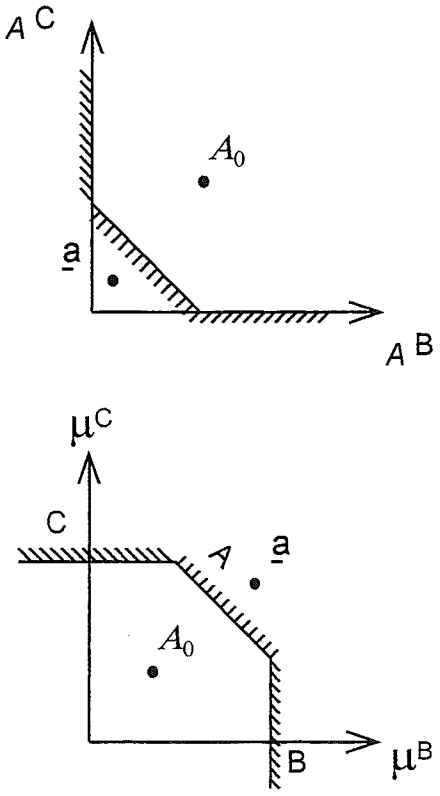

FIG. 66F

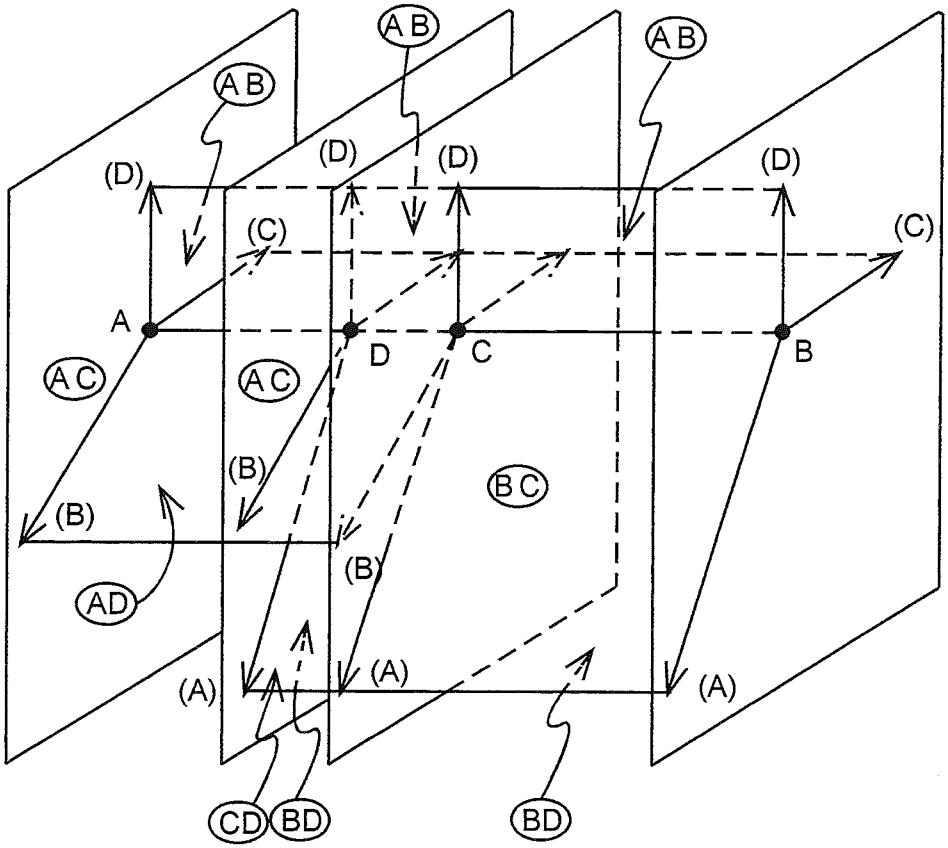

FIG. 67

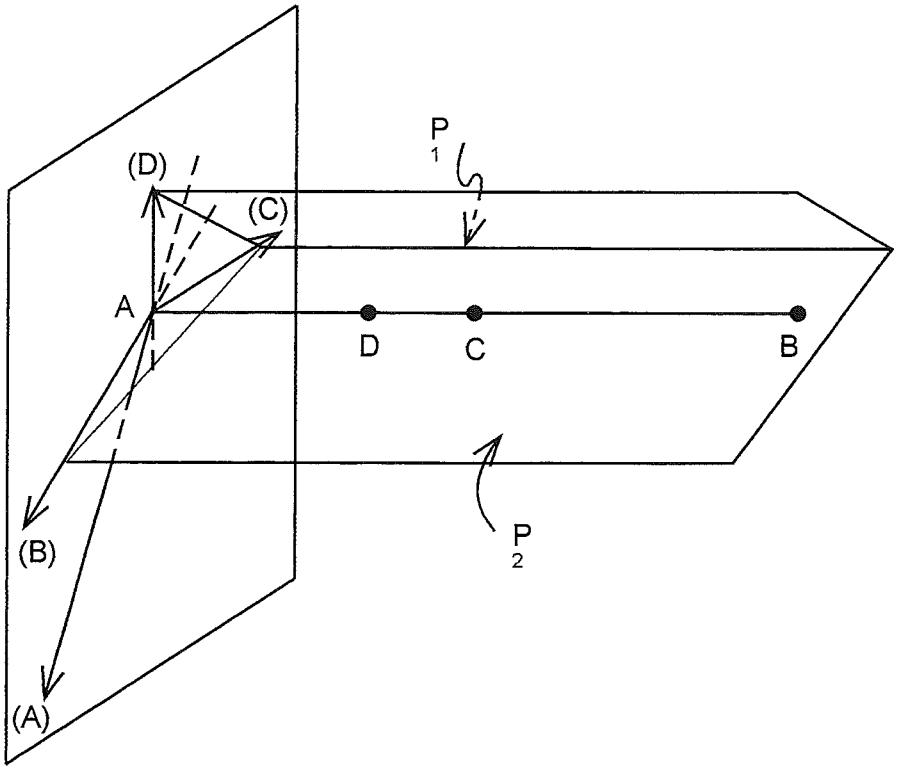

FIG. 68 A

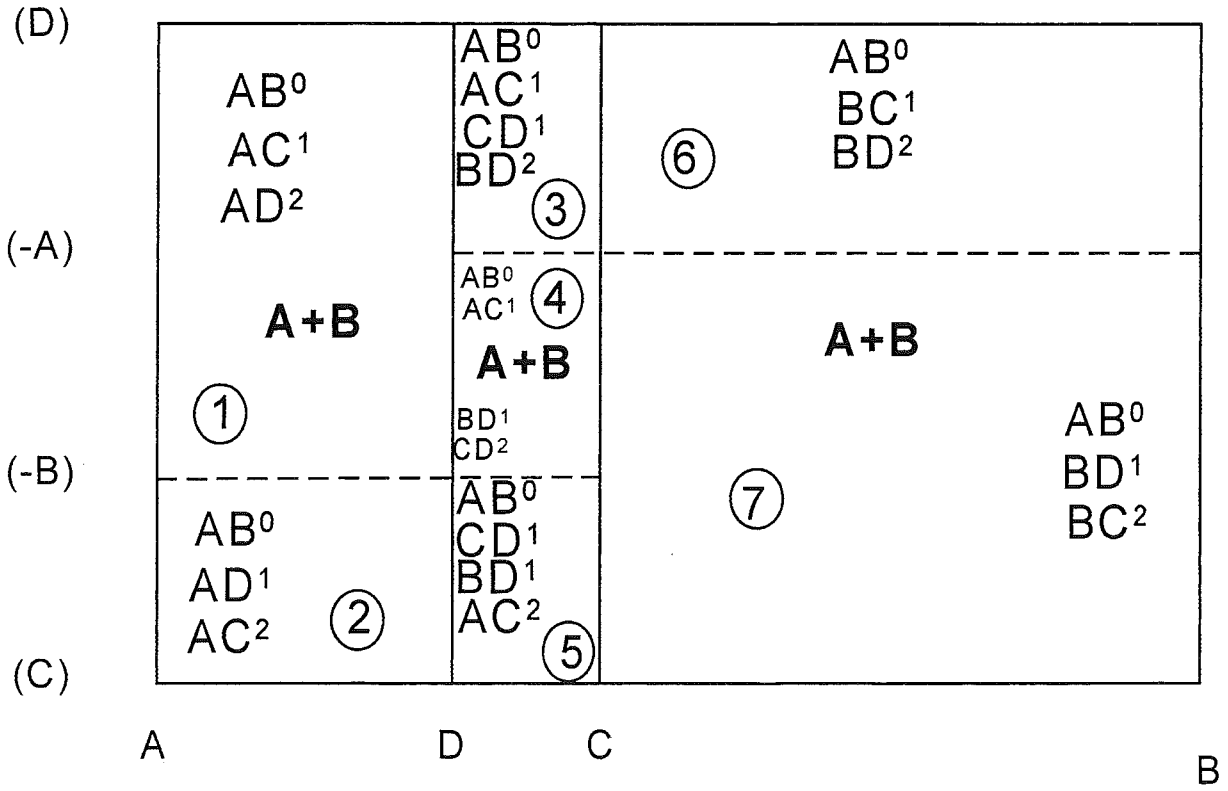

FIG. 68 B

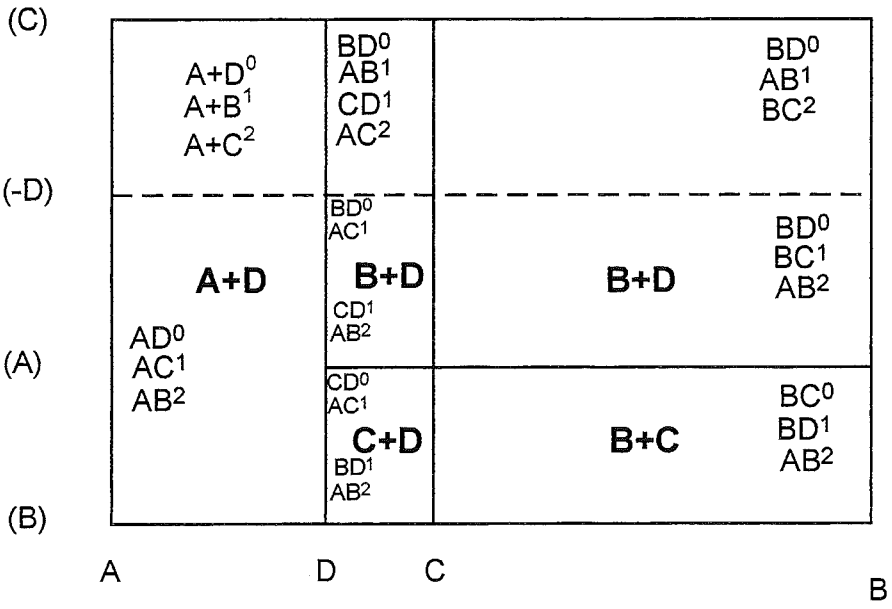
(C)
(-D)
(A)
(B)
A+D0
A+B1
A+C2
BD0
AB1
CD1
AC2
BD0
AB1
BC2
A+D
AD0
AC1
AB2
BD0
AC1
B+D
CD1
AB2
B+D
BD0
BC1
AB2
CD0
AC1
C+D
BD1
AB2
B+C
BC0
BD1
AB2
A
D
C
B

FIG. 68 C

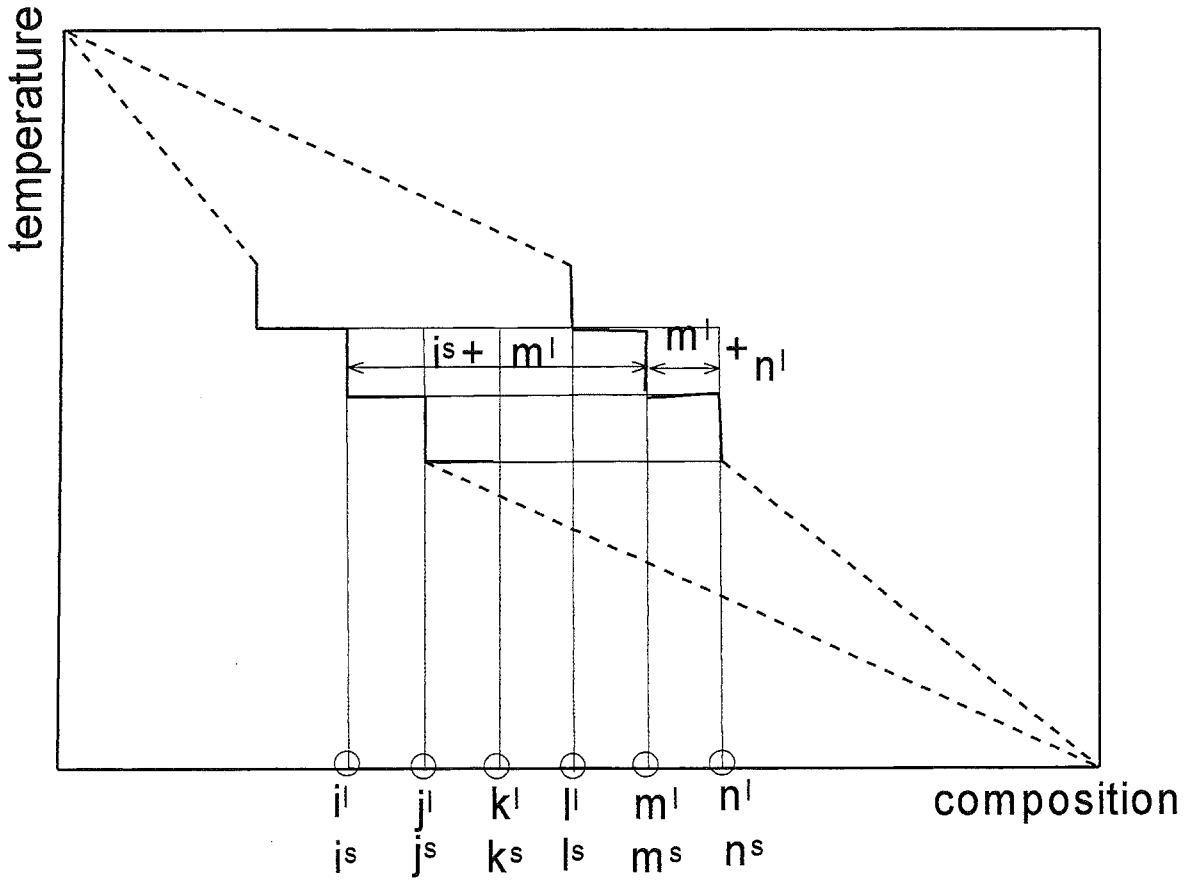
temperature
composition
$i^s + m^l$
$m^l + n^l$
i^l j^l k^l l^l m^l n^l
i^s j^s k^s l^s m^s n^s

Fig. 69